

CHAPTER I

GENERAL INTRODUCTION

1.1 Introduction

Nowadays dental amalgam fillings are widely being replaced by composite fillings. The main advantage of a direct dental composite over traditional materials such as amalgam is the superior cosmetic appearance. Composites can be made of a wide range of tooth colours allowing nearly invisible restorations of the teeth. They are glued onto the tooth with micromechanical bonding allowing a good adhesion of the restoration to the tooth. This means that there is no need for the dentist to create retentive features which destroy healthy tooth as it is the case when using silver or amalgam. Another reason for the increasing popularity of composite restorative materials is the controversy over the health risk in association with the mercury content in amalgam filling materials (Mackert, 1991, Mueller-Schneemayer, 2004, Schmalz and Arenhold-Bindslef, 2005). Furthermore, concern has been raised over environmental issues of amalgam (Mjoer, 1997, Maxson, 2007), especially mercury contaminated wastewater (Arenhold-Bindslef and Larsen, 1994 and 1998). These aspects clearly show the importance of composites as restorative filling materials.

During the last decades numerous studies have been carried out to address the improvement of the chemical and physical properties of the polymeric material (Moszner and Salz, 2001, Puckett *et al.*, 2007). The advanced composites are much stronger, show high wear resistance and colour stability (Li *et al.*, 1985, Braem *et al.*, 1989, Willems *et al.*, 1993). However, most of these sophisticated composite materials are still prone to fatigue damage (Trask *et al.*, 2007, Hickel, 2009, Jandt and Sigusch, 2009). In nearly all of the cases this happens due to cracks that had formed earlier deep

within the structure where manual repair is impossible (Truong and Tyas, 1988, Wool, 2001, Yuan *et al.*, 2008). These micro-cracks can lead to a drastic reduction in the physical and mechanical properties of the material. In practical application this means that the composite filling material becomes susceptible to fatigue failure and wear (Goovaerts *et al.*, 2002). The ageing process of the material is accelerated so that the tooth filling might fall apart ahead of time. If cracks build at the margin of a filling surface bacteria could penetrate and consequently enhance the susceptibility to caries.

The idea to create a dental restorative composite material with improved crack-resistance triggered this research work. This aim can be achieved by the application of a self-healing system. The probably most advanced concept of self-healing is being developed by aeronautical engineers at the University Illinois, US (White *et al.*, 2001). Their system contains microcapsules filled with a healing compound and a corresponding catalyst that are embedded into the polymeric host material. An upcoming crack would rupture capsules to release the healing agent into the crack plane which would then polymerize and seal the crack. Since microcapsules can encapsulate various substances and the coating can also be selected from a wide variety of natural or synthetic polymers it is possible to produce microcapsules for very special applications (Benita, 1996, Arshady and Guyot, 2002, Ghosh, 2006). The preparation of microcapsules for the incorporation in a dental composite matrix to create a self-healing filling material is one niche yet to develop. The main advantage of such a self-healing restorative material is its greatly improved durability. For the patient it would be extremely beneficial as a composite filling that can autonomically heal would be an aesthetic, cost and time saving solution.

1.2 Aim of the Present Investigation

The aim of the present work is to investigate a self-healing system that could be applied in a dental restorative composite to improve the performance of the material. The outcome of this research shall provide a sound foundation for further work on the development of dental polymeric materials with enhanced crack-resistance and therefore extended life-time. The findings of this study are not only beneficial for the creation of novel dental materials; potential applications of the self-healing system include any industrial area where polymeric materials are used.

The specific objectives of this project include the following:

- to define a self-healing concept applicable in a dental restorative composite material
- to determine a self-healing monomer-catalyst system
- to investigate the microencapsulation technology
- to prepare microcapsules and find appropriate methods to analyze the product
- to adjust the microencapsulation method and ingredients to meet the specific needs for the intended application
- to study the microcapsule incorporation in a dental composite matrix
- to examine the adhesion of the capsule shell to the dental host material
- to characterize the new material by mechanical test methods

1.3 Overview of the Dissertation

The present work reports the study of a microcapsule-based self-healing concept that could be applied in dental polymeric composite materials. The literature review in chapter 2 provides information on dental composites and self-healing materials in general. Next to the introduction of the novel epoxy-based dental material some background on common industrial epoxy resins is provided. A more detailed description is devoted to the microcapsule-based self-healing system and its chemistry. Furthermore, microencapsulation procedures are presented with the *in situ* emulsion polymerization technique being outlined. Finally, mechanical characterization methods are introduced that are suitable for studying the behaviour of the dental material after the incorporation of microcapsules.

The experimental section is divided into three chapters with the first part being the most comprehensive. It introduces the preparation process of the PUF/DCPD microcapsules. In addition, influences of the manufacturing parameters on the product properties are discussed. Also, changes in the capsule composition and their effects are described. Furthermore, chapter 3 deals with the evaluation of appropriate analytical methods to characterize the microcapsules. Besides, observations concerning the shelf-life of the microcapsules are reported.

Chapter 4 concentrates on the incorporation of microcapsules in an acrylic dental matrix. During the course of this study the enhancement of the microcapsule shell by the modification with melamine was explored to provide more robust capsules and better adhesion to the matrix resin. This section also outlines the fabrication of mechanical test specimens along with the test procedures. Eventually, mechanical properties of the microcapsule embedded dental material are presented.

In chapter 5 a new idea of a self-healing system that could be applied in an epoxy-based host material is explored. The preparation of the PUF/epoxy

microcapsules is reported next to first trials to incorporate the capsules into an epoxy resin matrix. This approach was mainly intended to examine the possible application in the novel silorane-based dental composite materials.

Finally, chapter 6 gives a summary of important results and conclusions of the research. In addition suggestions for future work are provided.

1.4 Basic Considerations for the Development of a Self-Healing Dental Restorative Material

Microcapsules containing DCPD in a PUF shell were identified to be able to meet the combined requirements on a self-healing dental material. The microcapsule-based self-healing system as described by White *et al.* (2001) consists of a monomer that is stored inside a capsule and a catalyst that selectively reacts with this ‘healing’-monomer. Both compounds are to be embedded in a conventional matrix resin which is in this study a dental composite material. The basic requirements on the self-healing dental system, the specific requirements on the healing monomer, on the corresponding catalyst, and on the microcapsules, in particular the microcapsule shell are outlined in the following sections.

1.4.1 General Requirements on the Self-Healing Composite System

The incorporation of the self-healing system may not have a negative impact on the good chemical, physical, and mechanical properties of the virgin material. For instance, the stability of the dental composite may not be reduced, the good aesthetics of the material should be maintained, and the handling may not be adversely affected. Furthermore, the strength and toughness of the cured self-healing material should be as high as those of the neat material.

1.4.2 Requirements on the Healing Monomer

Sriram (2002) has described some key characteristics for microcapsules in a self-healing polyester matrix material. One important factor he took into account was that the healing agent must be stored inside the microcapsule until it is ruptured by a propagating crack. Hence, it may not react beforehand and must be thermally and chemically stable for a long period of time. In the event of fracture, the healing monomer must easily flow into the crack plane for which low viscosity is required. Besides, it may not polymerize before it is distributed throughout the crack. However, the monomer must come into contact with the catalyst then and readily react to provide healing within an appropriate time frame. If the reaction takes too much time leakage or other side-reactions might occur. Furthermore, the chemistry of the healing resin must show good adhesive characteristics to be able to bond the crack planes and to provide a good adhesion to the matrix resin. It has to be considered that low shrinkage of the healing monomer upon polymerization is highly advantageous for a good adhesion to the matrix as it guarantees that the polymer film does not pull away from the crack surface during curing.

1.4.3 Requirements on the Specific Catalyst for the Healing Monomer

Likewise, the corresponding catalyst must be reactive enough to guarantee a fast polymerization of the healing monomer and complete reaction. It must be able to cure the monomer at ambient temperature which means for oral application approximately 37 °C. Besides, enough catalyst has to be available in the host material which is equally well distributed as the monomer. In addition, the catalyst must be selective as it may not react with the matrix monomers or be deactivated by the matrix curing system. And, it has to be stable for the same time period as the healing monomer. Also, both monomer and catalyst should be cheap and easily available.

Finally, for the application in a dental direct restorative material the compounds must be biocompatible.

1.4.4 Requirements on the Microcapsule Shell

The microcapsule shell must be impervious to leakage and diffusion of the encapsulated monomer to provide an adequate shelf-life (Brown, 2003). Furthermore, for the application of microcapsules in a self-healing dental polymeric system it is necessary that the capsule shell possesses sufficient strength to remain intact during the incorporation process into the host material yet rupture when the material is damaged. Moreover, the outer capsule shell must adhere very well to the matrix resin to avoid flaws that might reduce the physical and mechanical properties of the material. Well-bonded capsules could even increase the fracture toughness of the initial material according to Brown *et al.* (2002 and 2004). Also, a good adhesion is necessary to provide breaking of the capsule shell by an approaching micro-crack. Thus, the microcapsules must feature high bond strength to the host material next to a moderate strength of the microcapsule shell.

CHAPTER II

LITERATURE REVIEW

2.1 Dental Composites

2.1.1 Introduction

The development of dental restorative resin based materials started with the pioneer work of Bowen with monomers in the form of bis-phenol-A dimethacrylates in the 1950s (Bowen, 1956 and 1965). Very soon afterwards the poor properties of the resin matrix were greatly improved by the addition of filler particles which resulted in a new material class, the dental composite (Bowen, 1962). Based on this inventive idea, the first dental composites were launched from Johnson & Johnson (Adaptic) and 3M (Addent 15, Concise) which have been used in dental practices to restore teeth since the late 1960s (Roulet and Meyer, 2006). Some early materials employed polymethylmethacrylate (PMMA) as resin matrix. However, PMMA for this purpose was soon abandoned since Bis-GMA showed superior characteristics such as lower shrinkage, less volatility, decreased toxicity and also resulted in a harder polymeric material.

These first generation composites, however, had many artefacts such as a very rough surface resulting in poor workability and high abrasive wear, colour instability due to the benzoylperoxide-amine curing-system, x-ray invisibility which made the diagnostic of secondary caries difficult and immature bonding to the tooth (Phillips *et al.*, 1971, 1972, 1973). Thus, during the last decades a lot of work has been addressed to enhance the characteristics of the dental composite materials. Great effort has been devoted to the filler which resulted in composites of increased hardness and strength, improved workability, higher radiopacity, as well as reduced polymerization

shrinkage, thermal expansion and water sorption (Li *et al.*, 1985, Braem *et al.*, 1989, Willems *et al.*, 1993, Chen, 2010). A comprehensive review of the greatly improved performance and durability of the composite resin restorative materials *in vivo* is provided by Chadwick (1989). Apart from the works on the improvement of the composite filling material, adhesive systems have been developed that adhere well not only to enamel, but also to the moist dentin (Van Meerbeek *et al.*, 1998, Van Landuyt *et al.*, 2007).

Current dental composites consist of three essential components: a polymeric matrix, reinforcing filler particles such as glass or quartz, and a coupling agent to promote adhesion between organic matrix resin and inorganic filler particles (Rawls and Esquivel-Upshaw, 2003). Other favourable components of dental composites include pigments that help to match the tooth colour whereas ultraviolet absorbers improve the colour stability. Additionally, polymerization inhibitors are used to extend storage life and provide increased working time.

New developments of polymeric composites for restorative filling materials mainly focus on the decrease of the polymerization shrinkage next to the improvement of wear resistance and biocompatibility (Moszner and Salz, 2001). Various research groups have been investigating monomers that show low shrinkage upon curing, in particular monomers that polymerize in a ring-opening reaction mechanism. Bailey and Stansbury for instance have intensively studied spiro orthocarbonates (Bailey, 1990, Stansbury and Bailey, 1990, Stansbury, 1992, Stansbury and Dermann, 1997) for which examples are shown in Figure 2-1, whereas Eick and coworkers (1993, 2005, and 2006) have been investigating the spiro orthocarbonates in combination with conventional epoxy co-monomers such as bisphenol A diglycidylether (BADGE, Fig. 2-1 a) and 3,4-epoxycyclohexylmethyl-3,4-epoxycyclohexane carboxylate (ECHM-ECHC, Fig. 2-1 b). Further work was carried out by Moszner and his group

who concentrated on hybrid 2-vinylcyclopropanes (Moszner *et al.*, 1999); examples of structures are displayed in Fig. 2-3.



Figure 2-1 Spiro ortho carbonates: (a) general structural formula and (b) example of a spiro ortho carbonate as possible compound of a dental composite.

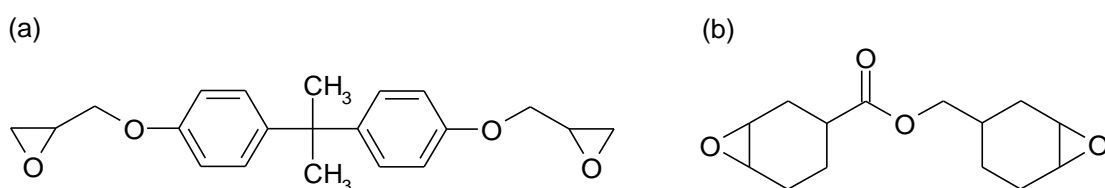


Figure 2-2 Structural formula of two diepoxide monomers that could be part of an epoxy-based dental matrix resin: (a) BADGE and (b) ECHM-ECHC.

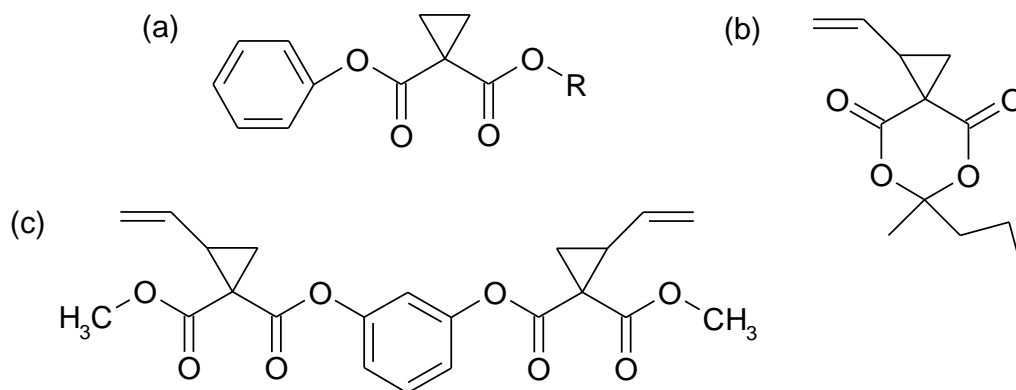


Figure 2-3 Examples of different types of 2-vinylcyclopropane monomers that might be interesting for the application in a novel dental composite matrix: (a) asymmetric substituted, (b) spirocyclic and (c) difunctional vinylcyclopropane.

Other research teams reported new dental monomers containing epoxy functional groups (Tilbrook *et al.*, 2000, Smith *et al.*, 2004) (Fig. 2-2). More advanced systems were studied by Belfield and Zhang (1997) and Guggenberger and Weinmann

(2000) who concentrated on silorane-based monomers. Both of them demonstrated promising matrix resins for dental composites that polymerize in a cationic ring opening polymerization (ROP). Eventually, Weinmann and his group (2002) managed to successfully prepare a dental composite that showed the good characteristics of the conventional radically polymerized materials along with significantly decreased shrinkage upon curing. Their novel silorane-based dental filling material was launched in 2007 (Filtek LS, 3M ESPE) and is the only restorative composite of this type available on the market so far (further details are provided in section 2.1.4).

2.1.2 Acrylate-Based Resin Matrix

The monomer structure of the resin matrix has a significant impact on the polymerization reactivity, water sorption, and fracture mechanics (Kawaguchi *et al.*, 1989, Peutzfeldt, 1997, Rey *et al.*, 2002). Most dental composites use a blend of aromatic and aliphatic dimethacrylate monomers. The hardening of unsaturated organic compounds such as methacrylates occurs via an addition polymerization mechanism (McCabe, 1998). A reactive species is required to initiate the reaction which is in most of the cases a free radical. Free-radical polymerization processes are chain reactions which follow a distinctive pattern as illustrated in Table 2-1.

Addition polymerization reactions generally produce linear polymers. Cross-linking is accomplished by adding cross-linking agents to the polymerizing monomer which provides bridges between the linear macromolecules to form a three-dimensional network (Rawls, 2003). The mixture of cross-linking dimethacrylates in resin-based composite restoratives gives rise to the formation of a polymer network of superior mechanical properties to those of linear polymers. Besides, the resulting highly cross-linked polymer matrix is not water soluble.

Table 2-1 Stages during the chain reaction process of a free radical addition polymerization

Stage	Description	Illustration*
Activation	Formation of radicals by external activation (e.g. radiation, heat)	$R-R^{**} + \text{external energy} \rightarrow 2 R\cdot$
Initiation	Radical reacts with monomer to form an active center	$R\cdot + H_2C=CH_2 \rightarrow RH_2C-CH_2\cdot$
Propagation	Addition of monomer molecules to the active chain end	$RH_2C-CH_2\cdot + H_2C=CH_2 \rightarrow RH_2C-CH_2-CH_2-CH_2\cdot$ $RH_2C-CH_2-CH_2-CH_2\cdot + H_2C=CH_2 \rightarrow RH_2C-(CH_2-CH_2)_2-CH_2\cdot \dots etc.$
Chain transfer	Transfer of active site to another molecule	$RH_2C-(CH_2-CH_2)_x-CH_2-CH_2-CH_2\cdot + H_2C=CH_2 \rightarrow$ $RH_2C-(CH_2-CH_2)_x-CH_2-CH=CH_2 + H_3C-CH_2\cdot \dots and similar$
Termination	Combination of active centers	$RH_2C-(CH_2-CH_2)_m-CH_2\cdot + \cdot CH_2-(CH_2-CH_2)_n-CH_2R \rightarrow$ $RH_2C-(CH_2-CH_2)_m-CH_2-CH_2-(CH_2-CH_2)_n-CH_2R \dots and similar$

* Illustration using ethylene as example monomer

** R-R: initiator, e.g. benzoyl peroxide

2,2-bis-[4-(2-hydroxy-3-methacryloyloxypropoxy)phenyl]propane (Bis-GMA, Fig. 2-4 a) is superior to other dimethacrylates because of its high molecular weight (MW = 512 g/mol) and stiff, partially aromatic molecular structure, providing rapid hardening, low polymerization shrinkage (6.1 v%), low volatility and a cured resin of outstanding mechanical properties (Moszner *et al.*, 2006, Floyd and Dickens, 2006). However, its high viscosity limits the potential filler load considerably. Hence, practically all composites employ next to Bis-GMA a low-viscosity monomer such as tri(ethyleneglycol) dimethacrylate (TEGDMA, Fig. 2-4 b) as a diluents monomer (Sideridou *et al.*, 2002).

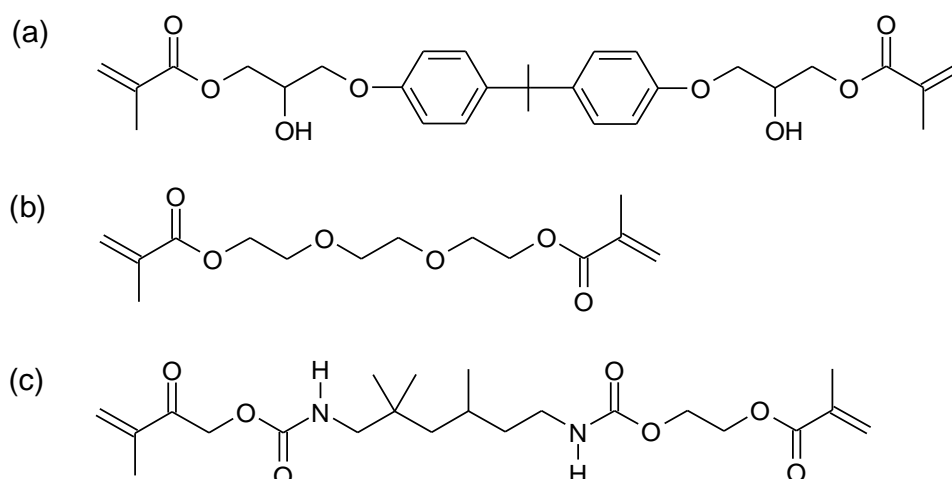


Figure 2-4 Chemical structures of common dental monomers: (a) Bis-GMA, (b) TEGDMA and (c) UDMA.

Further frequently used dental resins are urethane dimethacrylates with the most common type being 1,6-bis-(methacryloyloxy-2-ethoxycarbonylamino)-2,4,4-trimethyl-hexane (UDMA) displayed in Figure 2-4 c. UDMA consists of highly flexible urethane linkages, shows also relatively low polymerization shrinkage (6.5 v%) and additionally a considerably lower viscosity in comparison with Bis-GMA

(Barszczewska-Rybarek, 2009). One of the shortcomings of UDMA is the lower refractive index which significantly decreases the curing depth of composites based on radiopaque glass filler. Table 2-2 provides an overview of important properties of these three most relevant monomers in dental restorative resin matrices.

Table 2-2 Comparison of relevant properties of selected acrylic dental monomers

Monomer	Molecular Weight	Viscosity at 23°C	Refractive Index at 25°C	Polymerization Shrinkage
Bis-GMA	512 g/mol	1000–1200 Pa.s	1.549	6.1 v%
UDMA	470 g/mol	8–10 Pa.s	1.483	6.5 v%
TEGDMA	330 g/mol	0.01–0.05 Pa.s	1.458	>> 6.5 v%

v% = percentage by volume

2.1.3 Curing System for Acrylic Resin

Dental methacrylates polymerize by free-radical addition polymerization mechanism (as it is illustrated in Table 2-1). Free radicals are generated by either chemical activation or through the application of external energy such as heat, light, or microwave. For dental composite filling materials chemical activation or light activation or a combination of both is used (McCabe and Walls, 1998).

Chemical activation of acrylic resins requires a two component system which is supplied as two pastes, one of which containing the initiator benzoyl peroxide (BP) and the other the activator, a tertiary aromatic amine such as N,N-dimethyl-p-toluidine (DMT) or ethyl-p-dimethylaminobenzoate (EDMAB). When the two pastes are mixed together, the amine reacts with the BP to form free radicals which initiate the polymerization (Craig, 1981).

The use of a light-curing initiator system considerably improved the handling of the composite materials as they set on demand. First light-activated systems were formulated for UV light to initiate the free radicals (De Lange *et al.*, 1980). Benzoin alkyl ether was used to generate free radicals upon exposure to light of about 365 nm wavelength to trigger the polymerization.

Today blue-light-activated systems are used which are superior due to its greatly enhanced depth of cure and controllable working time, amongst others (Stansbury, 2000). The initiating system consists of a photosensitizer and an amine which do not interact as long as they are not exposed to light. However, under light exposure the photosensitizer reacts with the amine to form free radicals that initiate the addition polymerization. Camphorquinone (CQ) is a widely used photosensitizer which absorbs blue light with wavelengths between 400–500 nm whereas EDMAB and dimethylaminoethyl methacrylate (DMAEMA) are examples for amine reducing agents (Ferracane, 2001). The most successful and most frequently used types of light sources in daily clinical practice are quartz tungsten halogen lamps (QTH) and light emitting diodes (LED) units (Jimenez-Planas *et al.*, 2008).

2.1.4 Low-Shrinkage Epoxy-Based Resin Matrix

Although acrylic resins exhibit many excellent properties for the application in dental composite materials one major drawback is the shrinkage upon polymerization which challenges the tooth/composite interface (Peutzfeldt, 1997, Lu *et al.*, 2004). According to Weinmann (2005) imperfect margins resulting in marginal staining and eventually secondary caries are the most common reason for the need of replacement of the existing composite filling.

Since the shrinkage of the dental composite system is exclusively caused by the resin part, a lower proportion of resin in a composite decreases the general

shrinkage. Hence, the reduction of the polymerization shrinkage in dental restorative composites has been mainly achieved by the increase of the filler load. In the currently available composites the inorganic filler particles account for 45 to 87 v% in total (Rawls & Esquivel-Upshaw, 2003). Low filled composites like flowable composites exhibit volume reductions upon polymerization in the range of 4–5.5 v%, whereas highly filled systems like packable posterior materials reveal shrinkage values down to 1.7 v%. Table 2-3 summarizes the filler content and volume shrinkage of common acrylate-based dental composite classes which have been evaluated by different research groups (Nagem-Filho *et al.*, 2007, Chiang, 2009, Kuestermann, 2009).

Table 2-3 Volume shrinkage upon polymerization of selected acrylate-based direct restorative composite materials

Material Classification	Description	Filler Content in (wt%)	Shrinkage in (v%)
Flowable composites	Low filled composite	45–67	4–5.5
Hybrid composites	Common highly filled composite system	77–84	1.9–3.5
Nanohybrid composites	Highly packed composite with filler particle size < 0.1 micron	72–87	1.7–3.4
Compomers	Hybrid of dental composite and glass ionomer cement	59–77	2.6–3.4

Next to the increase of the filler load, another strategy to reduce the polymerization shrinkage is the reduction of reactive sites per volume unit. However, the use of high molecular weight monomers is limited by their viscosity, increased stickiness and generally unfavourable handling characteristics of the resulting restorative composite. Hence, recent attempts have been focusing on a change of the nature of the resin, in particular the investigation of lower shrinkage ring-opening

monomer systems. In contrast to the linear-reactive groups of methacrylates which polymerize via addition reaction mechanism, ring monomers such as epoxy compounds harden in an anionic or cationic ROP. The ROP process starts with the cleavage and opening of the ring systems which gains space and counteracts the negative volume change that occurs in the subsequent step, when the chemical bonds are formed (Sadhira and Luck, 1992).

The only ring-opening system successfully applied in a dental composite system from 3M ESPE (Filtek LS) is based on a combination of siloxane and oxirane moieties (Weinmann *et al.*, 2005). The novel silorane-based composite material exhibits shrinkage values as low as 0.79 v% and mechanical properties comparable to the methacrylate-based composites (Weinmann *et al.*, 2002, Eick *et al.*, 2007, Ilie *et al.*, 2006 and 2007, Lien and Vandewalle, 2010). The unique features of the silorane monomer (Fig. 2-5) derive from the hydrophobic cyclosiloxane backbone and the highly reactive cycloaliphatic oxirane sites (Eick *et al.*, 2006). The outstanding reactivity of the oxirane group (equivalent to the term ethylene oxide or epoxy group) is defined by an equilateral triangle which makes it highly strained.

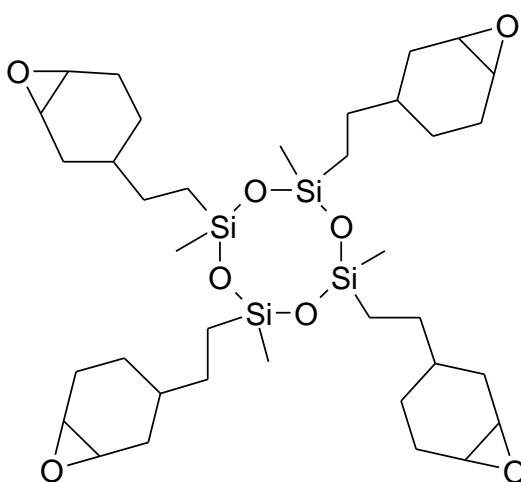


Figure 2-5 Silorane monomer.

The dental photo-activated silorane composite uses a three component initiating system, including CQ as photoinitiator, an iodonium salt and an electron donor such as dimethylaminobenzoate to harden the silorane in a cationic ring-opening reaction (Weinmann *et al.*, 2005).

In general, epoxy resins are a highly interesting alternative to the common acrylate-based dental composite materials since they provide the desirable properties which are: resistance to the aggressive oral environment, good adhesion to the tooth structure, colour stability, high compressive and flexural strength as well as adequate E-modules and hardness (Rawls & Esquivel-Upshaw, 2003).

2.2 Epoxy Resins in Industrial Application

2.2.1 Introduction

Whereas in dental restorative composite materials the curing is mainly initiated by light exposure, in industrial application such as coatings, paints, adhesives, fibre reinforced composites, etc. the use of two-component systems is common practice. The standard hardener comprises amines, polyamides, phenolic resins, anhydrides, isocyanates and polymercaptans with amine curing agents being the most widely used (Ratna, 2005). The most commonly used epoxy resin is the diglycidylether of bisphenol-A (DGEBA); its structure is illustrated in Figure 2-6. The DGEBA resin is available under different trade names such as ‘Epon 828’ or ‘Epikote 828’ from Hexion (formerly Shell Chemicals), ‘DER’ from Dow Chemical Company and ‘Araldite’ from BASF Schweiz AG (formerly Ciba Speciality Chemicals).

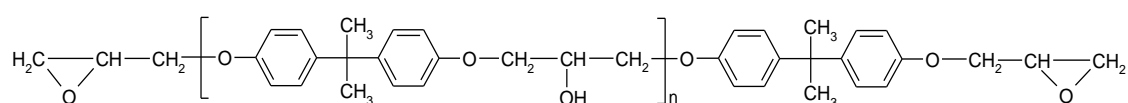


Figure 2-6 Structure of the common epoxy resin DGEBA.

2.2.2 Reactive Diluents

For the application in a dental self-healing filling material it is important that the encapsulated healing agent possesses low viscosity so that it can easily flow into the crack plane upon rupture. To alter the viscosity of epoxy resins reactive diluents are widely used (May, 1988). Besides, the addition of a reactive diluent permits higher filler loading and can therefore lower the polymerization shrinkage and enhance adhesion (Petrie, 2005). Preferably, the diluent should react with the curing agent at approximately the same rate as the resin, contribute substantial viscosity reduction at low concentrations and it should not react with the resin under normal storage conditions. Typical reactive diluents that are widely used in industry include n-butyl glycidyl ether (BGE), cresyl glycidyl ether (CGE), and 2-ethylhexyl glycidyl ether (EHGE), to mention just a few. BGE which is also known under the tradename ‘Heloxy Modifier 61’ (Hexion) produces maximum viscosity reduction (Dewprashad and Eisenbraun, 1994, Zalucha and Abbey, 2007); the structural formula is displayed in Figure 2-7.

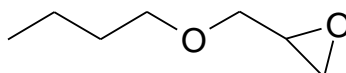


Figure 2-7 Structural formula of BGE which is commonly used in industry as a reactive diluent monomer to reduce the viscosity of epoxy resins.

2.2.3 Curing Agents

Amongst the required properties of the curing agent in a restorative filling material are low viscosity and colour, chemical and water resistance, it should produce rapid hardening of the epoxy resin at low temperatures and show a high degree of chemical cure. Furthermore, the hardener is supposed to provide a cured system of

increased strength, flexibility and toughness along with improved acid and water resistances. Diverse kinds of epoxy curing agents provide these properties, including polyamides, aliphatic amines and cycloaliphatic amines (May, 1988). Details of three different types of hardeners are given in Table 2-4.

Table 2-4 Examples of three different types of epoxy curing agents and their properties

Trade Name	Chemical Composition	Viscosity at 25 °C	Water Solubility
EPIKURE 3223	Diethylene triamine (DETA)	0.71 Pa.s	up to 5g/L
EPIKURE F205	Mixture of benzyl alcohol, isophoronediamine, bisphenol-A polymer with 5-amino-1,3,3-trimethylcyclohexanemethanamine and (chloromethyl) oxirane	0.5–0.7 Pa.s	0.567 g/L
EPIKURE 3140	Mixture of polyaminoamide and triethylenetetramine	13 Pa.s	slightly miscible

2.2.4 Polyaddition Reaction of Epoxide and Amine

When the epoxy resin and amine hardener are mixed together, the active hydrogen of the amine compound reacts with the epoxy group to form a covalent bond (Petrie, 2005). A generalized polyaddition reaction of an amine curing agent and an epoxy molecule is represented in Figure 2-8.

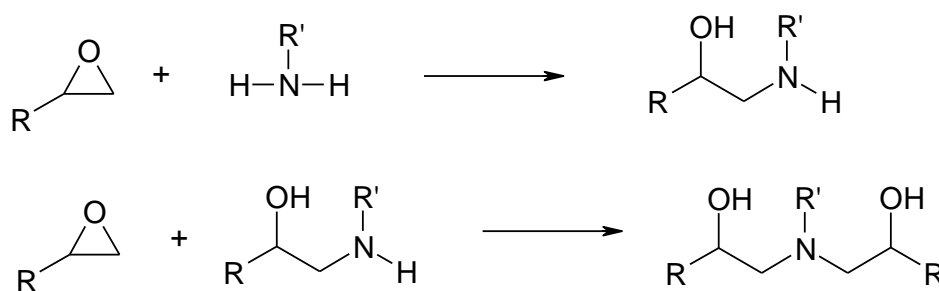


Figure 2-8 Illustration of the polyaddition reaction of an epoxy-amine system.

The curing agent forms part of the final epoxy network, thus the cured structure is a heteropolymer. Typical crosslinking agents are primary or secondary linear amines. Aliphatic amines show higher reactivity than aromatic amines and can therefore be used for hardening at lower temperatures. Diamines can build heavily cross-linked polymer networks as each NH group is able to react with an epoxide group (Fig. 2-9).

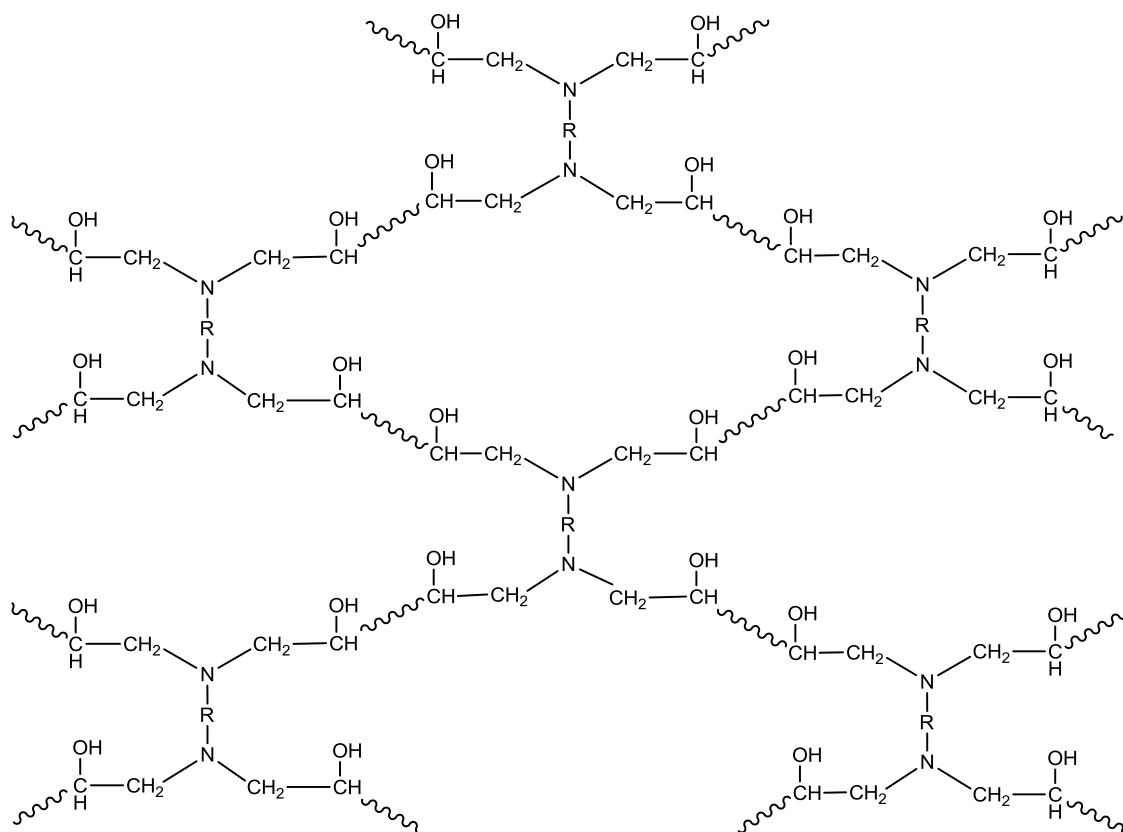


Figure 2-9 Diepoxy molecules and diamine molecules can react and tie together to form a heavily crosslinked polymer network.

The resulting network is chemical and heat resistant, shows very good mechanical and electrical insulating properties, as well as excellent adhesion. The chemistry of epoxies and the variety of commercially available epoxy resin mixtures

allow the production of polymers that suit almost any application. Epoxies can be made flexible or rigid, transparent or opaque coloured, fast setting or extremely slow setting. Various compounds can be employed to modify the properties of the epoxy-based material such as flexibilizers, tougheners, fillers, heat-resistant additives, thixotropic agents, defoaming agents, pigments, and diluents (Abuin, 2010). Hence, the range of application is extensive and includes paints, coatings, fibre and fibreglass reinforced composite materials. Epoxy resin materials are widely used in electronics industry and are known to be exceptional adhesives for wood, metal, glass, stone, and some plastics.

2.3 Self-Healing Polymeric Materials

2.3.1 Introduction

Polymers and polymer composites are often exposed to small scale damage, especially if they have to withstand strong impact. Damages in the form of cracks could significantly reduce the performance and useful lifetime of the polymeric material. Micro-cracks usually build deep within the structure of the material where they cannot be noticed and repaired on time by manual intervention. Reliance on polymeric materials in various fields and the need for improvement of the material performance has spurred several groups of researchers into action and led to the development of self-healing systems (Kessler, 2007, Wu *et al.*, 2008, Syrett *et al.*, 2010, Samadzadeh *et al.*, 2010).

A key focus of scientific research in the field of self-healing materials is the mimicking of biological systems in which damage triggers instantaneously and subconsciously a healing response (Trask *et al.*, 2007). The concept of a natural self-repairing system can be expressed in many familiar examples such as the grazing of the knee or cutting the finger. Blood would immediately rush to the side of the injury,

clot and finally the bleeding stops forming a scab over the damaged surface. Eventually, the scab falls off revealing new skin.

Inspired by this idea researchers from different fields have recently developed techniques for achieving self-healing functionality in polymeric materials. For instance, Dry (1996), Li *et al.* (1998), Motuku *et al.* (1999), Bleay *et al.* (2001), Pang and Bond (2005), and Thao *et al.* (2009) all reported the incorporation of glass fibres containing a healing system into the origin material. Upon crack intrusion the resin system (e.g. a two-part system) would simultaneously distribute in the crack plane and then react to polymerize and therefore ‘heal’ the crack. A similar approach was followed by researchers using spherical capsules that are filled with a healing monomer (Ni *et al.*, 1995, Hong and Park, 2000, White *et al.*, 2001, Cho *et al.*, 2006, Yuan *et al.*, 2008). The capsules were dispersed throughout the matrix material next to a corresponding catalyst which would initiate the polymerization of the released healing compound. Furthermore, Toohey and colleagues (2007 and 2009, Hansen *et al.*, 2009) demonstrated a self-healing system capable of repairing repeated damage events. Their bio-inspired coating-substrate design delivers the healing agent to cracks via a three-dimensional microvascular network embedded in the substrate.

Other approaches were made by Chen and co-workers (2002) who showed that polymeric materials possessing selective cross-links between polymer chains that can be broken under load and then reformed by heat offer healing efficiencies of 57% of the original fracture load. A similar motif was followed with a polymeric material hosting a second solid-state polymer phase that migrates to the damage site under the action of heat (Zako and Takano, 1999, Hayes *et al.*, 2006). Even though these systems provide the capacity for self-healing they require damage sensing and heating which is practically not applicable. A very different technique was investigated by Lee and his team (2005) with the use of nanoparticles dispersed in polymer films to deposit at a

damage site. Later work by Gupta and colleagues (2006), using fluorescent nanoparticles, has shown that selected ligands on these particles can help to direct the nanoparticles into a crack in a microelectronic thin film layer.

2.3.2 Microcapsule-Based Self-Healing Concept

Most of the works on self-healing materials as illustrated beforehand were primarily conceptual in nature and did not provide a substantial evidence of self-healing ability in the material. However, a very interesting and probably the most advanced approach is being followed by aeronautical engineers at the University of Illinois, US, who could also proof the self-healing ability of their system with excellent results (White *et al.*, 2001). They reported that the addition of urea-formaldehyde (UF) microcapsules filled with dicyclopentadiene (DCPD) as the ‘healing’ agent and a corresponding catalyst (e.g. Grubbs catalyst) significantly toughened the structural composite material with the critical load for virgin self-healing samples being up to 27 per cent higher than the control samples (without capsules and catalyst). Moreover they demonstrated recoveries of about 90% of the virgin fracture load (Brown *et al.*, 2002, Kessler, 2007).

Their system includes UF/DCPD microcapsules which are embedded in the polymeric matrix material along with a selective catalyst (Fig. 2-10 a). In the event of a crack the microcapsule shell will break and release the DCPD which distributes into the crack plane by capillary forces (Fig. 2-10 b). Finally, the healing monomer reacts with the catalyst to bond the crack (Fig. 2-10 c).

This self-healing system can be applied in any polymer and composite providing structural materials of longevity. Among others the use in dental materials seems highly attractive as the improvement of crack-resistance in dental restorative composite fillings is still of significant importance (Wool, 2001, Yuan *et al.*, 2008).

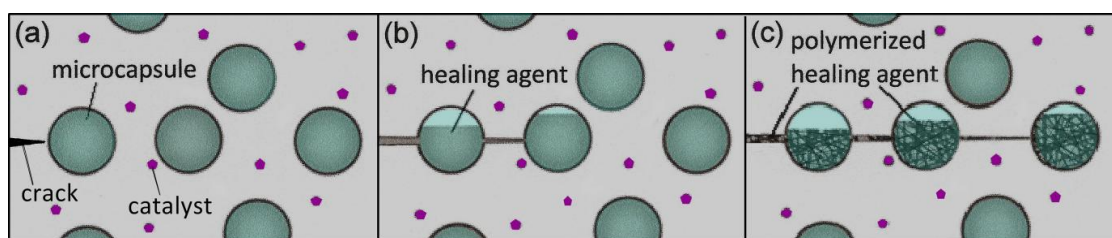


Figure 2-10 Illustration of a self-healing approach: (a) microcapsules filled with a healing monomer and a selective catalyst embedded in a dental host material; (b) an approaching crack ruptures microcapsules, releasing the healing monomer into the crack plane; (c) contact of the healing monomer with the catalyst, triggering polymerization and mending the crack.

2.3.3 The Healing-Compound

The requirements on the healing monomer are described in section 1.4.2. DCPD is a monomer that can meet these requirements as it possesses a long shelf life, low volatility, is able to rapidly polymerize at ambient conditions and shows low polymerization shrinkage. In addition, DCPD is cheap and easily available (Klosiewicz, 1983). The melting point of DCPD is approximately 32–34 °C. In liquid form it shows rather low viscosity and therefore the DCPD monomer could easily flow out of the microcapsules upon crack intrusion to fill the crack plane.

2.3.4 Ring-Opening Metathesis Polymerization (ROMP)

If DCPD comes into contact with a transition-metal alkylidene complex such as the Grubbs type catalysts it can solidify by a ring-opening metathesis polymerization (ROMP) (Grubbs and Tumas, 1989). Generally, in metathesis reactions, double bonds between carbon atoms are broken and reformed in a way that causes the atoms to change places. The ROMP is one variation of the metathesis reaction. It involves a molecule which contains a carbon-carbon double bond constrained in a ring structure such as DCPD. During ROMP, the double bond of the ring undergoes metathesis in which the double bond is cleaved and the ring opens up to form acyclic molecules

containing double bonds (Chauvin, 2006). This process is repeated many times to result in a high molecular weight polymer.

The driving force of chain growing is the relief of ring strain (Manners, 1995). Therefore, the ring that possesses the highest ring angle strain opens first which is displayed in an example of DCPD in Figure 2-11 where the double bond on the C-8 atom opens first in the presence of a subgroup element catalyst. The less strained double bond on the C-3 atom can only react afterwards induced by a strong catalyst (Grubbs, 2003).

The polymerizability of cyclic olefins is dependent on the size of the ring and the content of hetero atoms in functional groups since the latter can lower the activity of the ROMP-catalyst (Watkins *et al.*, 1994). Thus, the highest activity can be achieved if there are no hetero atoms in the monomer which is the case for DCPD.

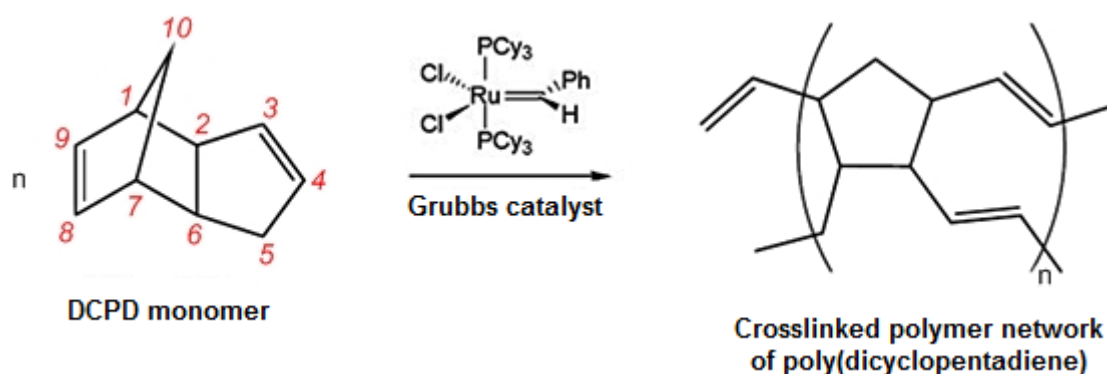


Figure 2-11 ROMP of DCPD creating a crosslinked polymer network of poly(dicyclopentadiene) (pDCPD).

2.3.5 ROMP Catalysts

Olefin metathesis only occurs in the presence of metallic catalysts of certain subgroup elements such as titanium, molybdenum, tungsten, ruthenium, osmium, rhodium, iridium, etc. (Osborn and Schrock, 1971 and 1976, Fogg *et al.*, 2007). The

polymerization of the ROMP monomer precursors can be effectively initiated by transition-metal alkylidene complexes like the Schrock, Grubbs, and Hoveyda catalysts (Schwab, *et al.*, 1996, Schrock and Hoveyda, 2003). The tungsten and the molybdenum-based Schrock catalysts show generally very good reactivity for metathesis reactions (Wengrovius, *et al.*, 1980, Feldman and Schrock, 1991, Schrock, 1990 and 2006). Unfortunately, they are rapidly deactivated when exposed to ambient conditions (Trnka and Grubbs, 2000). The very reactive ruthenium-based Grubbs catalysts of the first generation (Fig. 2-12 a) as well as analogue iridium and osmium compounds can tolerate functional groups and also show better tolerance for water and air (Grubbs and Chang, 1998, Huang *et al.*, 1999). However, Iridium and Osmium are impracticable due to their high costs.

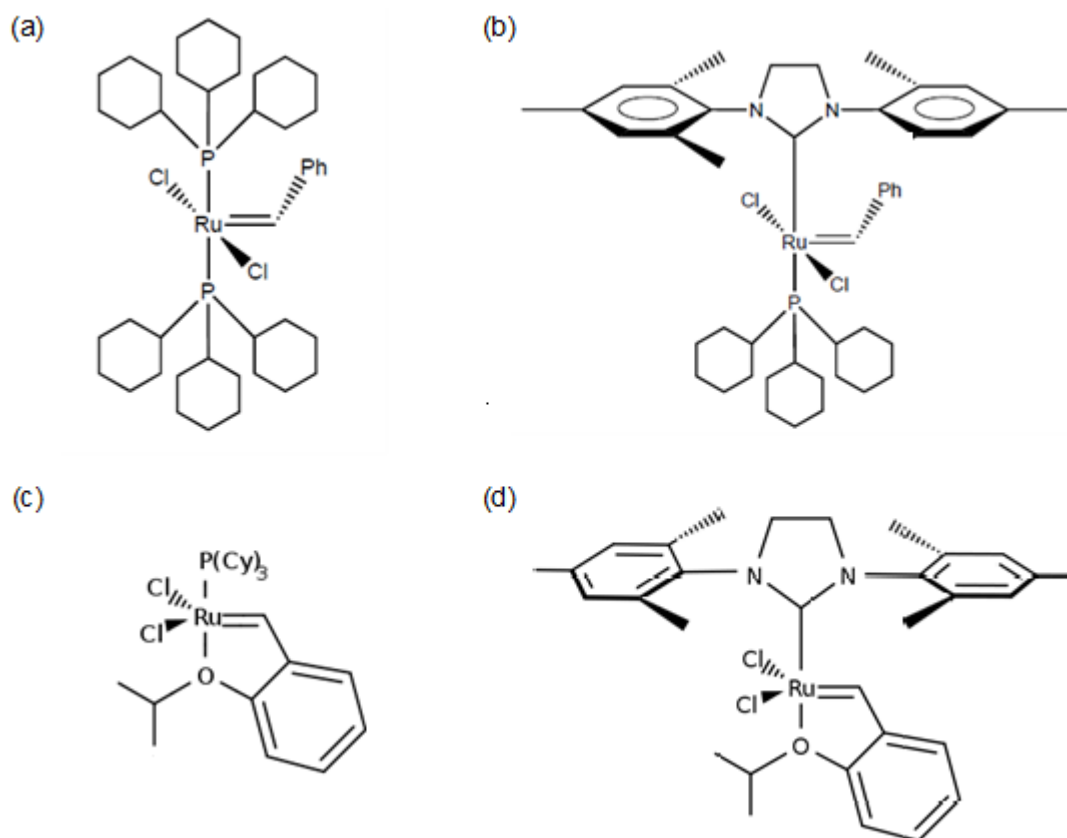


Figure 2-12 ROMP catalysts: (a) Grubbs 1st generation, (b) Grubbs 2nd generation, (c) Hoveyda-Grubbs 1st generation, and (d) Hoveyda-Grubbs 2nd generation.

Hence, Grubbs and his group addressed a lot of work to further enhance the properties of the ruthenium ROMP catalysts and developed a series of systems containing N-heterocyclic carbene ligands (Grubbs and Trnka, 2005, Grubbs, 2006). These so called second generation Grubbs catalysts (Fig. 2-12 b), as well as the Hoveyda-Grubbs catalysts (Fig. 2-12 c and d) show excellent metathesis activity with a high tolerance to a wide range of functional groups as well as oxygen and water (Scholl *et al.*, 1999, Hoveyda, 2008, Leitgeb *et al.*, 2010). Hence, they are most suitable for the application in a self-healing dental system as they can effectively produce self-healing and are sufficiently stable. Furthermore, Grubbs type catalysts can polymerize ROMP monomers such as DCPD quickly at room temperature once delivered into a crack plane (Rule, 2005).

2.4 Microencapsulation

2.4.1 Introduction

Microencapsulation means to enclose liquid drops or solid particles to obtain small containers that are spherical or irregular in shape with typical diameters ranging from 1 to 1000 μm . The process of microencapsulation was discovered and developed by Barrett K. Green from Ohio, US, in the 1940s (Green, 1957). He synthesized gelatine microcapsules in an oil-in-water emulsion system. Around 1950 Green and Schleicher introduced capsules containing dyes which were incorporated into paper for copying purposes (Green and Schleicher, 1953). This invention was successfully commercialized and already in 1974 the industrialized countries used about 500,000 tons of this carbonless paper which is equivalent to 50,000 tons of microcapsules (Sliwka, 1975).

Since then a lot of information on the manufacture of microcapsules has been stored in patents which shows the importance of this technique (e.g. Morishita *et al.*,

1976, Hayworth, 1985, Scher and Rodson, 1990, Janda *et al.*, 1995, Sumii and Yoshimura, 1996, Moy, 1998, Jordan *et al.*, 2000, Chao, 2002, Inui and Shigemura, 2004). Today, microencapsulation techniques are applied in diverse fields including medicine, biotechnology, food, agriculture and in different areas of the chemical industry. It involves many engineering skills and scientific disciplines.

2.4.2 Encapsulation Techniques

Several encapsulation techniques are available for the preparation of microcapsules depending on the type of material that is supposed to be encapsulated as well as the field of application (Ranney, 1969). For instance, the shell can be of natural or synthetic polymers and might be impermeable, permeable or semi-permeable; whereas the core materials could be gaseous, liquid, solid, or might be themselves an emulsion or suspension (Benita, 1996).

In general, the process of microencapsulation can be categorized into two groups: chemical processes and physical processes. The latter might be subdivided into physico-chemical and physico-mechanical techniques (Arshady, 1999). Examples of important microencapsulation techniques are summarized in Table 2-5. It has to be noted that some processes classified as mechanical technique can involve a chemical reaction, and some chemical techniques rely on physical events.

Although a huge variety of microencapsulation techniques is available, no single method is suitable for encapsulating different types of core material (Ghosh, 2006). The most suitable method depends on factors such as the type of the core compound and shell material, the desired particle size and other different required properties of the microcapsule. For instance, the diverse encapsulation techniques can produce capsules of certain diameters only as outlined in Table 2-6. Ultimately, the

microencapsulation process must be custom-tailored to achieve the desired product performance (Jyothi *et al.*, 2009).

Table 2-5 Different important microencapsulation techniques

Chemical Processes	Physico-Chemical Processes	Physico-Mechanical Processes
<ul style="list-style-type: none"> • Emulsion polymerization (e.g. oil-in-water and water-in-oil emulsion, miniemulsion) • Suspension polymerization • Dispersion polymerization • Interfacial polycondensation 	<ul style="list-style-type: none"> • Coacervation (simple and complex coacervation) • LBL (layer-by-layer) assembly of electrically charged particles • Sol-gel encapsulation • Phase separation • Supercritical fluid-assisted techniques: RESS[*], GAS^{**}, PGSS^{***} 	<ul style="list-style-type: none"> • Spray drying • Spray congealing • Spinning disk • Extrusion (e.g. co-extrusion, centrifugal extrusion, stationary nozzle, vibrating nozzle) • Fluidized bed coating (top, bottom, and tangential spray) • Pan coating

* *Rapid Expansion of Supercritical Solutions*

** *Gas anti-solvent*

*** *Particles from gas-saturated solution*

Table 2-6 Examples of possible particle sizes that can be produced by certain specific encapsulation techniques

Micoencapsulation Technique	Particle Size in (µm)
LBL assembly (polyelectrolyte multilayer)	0.02 – 20
Miniemulsion	0.1 – 0.5
Sol-gel encapsulation	1 – 20
In-situ polymerization, interfacial polymerization, solvent evaporation, coacervation, phase separation	0.5 – 2000
Spinning disk	5 – 1500
Spray drying, spray congealing	5 – 1000
Fluid bed coating	20 – 5000
Extrusion	1 – 5000
Pan coating	600 – 5000

2.4.3 Microencapsulation by *in situ* Emulsion Polymerization

The microcapsule synthesis by *in situ* oil-in-water emulsion polymerization requires vigorous agitation of the reaction slurry to obtain tiny droplets of the oil phase. The capsule shell forms around these droplets at the interface of the emulsion. For the preparation of UF/DCPD microcapsules, DCPD is suspended in an aqueous phase and droplets of the monomer are produced by continuous stirring. Urea and formaldehyde polymerize then around these droplets. The urea and formaldehyde first form a prepolymer when they mix in water. As the prepolymers gain molecular weight they move to the interface of the water and the DCPD droplets (Brown *et al.*, 2003). Eventually, these prepolymers cross-link to form a smooth microcapsule shell (Fig. 2-13). Higher molecular weight UF particles deposit around the smooth shell layer creating a rough outer surface.

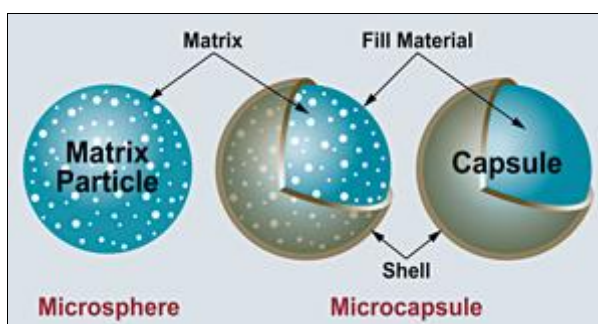


Figure 2-13 Droplets of the core material built by vigorous agitation; the shell materials move to the interface and react to form the shell around the microsphere (retrieved from <http://www.swri.org/3pubs/BROCHURE/D01/mne.htm>, 09-09-2010).

The agitation rate has a direct influence on the microcapsule diameter and thus can be adjusted to obtain the desired size range. A higher agitation rate would result in capsules of a smaller diameter and the other way around. Generally, by using the *in situ* emulsion microencapsulation technique capsule diameters of 10 to 1000 μm can

be produced with agitation rates varying from 200 to 2000 rpm. On average these UF/DCPD microcapsules contain 83–92 wt% DCPD and 6–12 wt% UF.

2.4.4 Urea Formaldehyde Shell Formation by Condensation Polymerization

UF polymers are produced in a highly exothermic reaction which takes place in two stages (Pizzi, 1994). In the first stage, urea is hydroxymethylated by the addition of formaldehyde to the amino group of urea. This step includes a series of reactions that lead to the formation of monomethylolurea, dimethylolurea, and trimethylolurea (Fig. 2-14) in an estimated ratio of 9:3:1, respectively (Pizzi, 1989). Tetramethylolurea has not been observed.

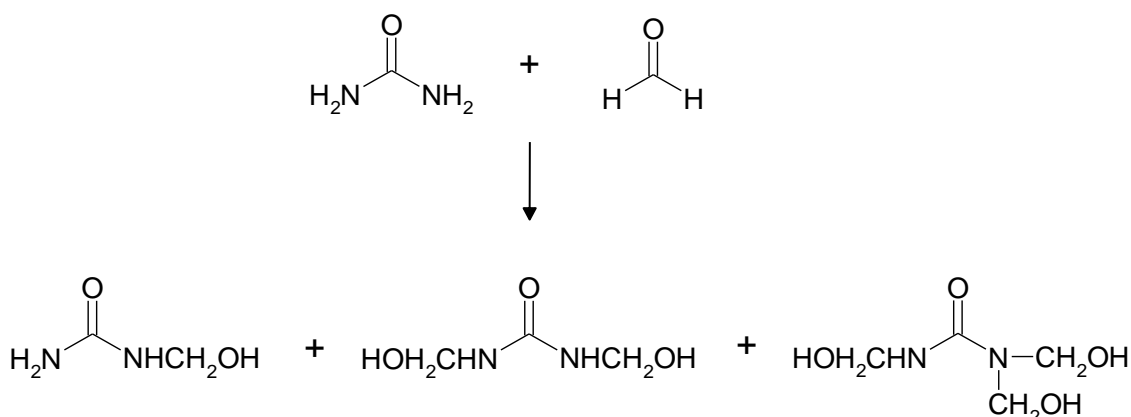
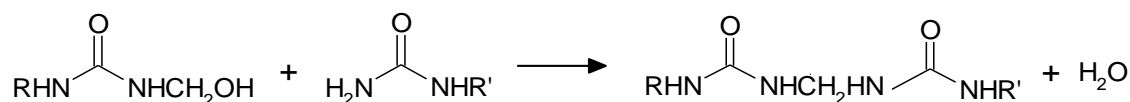


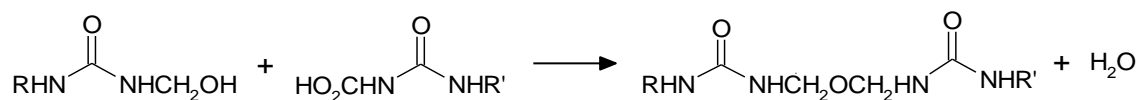
Figure 2-14 Formation of mono-, di-, and trimethylolurea by the addition of formaldehyde to urea in the first stage of the UF resin formation.

The second stage of the UF resin formation consists of condensation reactions of the methylolureas and the concurrent elimination of water resulting in low molecular weight condensates (Conner, 1996). Higher molecular weight oligomers and polymers are obtained by further condensation. The increase in the molecular weight to produce higher molecular weight products includes a combination of the following reactions:

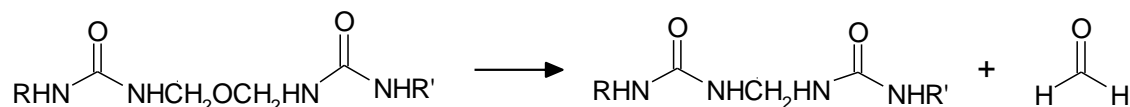
- (a) the reaction of methylol and amino groups of the reacting molecules leading to methylene bridges between amido nitrogens,



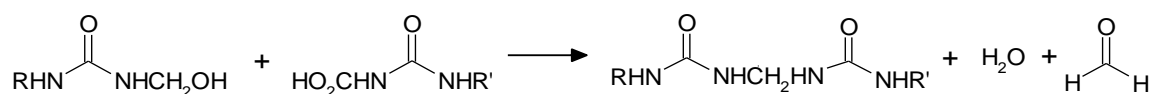
- (b) two methylol groups react to build methylene ether linkages,



- (c) the splitting out of formaldehyde from methylene ether linkages resulting in methylene linkages, and



- (d) the reaction of methylol groups in which water and formaldehyde are split out and methylene linkages are obtained.



The condensation reaction of methylolurea in the second stage requires an acidic pH whereas the precedent addition takes place over the entire pH range, however, the reaction rate is dependent on the pH. The urea-formaldehyde molar ratio used in industrial applications is commonly in the range of 1:2.0 to 1:2.4 (Pizzi, 1994, Christjanson *et al.*, 2006). Being aware of the health risks associated with

formaldehyde there is a general interest in reducing the formaldehyde content in these materials (Wijnendaele *et al.*, 2010). However, a decrease in the formaldehyde amount could have a negative impact on the characteristics of the polymeric material.

2.4.5 Urea-Melamine-Formaldehyde (UMF) Resin

Melamine (triamino-s-triazine) can polymerize with formaldehyde in a similar way to urea. First, methylol derivatives are generated that can contain up to six methylol groups (Allock *et al.*, 2003) as illustrated in Figure 2-15.

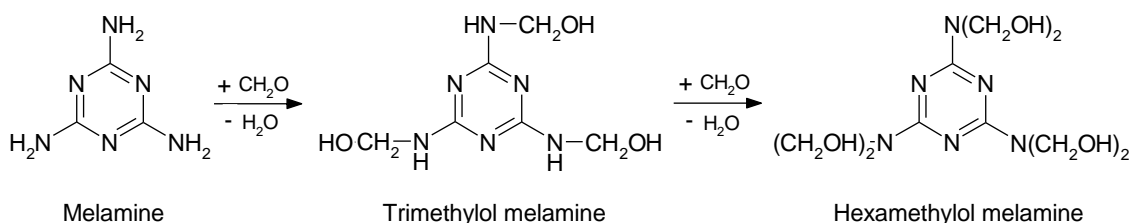


Figure 2-15 Illustration of the addition of formaldehyde to melamine to form methylol derivatives, e.g. trimethylol melamine and hexamethylol melamine.

In alkaline media melamine can react already at low temperatures very fast to hexakis(hydroxymethyl) melamine commonly referred to as hexamethylol melamine. Condensation of the methylol units can then occur via the formation of methylene or methylene-ether linkages, eventually resulting in a highly cross-linked polymer (Fig. 2-16).

Melamine-formaldehyde (MF) resins are, like UF resins, clear and colour stable. They are widely used in the manufacture of moulding compositions such as electro-insulating components (e.g. plugs, light switches, sockets), kitchen utensils (e.g. tableware) and other household utensils (e.g. plastic handles). Furthermore, MF

resins are applied as agents for paper and textile treatments, in wood products, adhesives and coatings. They are superior to UF materials especially in terms of durability as MF compounds are more resistant to water and heat (Pizzi, 1994). However, MF resins are more expensive in comparison to UF resins (Bono *et al.*, 2003). Therefore, blends are commonly used to enhance the properties of the UF material. UMF resins, for instance, can provide increased surface hardness and strength rather than the neat UF material, and they show lower volume contraction than the pure MF material (Hellerich *et al.*, 1996).

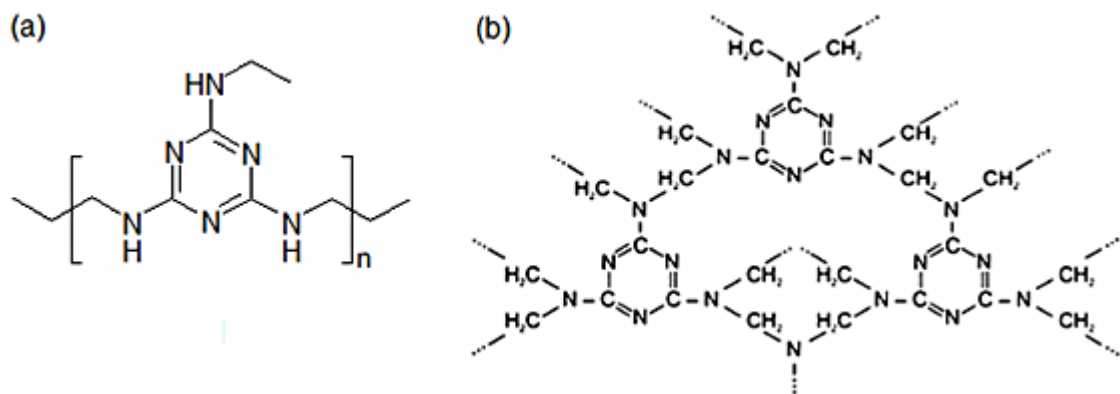


Figure 2-16 (a) Simplified representation of the melamine polymer and (b) possible network structure.

2.5 Mechanical Testing of Dental Material

2.5.1 Introduction

The clinical performance of dental restorations is best judged on the basis of long-term clinical trials. As this is not always possible mechanical test methods are applied to characterize the properties and behaviour of materials. One important factor is the strength of a material which represents the ability to resist induced stress without fracture or deformation. Whereas reversible deformation can be expressed in the

modulus of elasticity, permanent deformation might be defined in a hardness test, and a combination of elastic and plastic deformation in the measurement of toughness (Anusavice, 2003).

Generally, in fundamental research it is important to comprehend the chemical and physical properties of compounds. When these compounds are then applied it is necessary to understand whether the resulting material can meet the favoured properties for the particular application. For the development of a self-healing dental composite material the measurement of certain mechanical parameters is necessary to ensure that the good quality of the initial material can be maintained after the incorporation of the capsules. It is also possible that the addition of microcapsules to a polymeric matrix could help to increase its fracture toughness next to its function as self-healing system. For instance, Yuan *et al.* (2009) reported that the strengthening behaviour of microcapsules has been even more beneficial than that of solid particles.

To better understand how certain test methods are related to the performance of the material when applied it is helpful to have the basic knowledge on the mechanical test method and the data obtained. Therefore, some significant mechanical measurements and parameters for the characterization of a dental restorative filling material are described in the following sections which are:

- flexural strength,
- modulus of elasticity,
- toughness, and
- hardness.

2.5.2 Flexural Strength

Dental materials are often subject to tensile stress. Tensile stress is caused by a load that stretches a body but it can also be generated when structures are flexed.

Hence, to characterize the strength of a material, test samples are often exposed to flexural loading. For instance, the flexural strength or bending strength can be measured in a three-point-bending test where a test bar is supported at each end and a load is applied to the centre of the test rod as demonstrated in Figure 2-17 a. The maximum force needed to fracture the sample is normally used to characterize the strength of the material (Figure 2-17 b). A sample that reveals high strength values is referred to as a strong material whereas low values indicate a weak material (Schwarz, 1992).

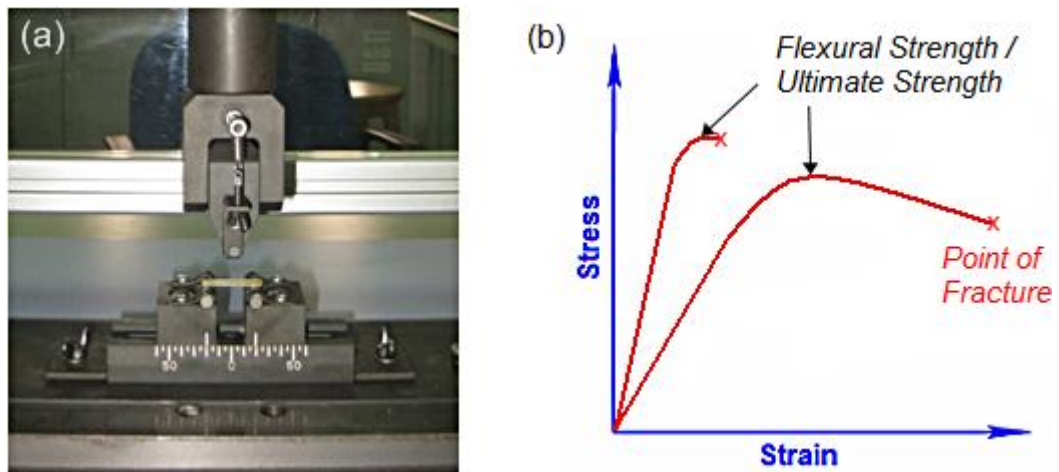


Figure 2-17 Illustration of (a) a three-point-bending test set-up and (b) the flexural strength data obtained from the measurement in a stress-strain diagram.

The flexural strength is also termed flexural stress or ultimate strength and can be calculated according to the following equation:

$$\sigma = 3 F l / 2 b h^2$$

where

- σ is the maximum stress in [Pa],
- F is the applied force or maximum load in [N],
- l is the distance between the supports in [mm],
- b is the width of the specimen in [mm], and
- h is the height or depth of the specimen in [mm].

According to the International System of Units (SI, 'Système Internationale d'Unités') the flexural strength is expressed in megapascal (MPa). The preparation and requirements for the flexural strength measurement of dental polymer-based restorative materials is standardized in the specifications from the International Standard Organization (ISO 4049:2000) and the American Dental Association (ANSI/ADA 27:1993).

2.5.3 Modulus of Elasticity

Another important property for the characterization of dental materials is the modulus of elasticity which gives an indication of the relative stiffness or rigidity of a material (Franck, 1996). It describes the tendency of a substance to be non-permanently (elastic) deformed when a force is applied. If the force is removed the strain may be recoverable so that the material returns to its original length or, in the opposite case the material stays deformed. Most of the materials are partially recoverable. The extent of recovery gives information about the elastic properties of materials. A high modulus (steep slope) implies a rigid material while low values are obtained from flexible materials (McCabe, 1998).

Mechanical testing machines often record automatically the strain as a function of stress and calculate the modulus of elasticity from the slope of the straight line

region (Fig. 2-18) which represents the reversible elastic part. Strain refers to the change in dimension when a force is applied on a test specimen. Thus, its numerical value is expressed by the change in length over the original length and therefore has no physical dimensions. The unit of the modulus of elasticity is Newton per square meter (N/m^2) or Pascal (Pa) and it is defined by the Hooke's law:

$$\lambda = \text{Stress} / \text{Strain}.$$

If the modulus of elasticity is calculated from a tensile test such as the three-point-bending test it is often referred to as Young's modulus or simply as elastic modulus. That means, the Young's modulus describes the tendency of an object to deform along an axis when forces are applied along that axis and therefore it is specified as the ratio of tensile stress to tensile strain. Other types of elastic moduli include the bulk modulus (volumetric elasticity) and the shear modulus which can be derived from viscosity or rheological measurements.

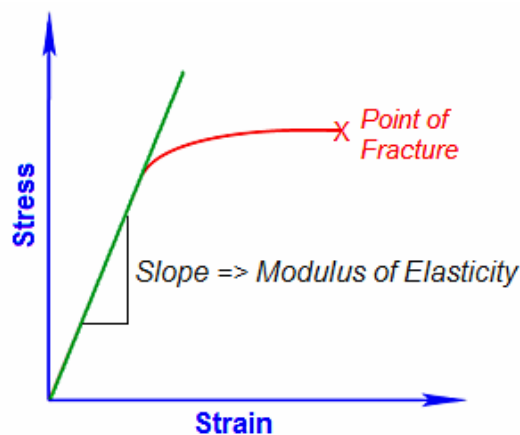


Figure 2-18 Calculation of the modulus of elasticity from the slope of the linear part of the stress-strain graph.

2.5.4 Toughness

Whereas strength indicates how much force a material can support, toughness indicates how much energy a material can absorb before it ruptures and is therefore a measure of resistance to breaking (Allcock *et al.*, 2003). A high amount of energy refers to a very tough material. On contrary, if the amount of energy absorbed is low the material is brittle. One way to measure toughness is by calculating the area beneath the stress-strain curve from a tensile test as it is illustrated in Figure 2-19.

The fracture toughness values can not only be obtained from a three-point-bending test but can also be calculated from impact test measurements such as the Charpy impact test. As the toughness expresses the energy of the mechanical deformation per unit volume prior to fracture its unit is Joule per cubic metre (J/m^3).

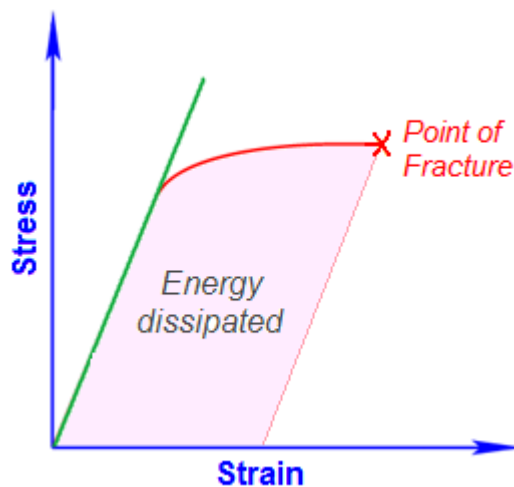


Figure 2-19 Fracture toughness measured as the total area under a plot of tensile stress versus tensile strain.

2.5.5 Hardness

Hardness is a characteristic of a solid material that expresses its resistance to deformation which can result from indentation, scratching, cutting or bending. Friedrich Mohs standardized the first hardness test method in 1822 and classified it

into various hardness scales (Tabor, 1951). His principle was based on scratching and is defined as the resistance to fracture or permanent deformation due to friction from a sharp object. Later, at the beginning of the 19th century, static indentation hardness tests using a spherical indenter were introduced by Brinell (1900) and Meyer (1908). A dynamic indentation test method followed soon afterwards by Shore (1918) in which the hardness is expressed in terms of the energy of impact and the size of the remaining indentation. In 1922, Smith and Sandland, engineers at the Vickers, Sons & Company Ltd. (United Kingdom), developed an indentation test that employed a square-based pyramidal indenter made from diamond, which became well known as so called 'Vickers' test method (Lloyd and Jeffrey, 1947).

Up to now hardness measurements follow the principles of either scratching or indentation (Zimmermann, 1991, Marxkors and Meiners, 1998). Especially indentation hardness measurements are nowadays widely used in industry for the quality control of plastic materials because they are quick and easy to carry out (Bell and Thwaited, 1999). If the resistance to plastic deformation is due to a constant load from a sharp object it is referred to as indentation hardness. The indentation hardness can be subdivided into static and dynamic methods (Tabor, 1951). While the static operation is defined by the extent of an impression that is left after a test probe was applied to the material, during the dynamic process usually the loss of energy is determined.

A selection of common types of indentation tests together with the main field of application is listed in Table 2-7. Standard hardness measurement methods to characterize dental resin-based materials are Vickers, Knoop, Shore, and Brinell which mainly distinguish from the shape of the indenter (Koerber and Ludwig, 1993). Indentation hardness can be measured on macro-, micro- and nano-scale. For dental composites the micro hardness and nanoindentation hardness methods are applicable as the measurements are more precise and can distinguish small variations that might

have a significant impact when applied. In addition, the latest microhardness and nanoindentation hardness testers allow the automatic calculation of other material properties such as elasticity and indentation work (toughness) next to the hardness number.

Table 2-7 Common methods for the determination of indentation hardness

Method	Abbreviation	Application
Shore	Shore A Shore D	Soft polymers, elastomers, rubbers Hard elastic materials
Vickers	HV	Hard and uniformly composed materials, tooth structure-like dental materials
Knoop	HK	Plastics, brittle materials, any dental restorative material
Brinell	HB	Soft to medium-hard materials, metallic dental materials
Rockwell	HRA, HRB, HRC	Metal sheets, metallic dental materials
Barcol	BH	Glass fibre reinforced plastics (GRP)
Janka	-	Wood
Martens	HM	Metals

The SI describes the kilopond (kp) as the unit of force rather than Newton (1 N = 0.102 kp). But most of the hardness values are expressed unit-free such as the Vickers hardness being express by ‘HV’ instead of using its unit kp/mm^2 (Strickling, 1988, Eichner and Kappert, 2005).

2.5.5.1 Vickers Microhardness

Macroindentation refers to methods that use an applied kilogram force of 1 kgf or more whereas in microindentation hardness testing the test load ranges from 1 to

1000 gf. Microhardness measurements can be performed when the volume of the material to be measured is restricted. Commonly Vickers or Knoop indenters are employed.

The Vickers test method was developed to overcome the disadvantages of the Brinell method which means that harder materials can be tested and the indentation is smaller and therefore less damaging (Strickling, 1988). The microhardness Vickers test has become standard practice for industrial quality control that requires measurements of metals and hard polymeric materials. Typical examples are wire materials, electronic parts, thin samples like razor blades and metal foil, small precision devices such as parts for clocks, sewing machines, and optical instruments, next to artificial teeth and artificial bones. Another common application is in research and development as this technique allows hardness measurements of all types of materials.

During the Vickers microhardness measurement the pyramid-shaped diamond indenter (Fig. 2-20 a) with an angle of 136° is forced into a test surface under controlled loading conditions (Marxkors *et al.*, 2008). Upon removal of the load the size of the impression produced is measured under a microscope. An example of a typical imprint is displayed in Figure 2-20 b.

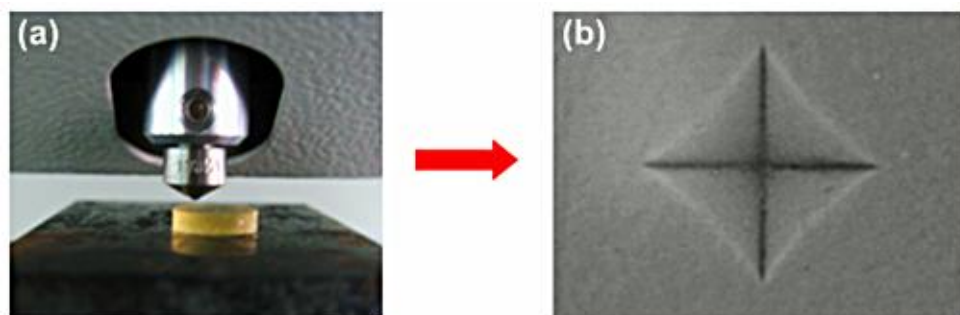


Figure 2-20 Images of a microhardness measurement showing (a) the Vickers indenter placed above a test specimen and (b) a micrograph of an indentation imprint on a dental polymeric material produced by a Vickers indenter.

The Vickers hardness number (HVN) is the number obtained from dividing the applied load by the surface area of the indentation. The latter is calculated from the mean of the measured diagonals of the indentation according to the following equation:

$$\text{HVN} = F / A_s = 2 F \sin(\alpha/2) / d^2 = 1.8544 F / d^2 ,$$

where

F is the maximum load in [kgf],

A_s the surface area of indentation in [mm²],

d the mean diagonal of indentation in [mm], and

α the face angle of indenter = 136°.

2.5.5.2 Nanoindentation Hardness

Although microindentation testing methods are still accepted and used, some claim that they no longer meet the requirements of modern hardness testing (Oliver and Pharr, 1992 and 2004, Woirgard *et al.*, 1998, Bell and Thwaite, 1999, Panich and Yong, 2005). The introduction of the ultra micro hardness (UMH) tester involved a change in the instrumentation and test principles of the common hardness measurements. The measurement is based on an electromagnetic force that presses an indenter against a specimen with the force being increased at a constant rate (Fig. 2-21 a). During the measurement, the depth of penetration is measured continuously. This allows dynamic measurement of changes that occur in the resistance of the specimen to deformation during the indentation process (dynamic hardness). If the indentation size is large enough to be observed with a microscope the hardness can also be calculated from the plastic deformation by measuring the span of

the indentation, e.g. the diagonal length in case of a Vickers indenter (Oliver and Pharr, 2004).

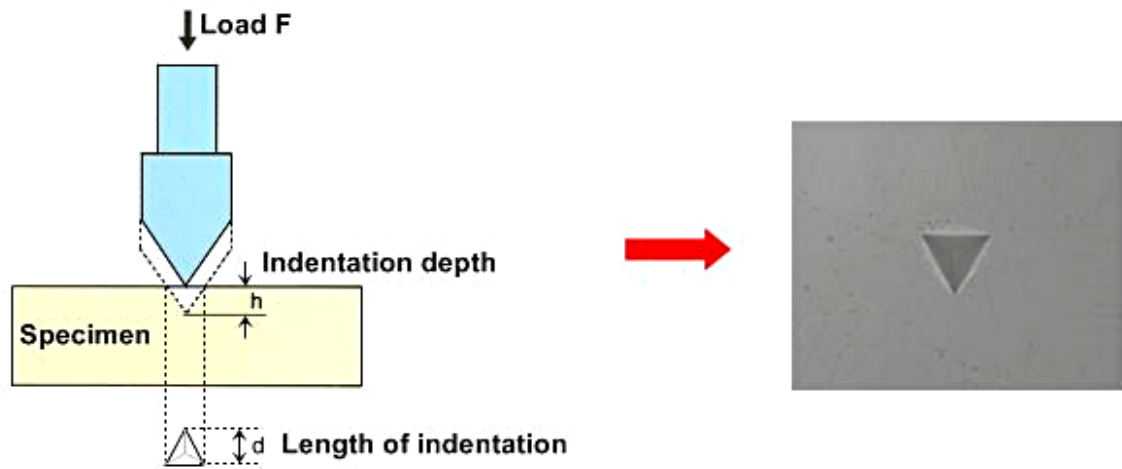


Figure 2-21 (a) Illustration of the measurement principle of a dynamic UMH tester and (b) indentation impression produced during nanoindentation hardness testing of a dental polymeric material using a Berkovich indenter.

Today, UMH measurements have become very important in material research and development next to the customarily employed microhardness tests (Bell *et al.*, 1991). UMH testing instruments, often referred to as nanoindentation tester, allow highly precise measurements of diverse materials properties. Since very small loads and tip sizes are used, the indentation area is only a few square micrometres or nanometres. Therefore, in industry they are employed for the quality control of a wide range of materials such as thin films, plastics, rubbers, fibres, microscopic electronic components, brittle materials as well as metallic materials.

Nanoindentation hardness methods typically employ the so called ‘Berkovich’ indenter which is a 115° triangular pyramid. An example for an imprint obtained from a Berkovich indenter during a nanoindentation hardness measurement is displayed in Figure 2-21 b. Further options are Vickers, Knoop, or a 100° triangular pyramid

indenter. The dynamic hardness (DHT_{115}) for the use of the standard 115° triangular pyramid indenter is calculated as follows

$$DHT_{115} = 3.8584 \times F / h^2,$$

where

F is the maximum load in [kgf], and

h the indentation depth in [mm^2].

The inclination of the tangent of the resulting unloading curve in the indentation depth-test force diagram (Fig. 2-22) can be used to determine the indentation elastic modulus which is equivalent to the Young's modulus (Oliver and Pharr, 1992, Steeger *et al.*, 2009). Toughness values are obtained from the indentation work which corresponds to the amount of plastic deformation done during the indentation.

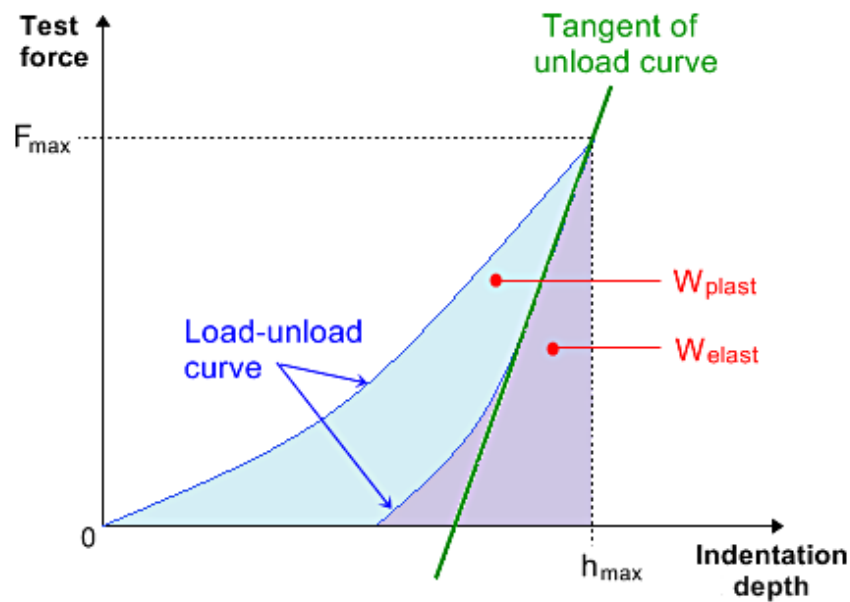


Figure 2-22 Diagram of a load-unload curve obtained from a nanoindentation measurement showing important parameters for the calculation of the test results.

CHAPTER III
MICROENCAPSULATION OF THE HEALING MONOMER
IN A POLY(UREA-FORMALDEHYDE) SHELL

3.1 Introduction

The *in situ* oil-in-water emulsion polymerization as it is described in literature by Brown *et al.* (2003) was identified to be best applicable for the preparation of the poly(urea-formaldehyde) (PUF) microcapsules containing DCPD in this work. First encapsulation experiments resulted in agglomerations of microcapsules that could not be broken and hardly any individual capsules were obtained. Apart from the intact microcapsules the product contained broken capsule matter and a lot of residual material which was found to be exclusively PUF particles. Therefore, it was necessary to study factors which might have an influence on the product quality, and eventually optimize the procedure to obtain higher yields of separate microcapsules.

Next to the adjustment of the process parameters this chapter discusses analytical methods to characterize the microcapsules. The comparison of the different analytical techniques was also meant to evaluate the most suitable methods to be applied in future analysis of similar systems.

3.2 Materials

The core material DCPD was purchased from Sigma-Aldrich and utilized as received. The microcapsule wall-forming materials consisted of urea, ammonium chloride and 1,3-dihydroxybenzol (resorcinol) which were acquired from Sigma-Aldrich whereas the additional wall-forming material formalin (37% formaldehyde in water) was supplied by System. Furthermore, 1-octanol, sodium hydroxide (NaOH)

pellets and 37% hydrochloric acid (HCl) solution were obtained from Sigma-Aldrich. For the pH adjustment a 3 molar NaOH solution and a 12 molar HCl solution were prepared. The solvents ethanol and acetone were purchased from System while methanol and chloroform were received from Merck, and isopropanol from HmbG Chemicals. The dental monomers, Bis-GMA, UDMA, methyl methacrylate (MMA) and TEGDMA were acquired from Sigma-Aldrich. All chemicals and solvents were of analytical grade. Ethylene maleic anhydride (EMA) copolymer powder of an average molecular weight (MW) of 400,000 was provided by Zeeland Chemicals. The EMA powder was mixed with distilled water and stirred at 60 °C over night to obtain a 2.5 wt% aqueous solution of the surfactant. All ingredients were used without further purification.

3.3 Method

3.3.1 General Procedure for PUF/DCPD Microcapsule Preparation

At room temperature (28-34 °C) 100 mL of distilled water and 25 mL of a 2.5 wt% aqueous solution of EMA copolymer were mixed in a 500 mL glass beaker. Under agitation the wall forming materials, 2.5 g urea, 0.25 g ammonium chloride and 0.25 g resorcinol were dissolved in the solution. Then, the pH was raised from about 2.70 to 3.50 by drop-wise addition of 3 molar NaOH and 12 molar HCl solutions using a Mettler Toledo pH meter. After that, the beaker with the reaction solution was suspended in a temperature-controlled water bath with external thermoregulator (Protech, Model 850). The solution was agitated with a digital mixer (IKA Labortechnik, Eurostar) at 450 rpm driving a three-bladed, 63.5 mm diameter low-shear mixing propeller that was placed just above the bottom of the beaker (setup in Fig. 3-1). Two drops of 1-octanol were added to eliminate surface bubbles. Then 30 mL DCPD were slowly added to form an emulsion that was allowed to stabilize for

15 minutes. After stabilization, 6.33 g formalin was added to obtain a 1:1.9 molar ratio of urea to formaldehyde. The emulsion was covered with aluminium foil and heated at a rate of 1 °C/min to the target temperature of 55 °C.



Figure 3-1 Setup for the preparation of PUF/DCPD microcapsules by *in situ* oil-in-water emulsion polymerization.

After 4 hours of continuous agitation the reaction slurry was removed from the water bath and left at room temperature for 30 minutes to slowly cool down. The suspension of the microcapsules (Fig. 3-2 a) was separated under suction with a coarse-fritted filter. The microcapsules were rinsed with distilled water. The filtered product was distributed on a watch glass and dried under the fan for 1 hour. After this, it was placed in a desiccator over night to separate the dry capsules by sieving the next

day. The resulting microcapsules appeared in the form of a free-flowing white powder (Fig. 3-2 b).

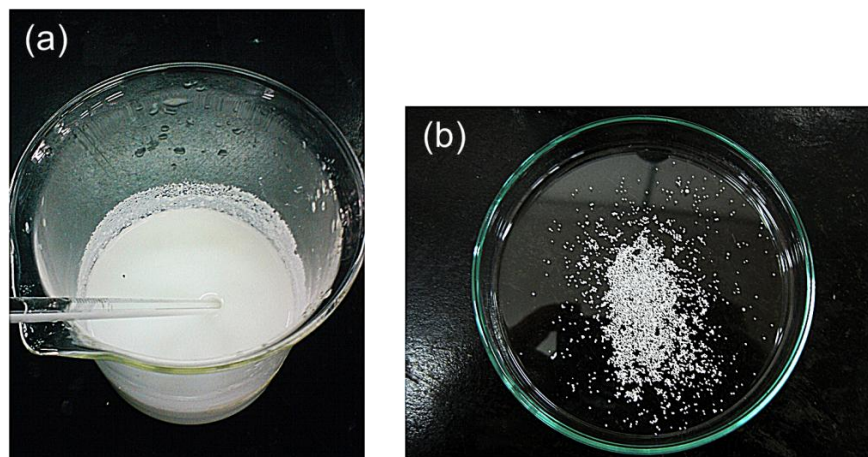


Figure 3-2 (a) Reaction slurry after the synthesis of PUF/DCPD microcapsules which was rinsed, filtered, and dried to obtain (b) the product in the form of a free-flowing white powder.

3.3.2 Study of Microencapsulation Process Parameters

A number of process parameters can control the quality of the resulting PUF/DCPD microcapsules. Amongst the most important parameters in the microcapsule synthesis are pH, reaction temperature, heating rate, reaction time, type and concentration of the emulsifier and the ratio of the compounds. These factors were partly elaborated by different works from research groups at the University of Illinois, US (Sriram, 2002, Brown *et al.*, 2003, Rule *et al.*, 2007). In this work certain other process parameters and their influence on the product were investigated.

All experiments described in the following were prepared according to the standard *in situ* encapsulation procedure as it is described in section 3.3.1. The same ingredients and equipment were used if not stated otherwise. Any variation in the process parameters and the amounts of the compounds is mentioned specifically.

3.3.2.1 Reaction Time

The reaction time in the microcapsule synthesis was varied to evaluate the influence on the quality of the resulting microcapsules, in particular to address the problem of agglomeration which might be the result of insufficient reaction time. Therefore, the microencapsulation process was followed as described earlier, except that the reaction slurry was allowed to stir for 1 hour, 2 hours, 3 hours, 4 hours, 5 hours and 6 hours. Afterwards the product was filtrated under suction, rinsed with distilled water and ethanol and dried before it was inspected with the help of digital microscopy.

3.3.2.2 Initial pH

To enhance the properties of the PUF/DCPD microcapsules, the encapsulation procedure was carried out at the four different initial pH values 3.1, 3.3, 3.5 (standard), and 3.7. After the synthesis the product was rinsed with ethanol to obtain individual capsules, then filtered and dried. The effect of the increasing initial pH on the product yield and quality was evaluated by digital microscopy. For clarification, this study only refers to the initial pH, changes in the acidity or alkalinity of the suspension during reaction time were not considered.

3.3.2.3 Product Treatment with Diverse Solvents

Another approach to separate the agglomerated microcapsules was followed by treating them with solvents. Therefore, the microcapsules were directly after the preparation separated in six equal parts. Each part was intensively rinsed with a different solvent which were water, ethanol, methanol, 2-propanol, acetone and chloroform. The samples were then filtered under suction. The procedure was repeated two more times. After this, the filter cakes were distributed on a watch glass each and

air dried under the fan for 1 hour. The dry capsules were then stored in a desiccator and inspected the following day by digital microscopy.

In addition, parts of the dry microcapsule samples were transferred to individual 250 mL glass beakers to be suspended in 100 mL of the same solvent again. Chloroform was not considered in this test series. The suspensions were agitated with the help of a mechanical stirrer at 200 rpm for 2 hours. The aim was to study the long-term impact of these solvents on the PUF capsule shell. After the exposure to the solvent the microcapsules were filtered under suction, dried and examined by digital microscopy.

3.3.2.4 Variation of Formaldehyde-Urea Ratio

An important factor that influences the capsule shell formation is the proportion of the compounds. In this section the effect of changing formaldehyde to urea ratio was elaborated. PUF/DCPD microcapsules were prepared with a formaldehyde/urea ratio in the range of 1.1 to 2.3. The amounts of the shell ingredients that differ from the standard recipe as described in section 3.3.1 are listed in Table 3-1. The resulting microcapsules were analyzed using digital and optical microscopy.

Table 3-1 Varying urea and formaldehyde amounts for the preparation of PUF/DCPD microcapsules

Sample No.	Urea-Formaldehyde Molar Ratio	Urea Weight (g)	Formaldehyde Weight (g)
1	1 : 1.1	3.56	5.29
2	1 : 1.5	2.92	5.93
3*	1 : 1.9	2.50	6.35
4	1 : 2.3	2.16	6.69

* *Standard*

3.3.3 Microencapsulation of Alternative Core Monomers

The following dental monomers were selected for the encapsulation in a PUF shell: MMA, Bis-GMA, UDMA, TEGDMA, and mixtures hereof. Bis-GMA and UDMA had to be diluted with TEGDMA due to their high viscosity. PUF microcapsules were produced following the general procedure as reported earlier in section 3.3.1. Bis-GMA and TEGDMA were mixed with ratios of 1:1, 1:3, 1:5, 1:7, 1:9 whereas the UDMA to TEGDMA proportions were 1:1 and 1:3. Besides, it was attempted to encapsulate the 1:9 Bis-GMA/TEGDMA mixture, and the 1:3 UDMA/TEGDMA mixture in the presence of a higher concentrated emulsifier solution which was 5% instead of the standard 2.5%.

3.3.4 Product Analysis

During the studies of the process parameters it was found that the product should be rinsed with ethanol after the synthesis to clear the microcapsules from any residual material and separate them to gain the maximum yield. Therefore, the following analytical measurements were all performed on microcapsule batches that were rinsed with ethanol after the synthesis. The product was then dried and sieved through the available precision test sieves of 50, 150, 300 and 500 microns mesh size (Endecotts, certified acc. to BS 410, ISO 3310). Except for the evaluation of the yield, and if not stated otherwise all tests were carried out on microcapsules of the size fraction 150–300 micron.

3.3.4.1 Microcapsule Size and Yield Evaluation

The microcapsule size can be controlled by the agitation rate during the synthesis. In this work the stirring rate was adjusted to 450 rpm to produce capsules of an average diameter of approximately 220 microns which was suggested by White *et*

al. (2001) for the application in a self-healing system. The total yield was obtained from the weight of the dry product and calculated from the mass of the starting materials, urea, formaldehyde, resorcinol and DCPD. Five samples of the dried product were measured and the weight percent calculated, assuming that no impurity was present. The microcapsules were then separated by sieving into 5 different size fractions which were < 50 μm , 50–150 μm , 150–300 μm , 300–500 μm , and > 500 μm . The weight of each size fraction was taken to evaluate the main microcapsule size fraction.

3.3.4.2 General Analysis by Digital and Optical Microscopy

The dried products were all analyzed with the help of a Dino-Lite digital USB microscope (AnMo Electronics) with the two possible magnifications of 5 times and 200 times. Further inspection at higher magnification was provided by Optical Microscopy (OM, Leica). It allowed the examination of the capsule shape and the shell wall. For the shell inspection capsules in the size range of 150-300 micron were dispersed in oil and measured using an oil immersion objective lens of 100 x magnification. The width of the outer capsule shell layer was taken from 3 images at 15 positions to calculate the average thickness of the microcapsule shell.

3.3.4.3 Examination of Microcapsule Shell by Field Emission Scanning Electron Microscopy (FESEM)

More detailed information can be obtained from field emission gun scanning electron microscopy (FESEM, FEI Quanta 250 FEG) which was applied for the study of the capsule shell morphology and thickness. Therefore, microcapsules were placed on a conductive carbon tape attached to a mounting piece for imaging. Some of them were ruptured with a razor blade to facilitate membrane thickness measurement. The

FESEM was operated under low vacuum with a fix electron accelerating voltage of 5 kV and a spot of 3.0. The samples were not sputter coated. For the evaluation of the capsule shell thickness 5 measurements of the outer and inner shell layers were performed.

Furthermore, elemental analysis of both surfaces the smooth shell layer and the rough part were conducted by means of FESEM. The energy-dispersive X-ray (EDX) spectroscopy option allows the determination of the chemical composition of the specimen. The silicon detector measures the energy of an incoming photon by the amount of ionization it produces in the detector material. EDX measurements were performed using a voltage of 10 kV; the magnification was 10,000 x.

3.3.4.4 Thermal Stability of Microcapsules by Thermogravimetric Analysis (TGA)

The TGA technique was used to investigate the thermal stability of the prepared microcapsules. Prior to the measurement the capsules were placed in the vacuum oven for 3 days at 38 °C and 0.3 bar to remove any possible moisture. The samples were then measured on a Perkin Elmer TGA 4000 in a nitrogen environment. Therefore, approximately 1 mg of the PUF/DCPD microcapsules was heated from 50 to 900 °C at a rate of 10 °C/min.

3.3.4.5 Verification of Microcapsule Core Content by Different Analytical Methods

Different analytical methods were considered to determine an appropriate easily available technique to confirm qualitatively the microcapsule core content. Since the chemical structure of the core monomer can be analyzed by spectroscopic techniques proton nuclear magnetic resonance (¹H-NMR) and Fourier transform

infrared (FTIR) spectroscopy were employed. In addition, knowing certain physical and chemical properties of the monomer, thermo-analytical techniques can be applied such as differential scanning calorimetry (DSC).

a. Fourier Transform Infrared (FTIR) Spectroscopy

FTIR spectroscopy of the dry capsule shell material, pure DCPD and the undamaged microcapsules was performed on a Perkin-Elmer RX1 FT-IR spectrophotometer using the potassium bromide (KBr) technique. Typical spectra were recorded in the range of 4000-400 cm^{-1} at a resolution of 4 cm^{-1} . The samples of the capsule shell material were prepared by grinding dry microcapsules with a pestle in a mortar. The crushed microcapsules were collected and washed with acetone several times to remove the DCPD, then dried at room temperature. Two samples of microcapsules were measured, one of the microcapsules with diameters in the range of 150-300 microns and another of the capsule size fraction of 300-500 microns. The weight of the initial microcapsules and the weight of the residue of the ground and extracted microcapsules were taken to calculate the quantitative core content in wt%.

In addition, intact PUF/DCPD microcapsules in comparison with the extracted shell material were analyzed on a Perkin Elmer Spectrum 400 FT-IR/FT-NIR Spectrometer employing the attenuated total reflectance (ATR) technique. The FTIR-ATR measurement was performed on two samples of microcapsules the standard capsules that were rinsed with ethanol after the synthesis, and microcapsules of the same batch that had been stirred for 24 hours in ethanol. This procedure was undertaken to ensure that there is no DCPD present on the outer microcapsule shell. The capsules were filtered and dried before the spectra were recorded from 4000-450 cm^{-1} . The resulting graphs of the microcapsules were compared with the spectrum of the extracted PUF shell material and with library data of pure DCPD.

b. *Differential Scanning Calorimetry (DSC)*

The sample preparation for the DSC measurement of the microcapsule shell material was identical to the one for the FTIR spectroscopy. Thermal analysis of the virgin microcapsules and the capsule shell material was measured on a Perkin Elmer Perkin Diamond DSC. For each sample a scan from 35 °C to 300 °C at a heating rate of 10 °C/min was performed, followed by cooling down to 35 °C and heating up again to 350 °C. For the second and third run a heating rate of 20 °C/min was employed.

c. *Nuclear Magnetic Resonance (NMR) Spectroscopy*

Finally, solution state ¹H-NMR of the microcapsule core content was recorded on a Lambda JEOL 400 MHz FT-NMR system. Therefore microcapsules were ground with a mortar and extracted with deuterated acetone. The extract was measured next to a reference sample of the neat DCPD which was dissolved in the same solvent.

3.3.5 Shelf-Life Test

All produced microcapsule batches were stored individually in brown glass containers at room temperature (27–36 °C) to study the shelf-life. After 1 month, 2 months, 3 months, 6 months, 9 months, and 12 months, and if applicable after 1 ½ year and 2 years storage time all microcapsule batches were visually inspected. Any change in colour or flowing behaviour was manually documented.

The stability of the core monomer of the PUF/DCPD microcapsules was measured by proton NMR spectroscopy after certain time periods. Therefore, samples of the microcapsules were taken after 3 months, 6 months, 1 year, 1 ½ year, and 2 years storage time and ruptured in a mortar each. They were then extracted with deuterated acetone to facilitate the ¹H-NMR measurements of the extracted core monomer.

Thermal analyses were performed at the same points in time as for the ¹H-NMR spectroscopy. DSC was employed for the measurement of the heat flow of the microcapsules in a single scan from 35–350 °C at a heating rate of 10 °C/min. A second run was not considered due to the expected evaporation of the DCPD at low temperatures which can only be observed in a first heating step. In addition TGA was utilized to reveal any possible physical changes in the polymeric shell structure. The weight loss of the microcapsule samples after 6 months, 1 year, 1 ½ year, and 2 years storage time were recorded at the temperature range of 50–900 °C; the heating rate was 10 °C/min. Prior to the thermoanalytical inspections all samples were placed in a vacuum oven at 38 °C and 0.3 bar for 3 days to remove any impurities that could lead to interferences during the measurement.

3.4 Results and Discussion

3.4.1 Impact of Selected Parameters on Product

The main drawback of first microencapsulation experiments was that the product contained a lot of residual material next to the microcapsules and most of the capsules appeared in the form of clusters that could not be separated. A low content of residual material means that the ingredients reacted completely and therefore the amount of microcapsules increases. Likewise, if the capsules are not agglomerated the yield will be higher. In this section the resulting microcapsule quality after the variation of certain distinct process parameters is discussed to eventually optimize the encapsulation procedure for the desired purpose.

3.4.1.1 Reaction Time

The aim of this study was to identify the necessary reaction time for the production of the maximum amount of intact microcapsules. The digital micrographs

of the capsules obtained after different reaction times revealed that after 1 hour some microcapsules had already formed (Fig. 3-3 a). After 2 hours reaction time more capsules had built. However, they still appeared in the form of dense clusters and no individual capsules were obtained (Fig. 3-3 b). Allowing the reaction another hour single microcapsules were produced next to many agglomerations of microcapsules (Fig. 3-3 c). The results of longer reaction times (4, 5 and 6 hours) are consistent with the 3 hour sample as it is obvious when comparing the micrographs in Figure 3-3 c with Figure 3-3 d which illustrate the product after 3 and 4 hours time, respectively. In summary, an increase in the reaction time does not have any beneficial effect on the product; a minimum reaction time of 3 hours is recommended to ensure that the reaction is completed.

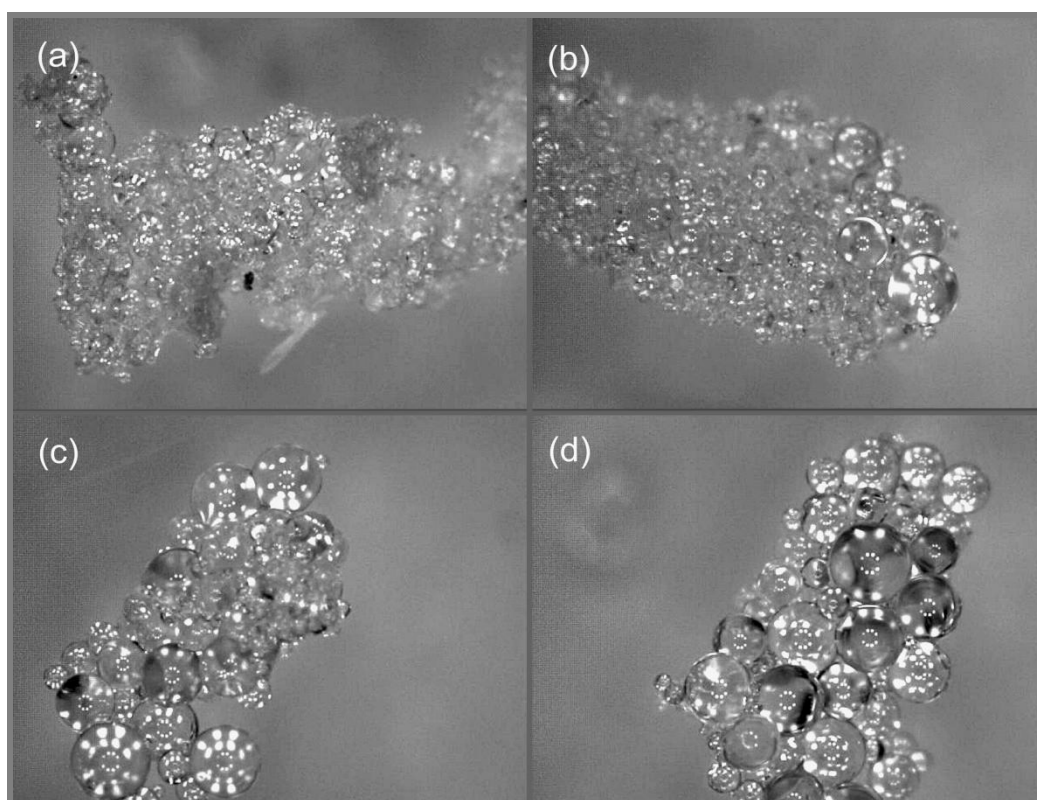


Figure 3-3 Influence of the reaction time on the PUF/DCPD microcapsule formation displayed in images obtained from digital microscopy. Reaction time: (a) 1 hour, (b) 2 hours, (c) 3 hours and (d) 4 hours.

3.4.1.2 Initial pH

Next to the study of the reaction time, the pH was varied in the range of 3.1 to 3.7. Cosco *et al.* (2006 and 2007) suggested that a decrease of the initial pH 3.5 has a positive effect on the yield. A similar observation was reported from Prasetya and Hasakowati (2010) who also claimed that a lower pH leads to the production of more PUF nanoparticles that attach to the microcapsule surface to build a thicker capsule shell. Whereas Lee *et al.* (2002) observed that the pH does not affect the yield but with increasing pH the particle size is reduced and the capsule shell becomes smooth lacking the deposition of PUF particles on the capsule surface. From these reports it can be concluded that the pH has a strong influence on the capsule shell formation in the microcapsule synthesis and is therefore an important parameter to be considered for the improvement of the product yield and quality.

The results of this study are illustrated in the images obtained from digital microscopy in Figure 3-4. It demonstrates the PUF/DCPD microcapsules produced at four different initial pH values which were 3.1, 3.3, 3.5, and 3.7. With the lowest pH of the test series (3.1) it was not possible to produce microcapsules. As Figure 3-4 a displays, only lumps of white powder were obtained. Whereas at pH 3.3 microcapsules are built, however, the product contained a lot of residual material next to the microcapsules (Fig. 3-4 b). Figure 3-4 c illustrates the product gained utilizing the standard pH 3.50. It shows perfectly round microcapsules and the yield was the highest in this test series. A slightly less acidic pH (3.7) resulted in many microcapsules, however, they were densely packed together and could not be separated by further processing using solvents (Fig. 3-4 d).

To sum up, with this study it was confirmed that the initial pH has a significant impact on the microcapsule preparation and the resulting product quality. The

observations of other researchers as mentioned above cannot be confirmed since the increase in the initial pH value showed an extension of the thicker outer shell wall. The optimum pH for the preparation of the PUF/DCPD microcapsules was found to be 3.50 which need to be accurately adjusted to obtain a high yield of individual microcapsules.

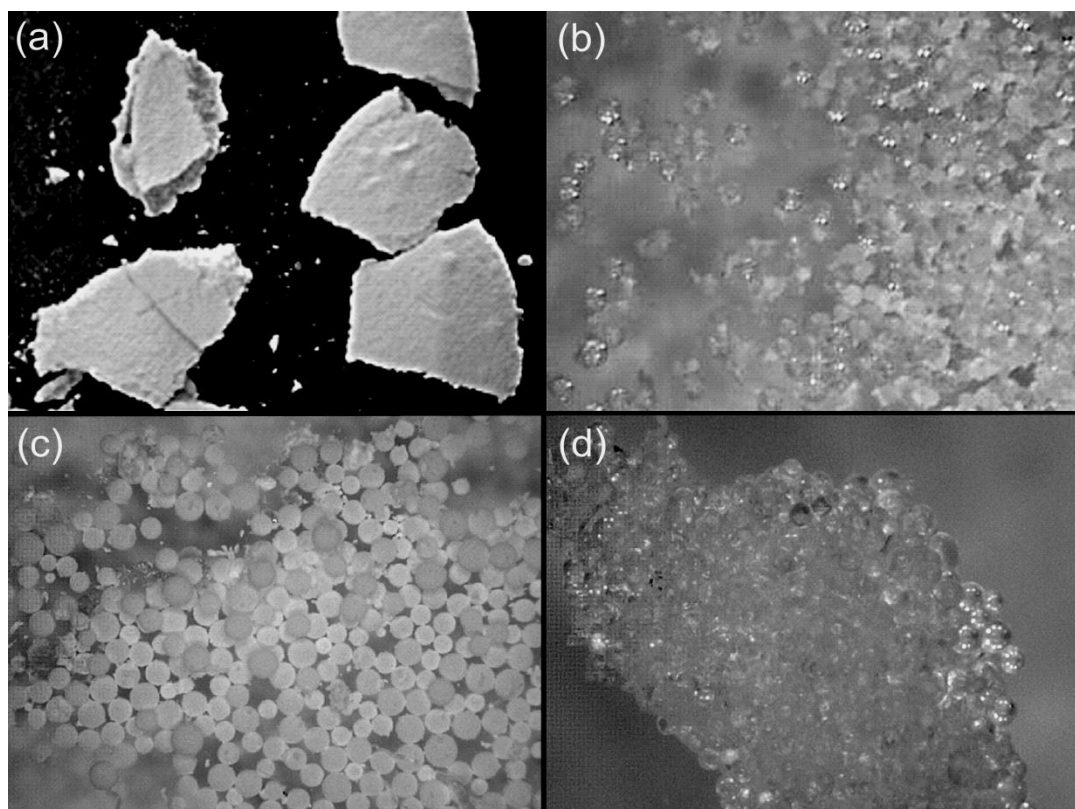


Figure 3-4 Digital micrographs of PUF/DCPD microcapsules prepared at different initial pH-values: (a) pH 3.1, (b) pH 3.3, (c) pH 3.5, and (d) 3.7.

3.4.1.3 Solvents for Microcapsule Separation

Different solvents were investigated to separate the product from other particles than microcapsules and clear the capsule shell. According to Brown and co-workers (2003) rinsing the product with water after the synthesis is sufficient to remove any remaining material next to the microcapsules. However, they did not mention the

strong tendency of the microcapsules to build agglomerations that cannot be separated by reprocessing. They further claimed that the treatment with solvents other than water would destroy the capsule shell. Yet, Cosco and his group (2006) reported the necessity of using chloroform to eliminate unreacted resin which was not encapsulated. Hence, it seems interesting to study the influence of certain solvents with the aim of removing undesired matter in the product and obtain a higher yield of individual microcapsules.

The microscopic images of the product after the treatment with different solvents (water, ethanol, methanol, 2-propanol, acetone, and chloroform) are outlined in Figure 3-5 and 3-6. The product that was rinsed with water was slightly sticking together containing many particles of residual PUF material (Fig. 3-5 a). The ethanol, methanol and 2-propanol rinsed samples showed similar results with separate capsules next to other residual material as it is obvious from the micrographs in Figure 3-5 b, c and d. Rinsing the microcapsules with acetone significantly increased the quality of the product since exclusively individual capsules were obtained as evident in Figure 3-5 e.

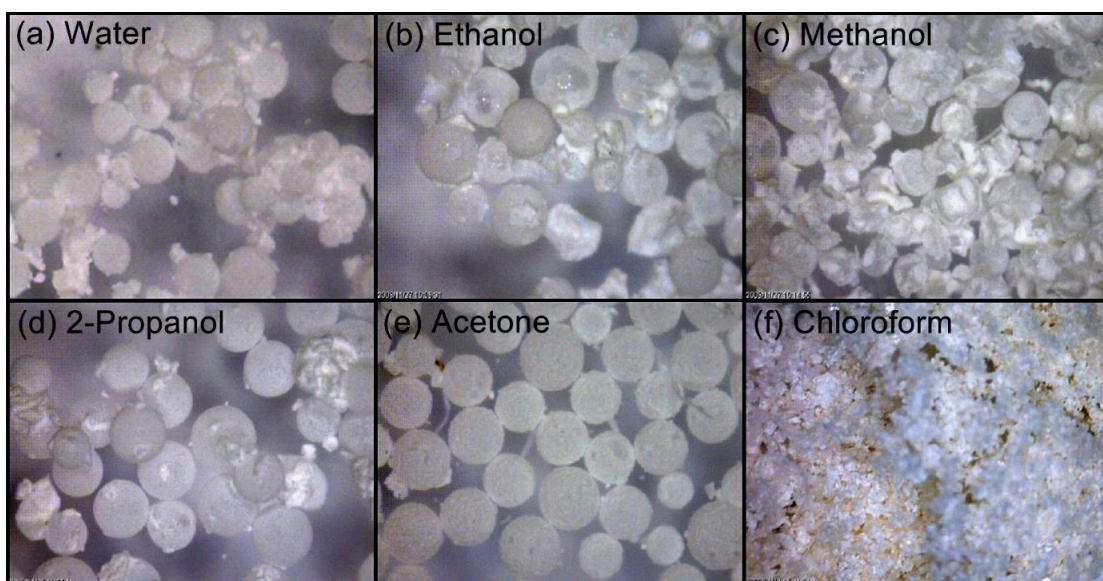


Figure 3-5 Micrographs of PUF/DCPD microcapsules demonstrating the effect of different solvents on the product.

In contrast, it was revealed that chloroform has a strongly destructive impact on the PUF microcapsule shell. After short exposure the microcapsules were devastated which is displayed in Figure 3-5 f.

After longer exposure to the solvent, the water, ethanol and methanol treated product showed less particulate matter (Fig. 3-6 a, b and c), however, the water and methanol samples appeared in the form of agglomerations. Whereas the ethanol exposure for 2 hours resulted in a free-flowing powder of individual microcapsules as it is clear from the micrograph in Figure 3-6 b. In contrary, 2-propanol would have a destructive effect on the capsules if exposed for a longer time (Fig. 3-6 d). Whereas rinsing of the product with acetone showed an extremely positive effect, extended exposure partly destroyed the capsule shell resulting in clusters and lumps of sticky material which can be seen in Figure 3-6 e.

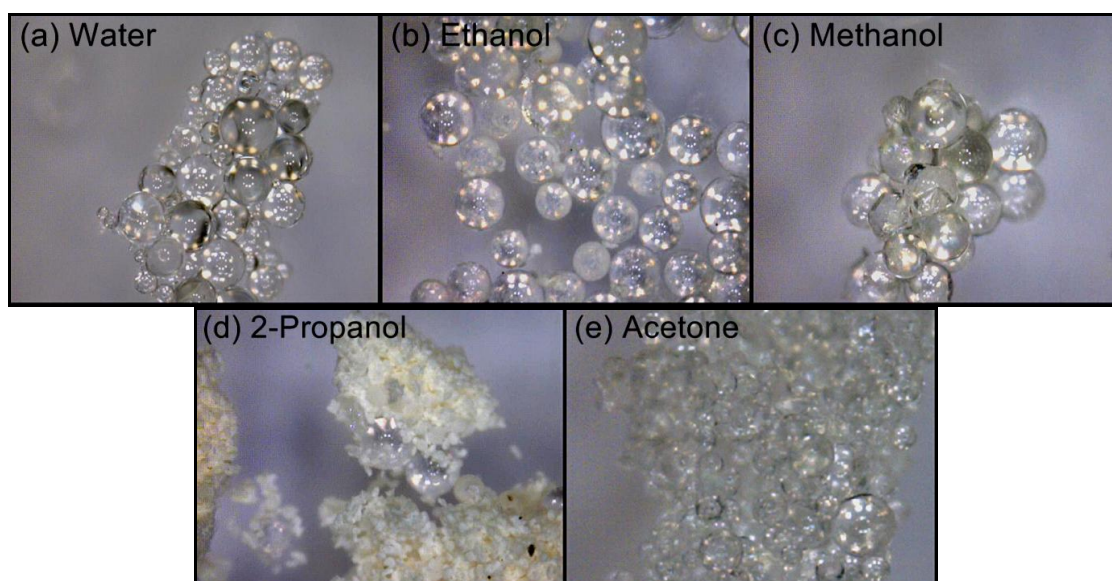


Figure 3-6 Micrographs of PUF/DCPD microcapsules illustrating the impact of the exposure to selected solvents for 2 hours.

To sum up, it was shown that water is not strong enough to separate the agglomerations in an aftertreatment whereas ethanol is very effective. By rinsing the

product with ethanol numerous individual microcapsules were obtained and hardly any residual matter was left. The result was improved after longer exposure to ethanol and no visible destructive effect on the PUF shell material was observed. In contrary, chloroform destroyed the capsules immediately. Furthermore, acetone showed high efficiency in clearing the product and separating the microcapsules, however, it might have a destructive impact on the microcapsule shell after extended exposure time. Hence, in following encapsulation experiments the product was rinsed with ethanol after the filtration to increase the yield of individual microcapsules.

3.4.1.4 Effect of Formaldehyde-Urea Ratio on Microcapsule Shell Formation

In industry the ratio of formaldehyde to urea commonly varies between 2.0 to 2.4. Lee and his group (2002) claimed that an increase in the formaldehyde amount has a positive impact on the microencapsulation efficacy. A low formaldehyde amount along with a low pH would lead to a weak capsule shell crushing easily. Thus, on the one hand a decreasing formaldehyde amount could reduce the residual PUF particles that were observed as these might stem from capsules that broke during the production process. On the other hand, an increase could result in higher yields. Therefore, it was of utter interest to investigate the effect of different formaldehyde and urea proportions on the microcapsule shell and the quality of the product.

Four batches of microcapsules with different formaldehyde to urea molar ratio were produced which were 1.1, 1.5, 1.9 (standard), and 2.3. Each product was examined by digital and optical microscopy. OM revealed that the microcapsules synthesized with a formaldehyde-urea molar ratio of 1.1 were of poor quality (Fig. 3-7 a) as the product contained a lot of broken capsules and other particulate matter. The capsule shell was not round and appeared wrinkled. Furthermore, the capsules lacked the relatively thick protecting outer shell layer which was observed in other batches,

for instance as obvious in Figure 3-7 c and d. Figure 3-7 b illustrates that with increasing formaldehyde content the capsules obtained their perfectly round shape. With a formaldehyde to urea ratio of 1.5 a relatively high yield and hardly any residual matter were produced which is obvious in the micrograph in Figure 3-8 a. Further raise in the formaldehyde amount exhibited the formation of a rough outer shell part. As Figure 3-7 c shows a formaldehyde-urea molar ratio of 1.9 produced spherical microcapsules surrounded by a relatively thick uneven outer capsule shell layer. An even higher formaldehyde part (urea-formaldehyde molar ratio 1: 2.3) led to an extension of this rough shell part (Fig 3-7 d) creating an irregular shell surface. The latter showed lower yields containing a lot of other residual material which is evident from the digital micrographs in Figure 3-8 b.

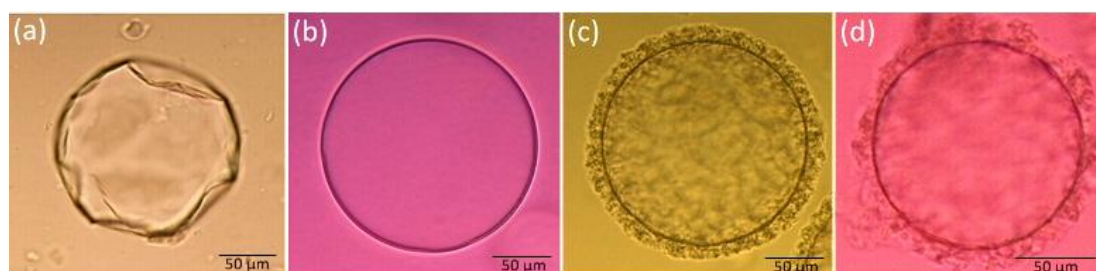


Figure 3-7 Optical micrographs of PUF/DCPD microcapsules produced with varying formaldehyde-urea molar ratio in the capsule shell: (a) 1.1, (b) 1.5, (c) 1.9 and (d) 2.3.

Generally, it was found that the formaldehyde-urea ratio has a significant impact on the formation of the microcapsule shell. A rise in the formaldehyde content resulted in an increase in the capsule shell thickness. Whereas low formaldehyde proportions led to a thinner, weak microcapsule shell. With a formaldehyde-urea ratio of 1.9 perfectly shaped microcapsules of high yields were produced.

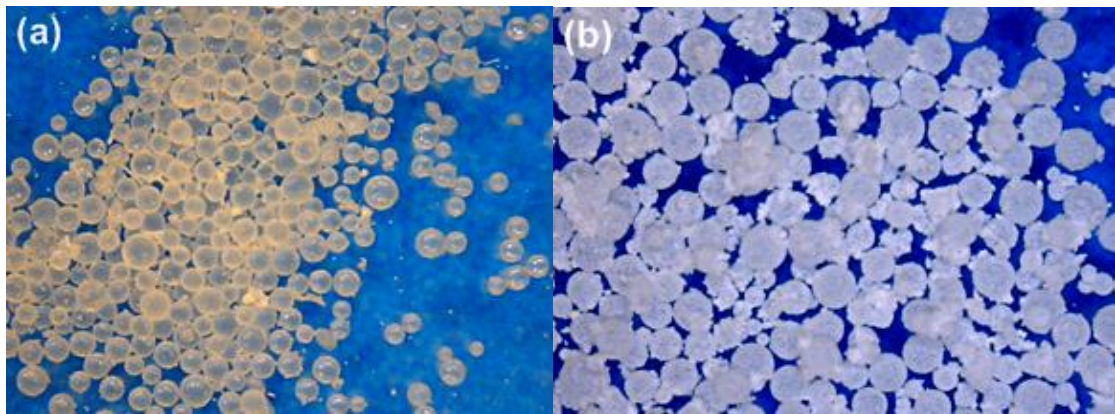


Figure 3-8 Digital microscopy images showing PUF/DCPD microcapsules obtained from two different formaldehyde-urea molar ratios: (a) 1.5 and (b) 2.3.

3.4.2 Microcapsule Yield and Size Fractions

The microcapsule medium size is controlled by the agitation rate during the synthesis (Tan *et al.*, 1991, Alexandridou and Kiparissides, 1994, Ovez *et al.*, 1997). With an agitation rate of 200–2000 rpm microcapsules of an average diameter of 10-1000 μm can be obtained. In this study an agitation rate of 450 rpm was used with which capsules of an average diameter ranging from approximately 50 to 500 microns were produced. The total yield was in the range of 78–85 % as also summarized in Table 3-2. The main capsule size fraction was for the capsules of 150–300 μm in size with an average yield of about 59 % relative to the total yield. The quantity of capsules smaller than 50 microns and bigger than 500 microns was negligible with 2 % and 5 % of the total yield, respectively.

Table 3-2 Total yield and yield according to different size fractions of PUF/DCPD microcapsules

Sample No.	Total Yield in (wt%)	Yield of Microcapsule Size Fractions in (wt%)				
		< 50 μm	50–150 μm	150–300 μm	300–500 μm	> 500 μm
1	78	0	13	51	30	6
2	80	1	6	60	24	9
3	82	3	8	59	27	3
4	85	1	10	64	21	4
5	81	7	26	63	3	1
Average	81	2	13	59	1	5

3.4.3 Microcapsule Analysis by Microscopic Methods

3.4.3.1 Product Characterization by Digital Microscopy

The handheld miniature microscope proved to be a very quick and effective tool to evaluate the successful preparation of microcapsules. Besides, this technique provided information about the purity of the product next to the size and shape of the microcapsules. Images were obtained from the two possible magnifications 5 x and 200 x (Fig. 3-9 a and b, respectively). After intensive rinsing of the product with ethanol many spherical microcapsules of different diameters could be produced by the *in situ* encapsulation method; there was hardly any residual material next to the microcapsules present. The inspection of the individual size fractions (50–150 μm , 150–300 μm , and 300–500 μm) showed no visible differences in the product quality.

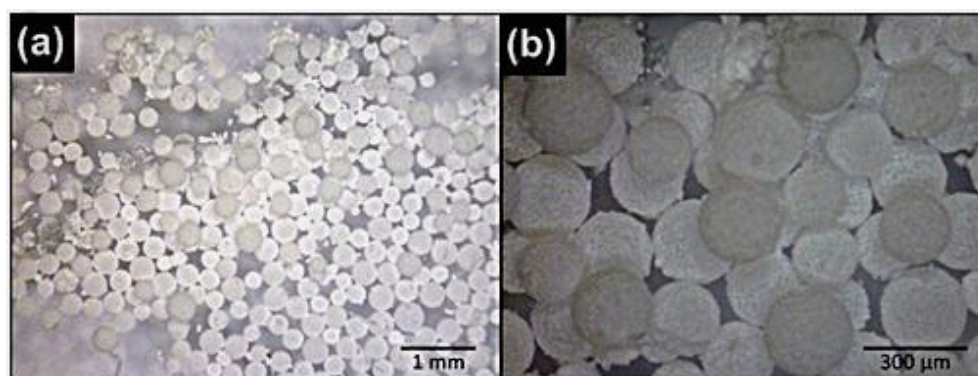


Figure 3-9 Images obtained from the miniature digital microscope showing spherical PUF/DCPD microcapsules at the two possible magnifications: (a) 5 x and (b) 200 x.

3.4.3.2 Shape and Shell Thickness by Optical Microscopy (OM)

OM supported the results obtained from digital microscopy which is the perfectly globular shape of the microcapsules. Further magnification allowed the inspection of the microcapsule shell wall. In Figure 3-10 (a) the thin smooth capsule shell layer is visible by a dark clear line enclosing the capsule core. This inner

membrane is surrounded by an uneven thick layer. The thickness of the inner shell layer was less than 1 μm whereas the outer shell layer measured approximately 12–16 μm (Fig. 3-10 b).

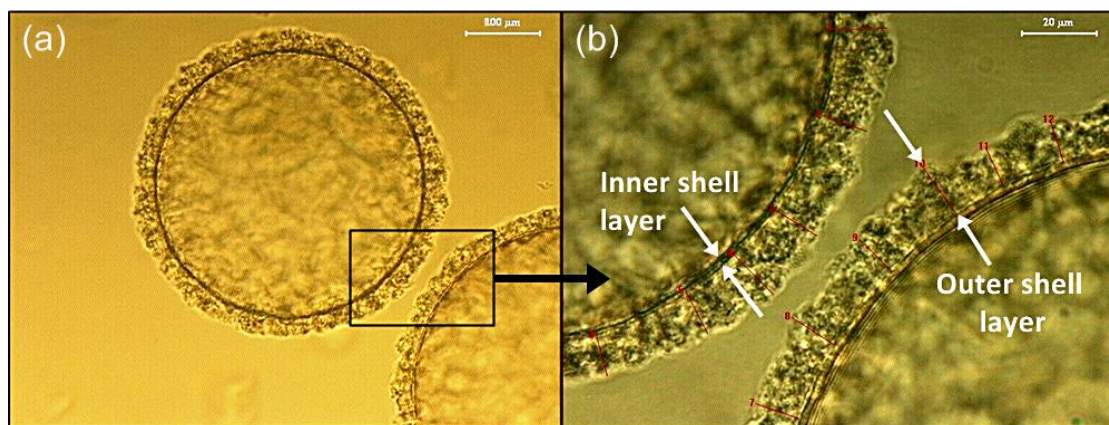


Figure 3-10 Optical micrographs of (a) spherical PUF/DCPD microcapsule displaying the inner shell membrane as a dark clear line surrounded by an uneven outer layer, and (b) the thickness measurement of the two shell layers.

3.4.3.3 Shell Composition and Morphology by FESEM-EDX

The surface morphology of the microcapsule shell was studied by FESEM. Figure 3-11 (a) shows the outer surface of the round microcapsules which is rough and irregular. When zooming in the surface of a continuous smooth inner shell wall becomes visible on which numerous tiny beads of annular shape are sticking (Fig. 3-11 b). Brown *et al.* (2003) suggested that the smooth capsule wall is the result of the deposition of low-molecular weight prepolymer at the DCPD-water interface during synthesis. After this shell layer is formed PUF nanoparticles, which are precipitations of higher molecular weight prepolymer, deposit on the smooth capsule shell to build the rough porous outer shell layer. That means that the outer shell wall consists solely of agglomerations of globular PUF nano-sized particles which were in the size range of 80-350 nm as evaluated by FESEM.

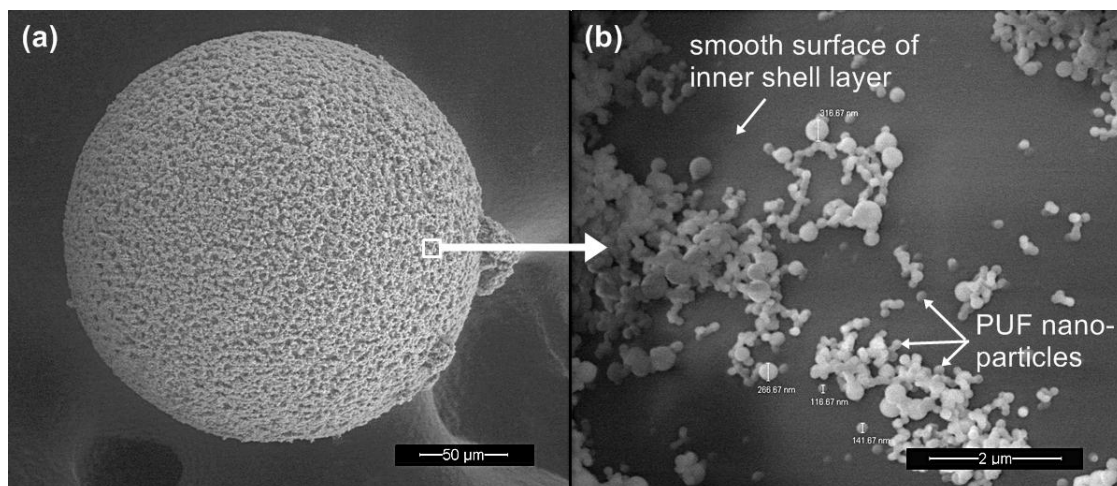


Figure 3-11 FESEM images of PUF/DCPD microcapsules illustrating (a) the uneven porous outer shell layer and (b) the surface of the smooth continuous inner shell wall on which precipitations of PUF nano-beads are adhered.

Elemental analysis was performed by FESEM-EDX spectroscopy which showed the presence of carbon (C), nitrogen (N), and oxygen (O) as well as negligible amounts of alumina (Al) on both surfaces, the smooth shell membrane and the rough outer layer. The traces of Al might be impurities deriving from the starting materials. The distribution of the elements within the two surface layers is displayed in Table 3-3. The data gained from both measurements is typical for a UF polymer.

Table 3-3 Composition of the smooth inner membrane and the rough porous outer layer of the microcapsule shell obtained from FESEM-EDX analysis

Element	Inner Continuous Shell Layer		Outer Porous Shell Layer	
	weight%	atomic%	weight%	atomic%
C	54	59	44	49
N	30	28	34	32
O	15	12	21	18
Al	< 1	< 1	< 1	< 1

The CNO ratio varies between the porous and non-porous zone. For instance, the continuous capsule shell layer consists of more carbon (about 10 % more), less oxygen and less nitrogen (6% and 4%, respectively) than the PUF nanoparticles. This can be explained by the different molecular weight ratio in the two membrane zones.

3.4.3.4 Membrane Thickness by FESEM

With the help of OM the thickness of the shell membrane could be roughly determined. A more precise measurement is provided by FESEM as it allows much higher magnification. The resulting images of the broken microcapsule shell revealed that the rough porous outer layer measured about 10 to 15 microns (Fig. 3-12 a). The thickness of the inner shell layer was in the range of about 120 to 140 nm as it is displayed in Figure 3-12 b.

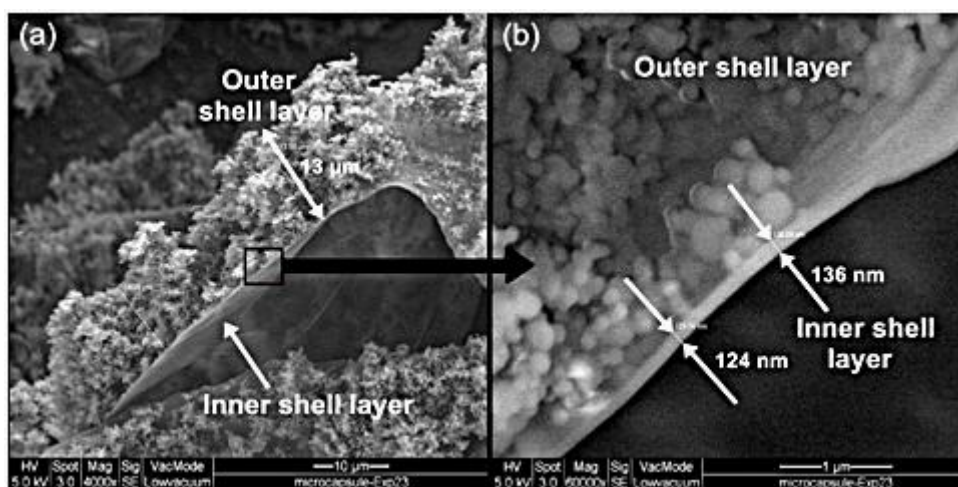


Figure 3-12 FESEM micrographs of ruptured PUF microcapsule shell showing (a) the rough porous outer shell layer and (b) the smooth continuous inner shell.

The continuous inner shell layer is important as it protects the core compound by avoiding diffusion and leakage of the enclosed monomer; whereas the rough porous outer layer prevents the capsules from sticking together. Furthermore, the porous part

allows the matrix resin to penetrate through when embedded in a polymeric host material. Upon hardening it would provide a good adhesion of the microcapsules to the matrix polymer allowing mechanical retention.

3.4.4 Thermal Stability of Microcapsules by TGA

Figure 3-13 illustrates the nonisothermal TGA result of the PUF/DCPD microcapsules. The sample showed a gradual weight reduction starting at about 150 °C. Around 200 °C the mass abruptly drops approximately 80 %. According to Kessler (2002) the rupture of the microcapsules which would cause a weight loss due to the release of vaporizing DCPD occurs at around 220 °C. Hence, the sudden decrease in mass could be partly referred to the breaking of the microcapsule shell in connection with the evaporation of the core monomer. This becomes clear when considering the boiling point of DCPD which is about 170 °C. The other part of the mass loss refers to the decomposition of the PUF shell which takes place at the same time and continues until around 660 °C.

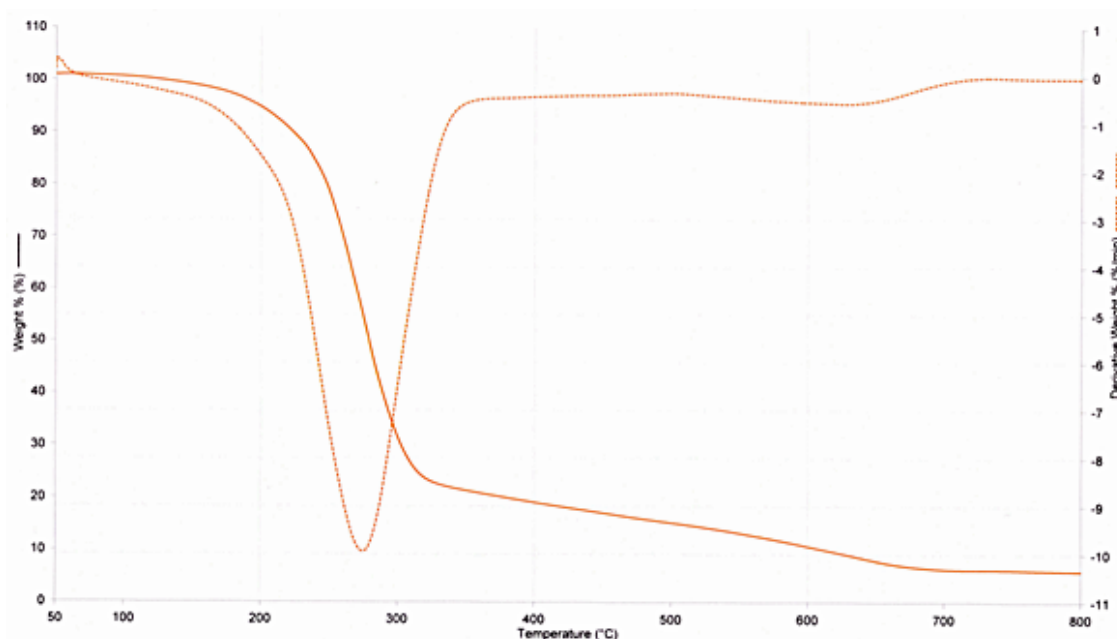


Figure 3-13 TGA diagram of PUF/DCPD microcapsules.

3.4.5 Verification of Encapsulated DCPD

The quantitative microcapsule core content was calculated from the initial microcapsule weight and the weight of the capsule shell material after extraction. It was found that the microcapsules in the size range of 150–300 microns contained about 75–79 wt% DCPD whereas for the microcapsules with diameters ranging from 300–500 microns the core monomer accounted for approximately 90 wt% of the total microcapsule composition.

For the qualitative verification of the microcapsule core monomer diverse analytical methods were considered which included FTIR spectroscopy, $^1\text{H-NMR}$ spectroscopy and DSC. In the following the resulting spectra are discussed with the aim of identifying the most suitable technique for future microcapsule core analysis.

3.4.5.1 FTIR Spectroscopy of Microcapsules and PUF Shell Material

Figure 3-14 shows the plot of the FTIR spectra obtained from the extracted microcapsule shell materials and the microcapsules of two different size fractions in comparison with the pure DCPD. The spectra of the microcapsules and the extracted microcapsule shell material showed all the expected peaks in the area between 3000 to 3400 cm^{-1} , at around 1642 cm^{-1} and 1400 cm^{-1} which are the characteristic absorptions of N–H stretching, amide C=O stretching, and methylene C–H bending vibrations, respectively. These three primary peaks indicate the formation of the UF wall material.

It was expected that in the spectra of the intact microcapsules additional peaks related to DCPD would appear which is not present in the extracted microcapsule shell material. However, no additional peaks that might correspond to DCPD were observed in the sample of the microcapsules in the size range 150–300 microns which spectrum is shown in Figure 3-14 c. When compared with the spectrum of the pure DCPD it became obvious that the characteristic absorptions at 2930 cm^{-1} , 2964 cm^{-1} and

3048 cm^{-1} next to the C–H out of plane (OOP) absorptions at 724 cm^{-1} and 755 cm^{-1} are not present. This observation might lead to the assumption that the encapsulation of the DCPD monomer did not occur.

Surprisingly, in the spectrum obtained from the microcapsules of the size fraction 300–500 microns these absorptions were observed. This phenomenon can be justified by the bigger spheres being able to incorporate a higher amount of the core monomer which could be detected by the applied FTIR method. The spectrum is displayed in Figure 3-14 b in which the DCPD specific peaks are present at 2965 cm^{-1} (C–H stretching vibration of CH_2) and around 724 cm^{-1} and 755 cm^{-1} (C–H bending vibrations). Therefore, the presence of the core monomer in the microcapsules of 300–500 microns size was clearly demonstrated.

The FTIR-ATR option was employed as it allows the direct measurement of materials without destroying them as it is the case when using the KBr method. Further advantages associated with this technique include the increased sensitivity, improved reproducibility and the much faster and easier sampling. Since the ATR technique measures maximal 5 microns beyond the surface of a sample it was expected solely to detect the absorptions of the PUF shell material.

In Figure 3-15 the FTIR-ATR spectrum of the intact microcapsules of the size range 150-300 microns is displayed in comparison with the library spectrum of pure DCPD and the extracted PUF shell material. The latter spectrum shows the characteristic absorption peaks of the N–H and C=O vibrations of PUF (Fig. 3-15 a). In the spectrum of the microcapsules (Fig. 3-15 b) the strong band of the N–H stretching absorption appears around 3325 cm^{-1} , the C=O stretching vibrations in the area of 1610-1650 cm^{-1} , and the bending absorption of the N–H bond at around 1549 cm^{-1} which all correspond to the PUF microcapsule shell material.

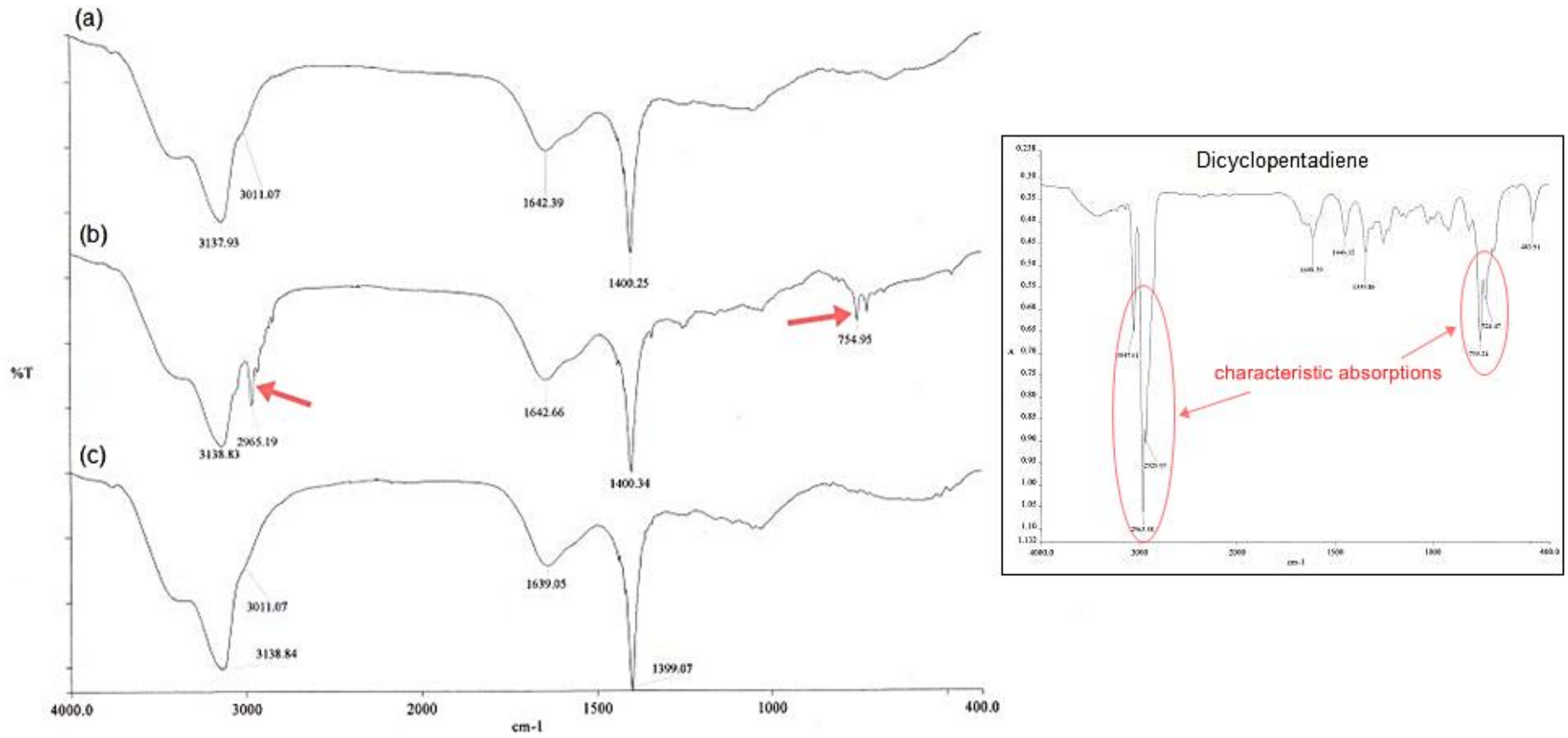


Figure 3-14 FTIR spectra of (a) the extracted PUF capsule shell material, (b) PUF/DCPD microcapsules in the size range of 300-500 microns and (c) PUF/DCPD microcapsules of 150-300 microns diameters, in comparison with the spectrum of the neat DCPD.

When comparing the spectra with the library data (Fig. 3-15 c) it was found that all characteristic peaks for DCPD are present. For instance, the typical vibration of sp^2 C–H is obvious at 3046 cm^{-1} , next to the sp^3 C–H stretching absorptions between 2844 cm^{-1} to 2962 cm^{-1} which appear in the DCPD library spectrum at 3050 cm^{-1} and 2845 cm^{-1} to 2964 cm^{-1} , respectively. Furthermore, the OOP bending absorption peaks of C–H are evident with strong intensity at 753 cm^{-1} and 725 cm^{-1} which match the corresponding signals in the DCPD spectrum. Hence, DCPD was clearly identified in the microcapsules of the size fraction 150–300 microns by this FTIR-ATR technique.

It has to be noted that to undertake the measurement the sample is placed on a crystal area and pressure has to be applied from the top to push the sample onto the diamond surface. The force used was kept to a minimum which was adjusted by previewing the spectra and collecting data as soon as a satisfactory spectrum was obtained. Nevertheless, the capsules might have been partly ruptured in the course of the action.

To ensure that the outer capsule surface was clear of any DCPD another sample was measured for which the microcapsules were stirred in ethanol over night. The resulting spectrum was consistent with the one of the standard microcapsules (Fig. 3-15 b). With this it was proofed that the detected DCPD solely stemmed from the core verifying the successful encapsulation of the monomer.

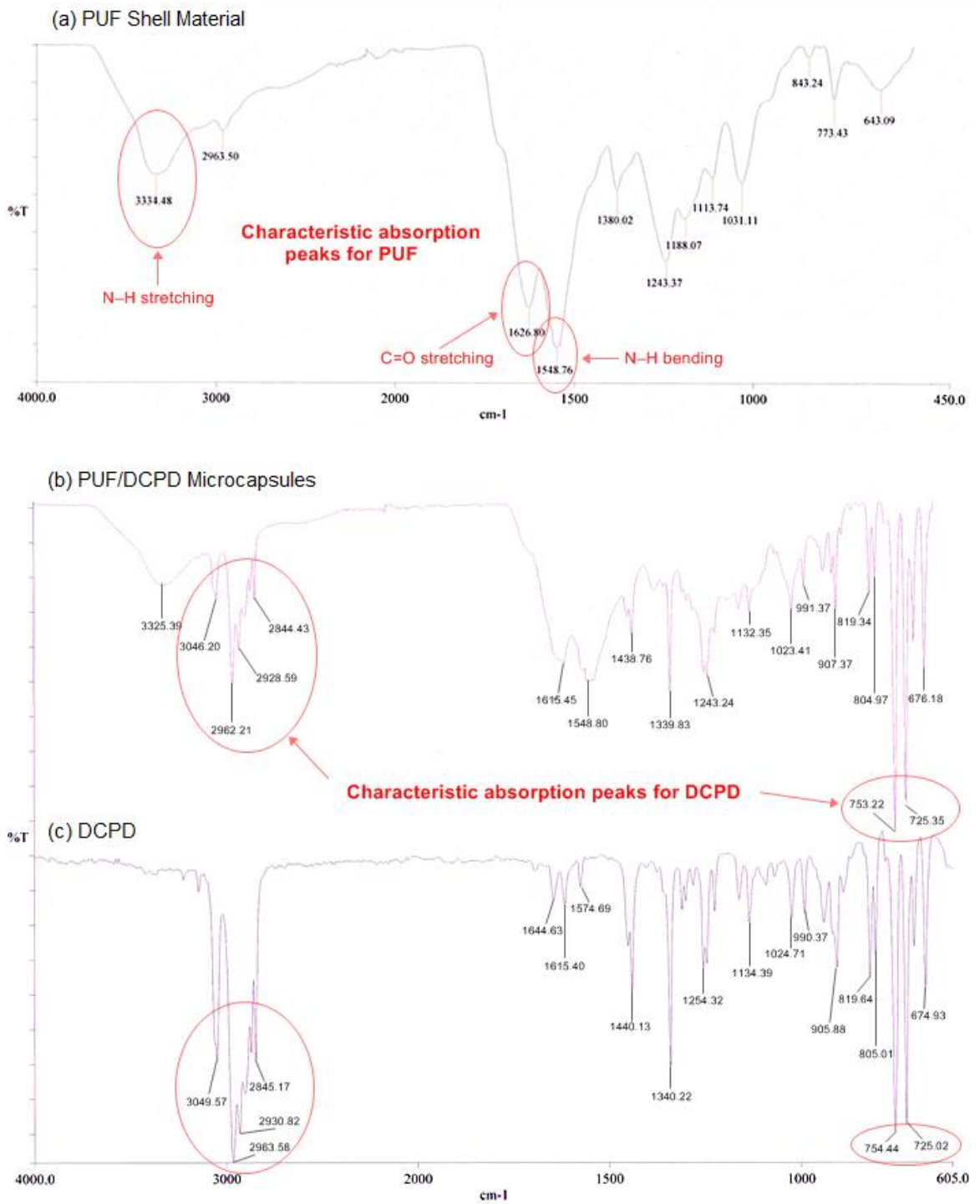


Figure 3-15 FTIR-ATR spectra of (a) extracted PUF shell material, (b) PUF/DCPD microcapsules and (c) pure DCPD.

3.4.5.2 DSC of Microcapsules and PUF Shell Material

For the evaluation of the DSC results only the first heating scans were considered since the intention was to observe the DCPD melting and evaporating. Once the microcapsules are broken and the core monomer is evaporated it cannot be recovered. Thus any information that can be obtained from further heating steps is insignificant for the verification of the DCPD core.

The DSC plot of the initial PUF/DCPD microcapsules showed a rise in the enthalpy of transition (ΔH) from the starting temperature (35 °C) reaching an apex at 62 °C (Fig. 3-16) which illustrates the melting of DCPD. The following gradual increase of ΔH starting at about 160 °C might indicate the boiling of DCPD which boiling point is 170 °C. Then, the heat flux curve reaches another peak at 219 °C when the capsules rupture, obviously merging with the melting peak of the PUF shell material which is indicated by the shoulders at about 245 °C and 260 °C.

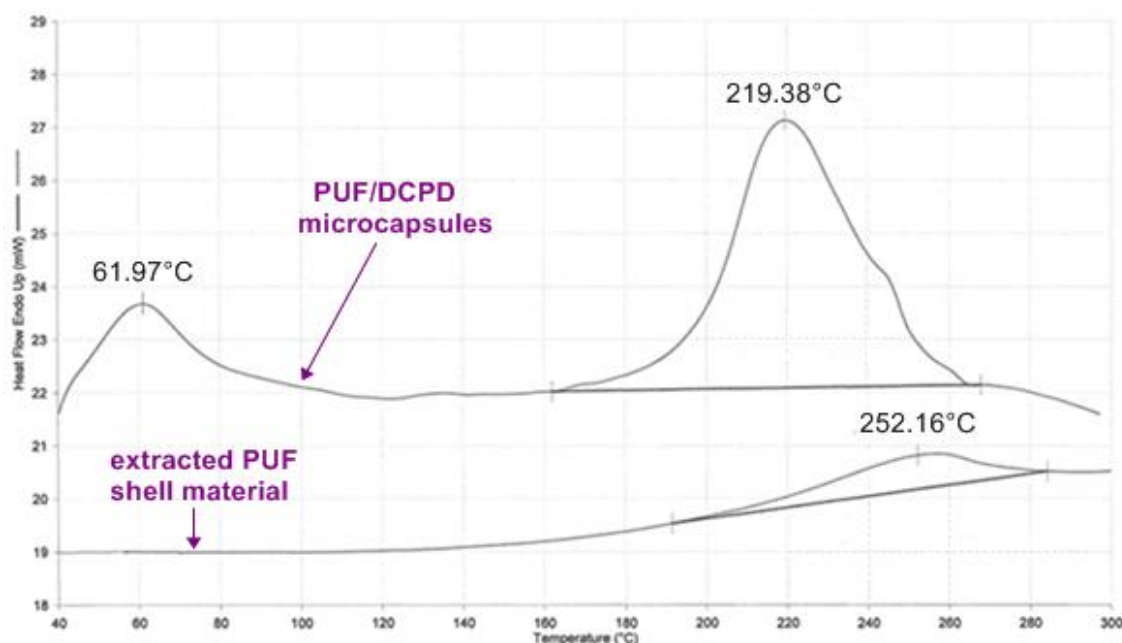


Figure 3-16 DSC plots of PUF/DCPD microcapsules and extracted PUF microcapsule shell material.

The DSC trace of the extracted PUF shell material shows a moderate increase in enthalpy only at higher temperatures to reach a maximum at 252 °C. The evident climax of DCPD in the plot obtained from the intact microcapsules which does not appear in the extracted PUF shell material clearly proved the presence of the encapsulated monomer.

3.4.5.3 Proton NMR Spectroscopy of Core Monomer

Proton NMR in deuterated acetone was measured of the microcapsule extract containing the core monomer and the pure DCPD diluted in the same solvent. The successful encapsulation of the core monomer was indicated by the presence of the characteristic signals corresponding to DCPD in the ^1H -NMR spectrum of the microcapsule extract. The result is displayed in Figure 3-17 showing all the typical

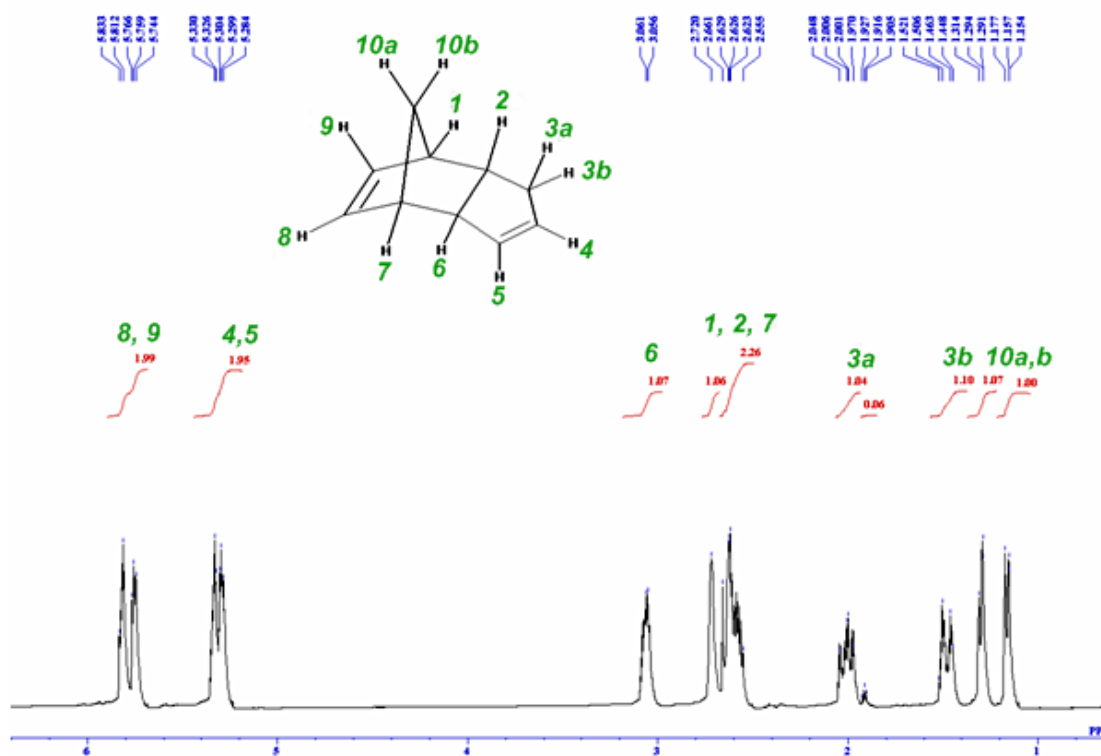


Figure 3-17 Proton NMR spectrum in acetone of the extracted core monomer of the PUF/DCPD microcapsules.

peaks of DCPD at 1.17 ppm (d,1H); 1.30 ppm (d,1H); 1.45-1.52 ppm (m,1H); 1.97-2.05 ppm (m,1H); 2.56-2.66 ppm (m,2H); 2.72 ppm (s,1H); 3.06 ppm (m,1H); 5.28-5.33 ppm (m,2H); 5.74-5.83 ppm (m,2H). Since the measured spectrum resembles the spectrum of neat DCPD with all characteristic absorptions being present the encapsulated monomer was unequivocally verified. Thus, proton NMR spectroscopy is a most suitable method for the analysis of the core content in the case of DCPD.

3.4.6 Encapsulation of Dental Monomers

The use of dental acrylate-based monomers as healing agents could be a promising solution for the creation of a self-healing system to be applied in a restorative material due to diverse factors. For instance, long term experiences with the diverse dental monomers eliminate any possible health concern. Furthermore, an acrylic healing agent that polymerizes in the crack plane would adhere very well to the matrix resin which is of the same chemistry. Besides, these healing monomers might be polymerized in the crack plane by free radicals that are already available in the host material. This would also mean that no additional selective catalyst for the healing compound is needed. If the acrylic monomers employed for this purpose are derived from palm-oil it would be an ecological friendly and cost-saving solution by taking advantage of local resources.

TEGDMA was successfully encapsulated in a PUF shell with a high yield of microcapsules as revealed by digital microscopy (Fig. 3-18 a) and OM. The product appeared as a white free-flowing powder. Microcapsules could also be produced when a 1:1 mixture of Bis-GMA to TEGDMA was used as core resin. However, the capsules tended to stick together and the capsule shell seemed wrinkled as it can be seen in the optical micrograph in Figure 3-18 b. When using other Bis-GMA/TEGDMA mixtures

similar results were obtained. Neither MMA nor the UDMA/TEGDMA mixtures could be enclosed by the *in situ* oil-in-water emulsion encapsulation method which is probably due to the higher intolerance of these monomers towards water. Besides, it seemed that the viscosity of the monomer to be encapsulated is a relevant parameter for the formation of the PUF shell around the monomer droplets.

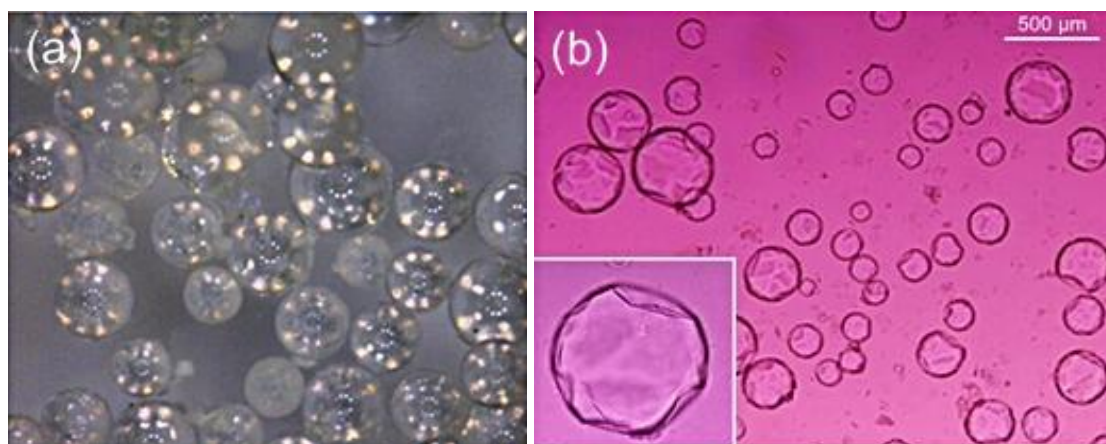


Figure 3-18 (a) Digital micrograph showing PUF/TEGDMA microcapsules and (b) optical micrograph illustrating PUF microcapsules that contain a 1:1 Bis-GMA/TEGDMA mixture.

Finally, the increase in the amount of the emulsifier did not show any positive effect on the formation of the microcapsules. In summary, this study showed that it is possible to encapsulate other dental monomers by this *in situ* microencapsulation method. Depending on the chemistry of the core monomer the process parameters might have to be adjusted.

3.4.7 Shelf-Life of Microcapsules

One consideration when choosing the compounds for the self-healing system was the stability of the healing agent and the impermeability of the PUF capsule shell.

Only as long as the DCPD is stored inside the capsule the applied healing system can effectively stop the growing of a crack. Hence, a long shelf-life of the microcapsules is extremely important.

Generally, any leakage of the core monomer would result in a discolouration of the product showing the yellow colour of DCPD along with the development of the strong typical smell of the DCPD monomer. If this is the case the capsules would also show the tendency to stick together and the powder would not be free-flowing anymore. This means that important indications concerning the stability of the capsules can be visually obtained. Chemical and physical changes were detected by spectroscopy and thermoanalyses, respectively.

3.4.7.1 Discolouration and Flowing Behaviour after Storage

All microcapsule batches were visually examined for discolouration and flowing behaviour after certain storage times ranging from 1 month to 2 years (if applicable). Special consideration was given to the samples that were post treated with different solvents and the batches of varied formaldehyde to urea ratio in the capsule shell (details in section 3.3.2.3 and 3.3.2.4, respectively). The PUF/DCPD microcapsules that were washed with ethanol and stored up to 2 years did not show any visible change; they all were still of white colour and free-flowing. Furthermore, there were no perceptible changes in the appearance after 1 ½ year storage time among the microcapsules that were rinsed with acetone. Hence, the treatment with alcohol or acetone to clean and separate the capsules did not have any apparent negative impact on the capsule shell.

The microcapsules that were produced with lower formaldehyde content in the shell showed after 2 months a strong discolouration and smell of the DCPD monomer

along with the building of lumps. Higher formaldehyde content led to the formation of a thicker outer capsule shell layer which resulted in an extended storage time. The samples with a formaldehyde-urea ratio of 1.9 and 2.3 were still intact after 1 ½ year.

Finally, the PUF microcapsules that incorporated the TEGDMA monomer appeared still flawless after 12 months storage time whereas after 18 months the capsules had become a slight yellowish touch and were clumped together. Linear backbone type monomers might easier penetrate through the capsule shell rather than a monomer of the DCPD structure which might result in a reduced storage time of PUF capsules containing TEGDMA.

3.4.7.2 Chemical Stability of the Core Monomer

Chemical changes in materials can be identified by spectroscopic methods. In the case of the DCPD monomer proton NMR spectroscopy is applicable. Therefore, the extracted core compound of the PUF/DCPD microcapsules was analysed at time periods ranging from 3 months to 2 years. The resulting spectra demonstrated that there was no change in the structure of the encapsulated monomer after up to 2 years storage time with the peaks of DCPD appearing at the typical frequencies. The single spectra of this set of analyses as well as the absorption data of each spectrum are not provided since they all showed exactly the same pattern as it was reported earlier in this work (page 79, section 3.4.5.3, Fig. 3-17).

3.4.7.3 Physical Stability of the Microcapsule Shell

Possible physical changes in the PUF shell material can be revealed using thermoanalytical techniques. For example, an increasing melting temperature with storage time could indicate further cross-linking which might happen within the

polymeric material whereas a decrease might be the result of degradation. TGA and DSC were applied to detect possible physical changes of the standard PUF/DCPD microcapsules after 3, 6, 12, 18, and 24 months storage.

The DSC plots of the microcapsules showed no significant changes after the different time periods. Figure 3-19 illustrates the heat flux curves which all indicate a slight increase in the heat flow due to the boiling of DCPD followed by the melting of the PUF shell material at around 250 °C. Furthermore, the TGA results did not reveal any obvious discrepancies with increasing storage time. All TGA diagrams showed a sudden weight loss resulting in a peak in the temperature range of 240-290 °C which can be referred to the vaporization of the DCPD. The thermograms of the PUF/DCPD microcapsules after 6 months, 1 year, 1 ½ and 2 years storage time can be found in appendix B.

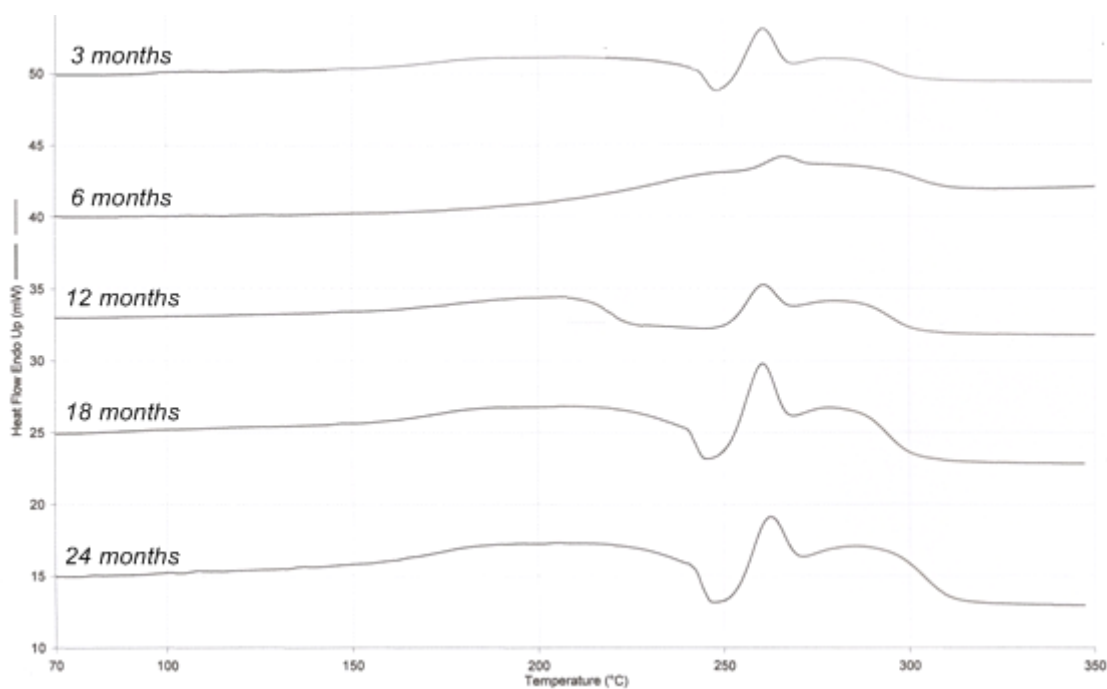


Figure 3-19 DSC curves of PUF/DCPD microcapsules after different storage times.

In summary, these tests showed that the quality of the PUF/DCPD microcapsules remained unaffected for more than two years. This means the capsules can be stored at room temperature for this period of time without undergoing chemical or physical changes.

3.5 Summary and Conclusions

PUF microcapsules filled with DCPD were successfully prepared by *in situ* condensation polymerization of the UF shell materials. The aftertreatment of the product with ethanol and acetone, significantly improved the quality of the product.

With a shear rate of 450 rpm microcapsules in the size range of 50–500 microns were produced. High yields (78–85 %) of spherical microcapsules were obtained which appeared in the form of a free-flowing white powder. The optimum pH for the synthesis was 3.5 and it was found that the reaction needed a minimum of 3 hours to be completed. In the end the product has to be rinsed with ethanol or acetone to obtain individual capsules.

The shelf-life of the PUF/DCPD microcapsules is more than two years when stored at room temperature (26–35 °C). The PUF shell material exhibited the same thermal stability after this time period. It provided a protective barrier of the encapsulated monomer which structure remained unchanged.

Furthermore, it was shown that ¹H-NMR spectroscopy, FTIR spectroscopy and DSC are all useful methods to verify the DCPD core monomer whereas the capsule shell was examined by different microscopic methods. The microcapsule shell consisted of a smooth inner PUF membrane of about 120–140 nm in size as determined by FESEM. This continuous inner shell membrane is essential as it prevents leakage of the core monomer. The inner membrane is surrounded by a rough

porous outer layer, consisting of PUF nanoparticles, which measured about 10–15 μm . OM revealed that with increasing formaldehyde content the outer shell wall can be extended. The rough porous layer is important as it would promote the adhesion of the capsules to the matrix resin when embedded in a polymeric host material. A good adhesion is necessary to maintain the properties of the virgin material.

CHAPTER IV

MELAMINE MODIFICATION OF THE PUF MICROCAPSULE SHELL AND INCORPORATION OF THE MICROCAPSULES IN A DENTAL MATRIX

4.1 Introduction

First tests showed that the PUF/DCPD microcapsules break easily when incorporating them into a dental composite host material. Therefore it was necessary to produce microcapsules with a tougher and more robust shell than UF resins provide. Urea-melamine-formaldehyde (UMF) polymers are known to have higher bond qualities and strength in comparison to UF resins due to the eminent cross-linking ability of melamine (Tohmura *et al.*, 2001, Pizzi and Mittal, 2003). Even small amounts of melamine can significantly toughen the UF material.

To enhance the properties and performance of the microcapsules for the application in a dental composite a series of PUF/DCPD microcapsules were prepared with melamine amounts ranging from 0% to 5% relative to the urea amount in the capsule shell. The microcapsule manufacture was carried out according to the procedure which is described in section 3.3.1 using the same instruments and equipment if not stated otherwise. The capsule performance when applied in a dental host material was then investigated by microscopic methods and mechanical tests.

4.2 Materials

Urea, ammonium chloride, resorcinol, DCPD, 37% HCl and 1-octanol were acquired from Sigma-Aldrich. The 37 wt% aqueous formaldehyde solution was purchased from System, the additional wall-forming material hexamethoxy-

methylmelamine (Cymel 303) from Cytec Industries and ethanol from HmbG Chemicals. NaOH pellets were supplied from R&M Chemicals which were dissolved to obtain a 3 molar NaOH solution, whereas HCl was received from Merck and diluted to provide a 12 molar HCl solution. The emulsifier EMA with an average $M_w = 100,000\text{--}500,000$ was purchased from Sigma-Aldrich and dissolved in water to produce a 2.5 wt% solution. The dental materials which were acquired from Sigma-Aldrich included the monomers Bis-GMA and TEGDMA as well as the light-curing system EDMAB and CQ. All chemicals and solvents were of analytical grade except for the Cymel 303 which was of technical grade. They were all used as received.

4.3 Method

4.3.1 Preparation of Melamine Modified PUF/DCPD Microcapsules

The microcapsules were prepared following the general procedure for the preparation of PUF/DCPD microcapsules, except for the stirring speed and the urea amounts which were partly replaced by the Cymel 303. The urea and melamine parts are therefore listed in Table 4-1.

Table 4-1 Urea and melamine parts used for the preparation of the melamine modified PUF/DCPD microcapsule test series

Sample No.	Cymel in (%)	Cymel in (g)	Urea in (g)
1	0	0.000	2.500
2	0.5	0.025	2.488
3	1	0.053	2.475
4	2	0.105	2.450
5	3	0.158	2.425
6	4	0.210	2.400
7	5	0.263	2.375

The melamine component was dissolved in a minimum amount of ethanol before it was added. The agitation rate was increased from 450 rpm to 500 rpm to obtain capsules of a slightly smaller average diameter than in the previous experiments. The product was rinsed with ethanol and sieved through precision test sieves of 50, 300 and 500 microns mesh size. The size fraction of 50-300 microns was separated for further processing whereas the product with diameters less than 50 microns and higher than 500 microns was discarded.

4.3.2 Characterization of Melamine Modified Microcapsules

4.3.2.1 General Analysis

The product analysis which was performed on each of the melamine modified PUF/DCPD microcapsule batches included the yield, microscopic inspections, and the proof of the core content by proton NMR. The yield was calculated from the total mass of the dry microcapsules in the size range of 50 to 500 microns as the weight percent of the starting materials of the microcapsule constituents. The shape and purity of the product were examined by digital microscopy. For the verification of the core content the dry microcapsules were ground with a pestle in a mortar and extracted with deuterated acetone to be measured by $^1\text{H-NMR}$ spectroscopy.

4.3.2.2 Determination of Shell Composition

FTIR-ATR analysis was employed for the inspection and comparison of the neat PUF/DCPD microcapsules with the sample in which 5% urea was replaced by melamine. To determine the melamine amount in the capsule shell, FTIR spectroscopy was also measured on the extracted shell material of the two samples. Therefore, the microcapsules with 5% melamine content referring to the urea part were ground with a

pestle in a mortar. The crushed material was collected and intensively washed with acetone so that it was free of DCPD. The same procedure was undertaken with capsules of the pure PUF shell (0% melamine). The FTIR spectra of the dried powders were then recorded from 4000-450 cm^{-1} each.

Furthermore, thermal analyses were performed for the differentiation of the melamine modified shell from the neat PUF material. The heat flow of the two samples of extracted shell material were measured using DSC from 35 °C to 350 °C at a heating rate of 10 °C/min in a single scan. In addition, TGA was employed for which small amounts of the samples (approximately 5 mg) were scanned from 50 to 900 °C at a rate of 10 °C/min. Prior to the thermoanalytical measurements, the samples were placed in the vacuum oven for 3 days at 38 °C and 0.3 bar to remove any possible moisture.

4.3.2.3 Examination of Shell Morphology

The microcapsule shell morphology of both samples, the neat PUF/DCPD microcapsules and the 5% melamine modified capsules, was examined and compared by FESEM. Samples were taken from microcapsules in the size range of 50–300 μm from each batch. They were mounted on a conductive stage and part of the capsules was ruptured with a razor blade to facilitate shell membrane inspections. Low vacuum was applied and the samples were measured without being sputtered using a voltage of 5 kV and a spot of 3.0.

4.3.3 Incorporation of Microcapsules in Dental Host Material

To increase the strength of the microcapsule shell the initial PUF shell membrane was modified with small amounts of melamine ranging from 0.5–5%

referring to the urea part. The following tests concentrate on the performance of these microcapsules when embedded in the dental acrylic host material to evaluate the strengthening effect of the increasing melamine amounts. Thus, the addition of filler particles and ruthenium catalyst were neglected. Relevant design parameters are the adhesion of the interface between the microcapsule and the matrix, and the hardness and flexural strength of the resulting material.

4.3.3.1 Specimen Preparation

The monomers Bis-GMA and TEGDMA were mixed together in the ratio of 7 to 3 by weight. In a dark environment, the corresponding initiator system consisting of 2.3 wt% EDMAB and 0.7 wt% CQ was added. The ingredients were homogeneously mixed and degassed in an ultrasonic bath to obtain the dental host material. The microcapsules were carefully added and the mixture was sonicated for another 30 minutes to remove any air bubble. Two different weight percentages of microcapsules of the size fraction 50 to 300 microns were incorporated. In the first set a series of 6 wt% of the microcapsules in which 0.5%, 1%, 2%, 3%, 4% and 5% of the urea was replaced by melamine were added. In a second set a series of 3 wt% microcapsules of the 1%, 3%, and 5% melamine modified capsules were added. As reference material for each test series resin mixtures were prepared in which 6 wt% and 3 wt% DCPD filled microcapsules with the neat PUF shell (0% melamine) were incorporated. Furthermore, one sample of the virgin host material without microcapsules served as a reference in both test series.

The prepared matrix resin was poured into cylindrical metal moulds (dimensions: $h = 2 \pm 0.1$ mm, $d = 8 \pm 0.1$ mm) for hardness measurements after curing. Beforehand a strip of transparent film was placed on the bottom of the mould and a

thin layer of wax was applied on the metal surfaces beforehand to facilitate removal of the cured specimen. After filling the moulds with the resin they were covered with a polyester film and a flat glass plate. Gentle pressure was manually applied to displace excess material. The pressure was kept whilst hardening the samples by light-curing. Therefore, the exit window of a halogen curing light (Dentsply) was placed at the centre of the specimen on the glass plate and the specimen was irradiated for 60 minutes. The mould with the samples was then turned around to irradiate the samples from the other side for another 60 minutes. Five specimens of each sample of the 3 wt% and 6 wt% microcapsules containing series were prepared for microhardness tests. An additional specimen of each sample that incorporated 6 wt% microcapsules was produced for nanoindentation hardness measurements.

Furthermore, bar shaped specimens to determine the flexural strength in a three-point-bending test were prepared (dimensions: $l = 25 \pm 2$ mm, $h = 2 \pm 0.1$ mm, $t = 2 \pm 0.1$ mm) according to ISO 4049:2000. Each flexural strength specimen was irradiated for 100 seconds in total from either side (5 sections, 20 minutes each). After the specimens were removed from the moulds any flash was carefully trimmed away using 600, 1000, 1500 and 2000 grit abrasive papers. For the three-point-bending test eight test specimens were prepared each. All samples were stored in distilled water at 37 ± 1 °C for 24 hours prior to testing.

4.3.3.2 Examination of Embedded Microcapsules by Microscopy

After the incorporation of the microcapsules into the dental host material, the distribution of the microcapsules in different three-point-bending test specimens was examined using a Meiji Techno RZ stereo microscope. Seven samples of the

specimens that contained 3 wt% microcapsules and another seven samples of the specimens incorporating 6 wt% microcapsules were inspected.

Furthermore, FESEM was employed to study the microcapsule shell adhesion to the host material. Therefore, three-point-bending test specimens that contained 6 wt% microcapsules with a pure PUF shell and specimens with the 5% melamine modified PUF shell were placed in the freezer. After a few hours they were removed and immediately ruptured to obtain a smooth cut. The interface between capsule and host matrix was then inspected by FESEM on the broken surface.

4.3.3.3 Mechanical Tests

The flexural strength measurement was performed according to ISO 4049:2000 using a Shimadzu AG-X high precision universal testing machine. The setup consisted of two rods (2 mm in diameter), mounted parallel with 20 mm distance, on which the test specimen was placed. The load was applied to the specimen at a cross-head speed of 0.75 ± 0.25 mm/min until the specimen fractured. Prior to testing the dimensions of each three-point-bending test specimen were measured to an accuracy of ± 0.01 mm using a vernier calliper. Eight specimens of each sample were measured.

Vickers hardness tests were carried out on a Shimadzu HMV-2 microhardness measuring machine according to ASTM E 384 - 89:1990 using a test force of 980.7 mN (HV0.1) and 5 seconds indentation duration. Measurements were obtained from 5 specimens with 5 indentations each, so that in total 25 indentations were analysed per sample. The nanoindentation hardness was determined on a dynamic UMH tester (Shimadzu DUH-211) using a Berkovich indenter. Load-unload tests were performed applying a test force of 50 gf (490.33 mN) and a hold time of 5 seconds. Nine indentations were measured on each specimen.

4.4 Results and Discussion

The first part of this section concentrates on the microcapsule analysis with the main focus on the determination of the small melamine amount in the microcapsule shell. In the second part the results of the microcapsules after the incorporation are presented, in particular the mechanical properties and the microcapsule shell adhesion to the matrix resin.

4.4.1 Microcapsule Analysis

4.4.1.1 Yield, Quality and Shell Morphology

PUF/DCPD microcapsules in which the urea was partly replaced by melamine in varying amounts (as it is described in Table 4-1) were successfully prepared. The yields for the microcapsule size fraction of 50–500 microns were in the range of 76–89%. The product of each batch was examined using a digital microscope which all looked alike. The microcapsules were of globular shape and appeared in the form of a free-flowing white powder. The amount of residual matter was negligible. FESEM did not reveal any significant difference between the pure PUF and the melamine modified PUF capsule shell morphology.

4.4.1.2 Verification of Core Content

The determination of the capsule fill content by $^1\text{H-NMR}$ spectroscopy clearly proved the presence of the core monomer. All spectra obtained from the different microcapsule extracts resembled each other showing the characteristic peaks of neat DCPD as it was illustrated earlier in section 3.4.5.3, Figure 3-17. The result was confirmed by the FTIR analysis of the PUF/DCPD microcapsules in which 5% of the urea part was replaced by melamine in comparison with the corresponding extracted

shell matter. The spectra of the DCPD filled microcapsules contained all the characteristic peaks of the core monomer which were not present in the spectra of the shell material; details on the interpretation were discussed beforehand (section 3.4.5.1, Fig. 3-15).

4.4.1.3 Shell Composition by FTIR Spectroscopy

In addition FTIR spectroscopy was used to differentiate the melamine modified shell from the neat PUF shell. Figure 4-1 displays the overlaid spectra of the two samples of the extracted shell material. All typical absorptions of PUF are visible in both spectra such as the N-H, H-C-H and NH-CO-NH vibrations at 3334 cm^{-1} , 2963 cm^{-1} and 1627 cm^{-1} , respectively.

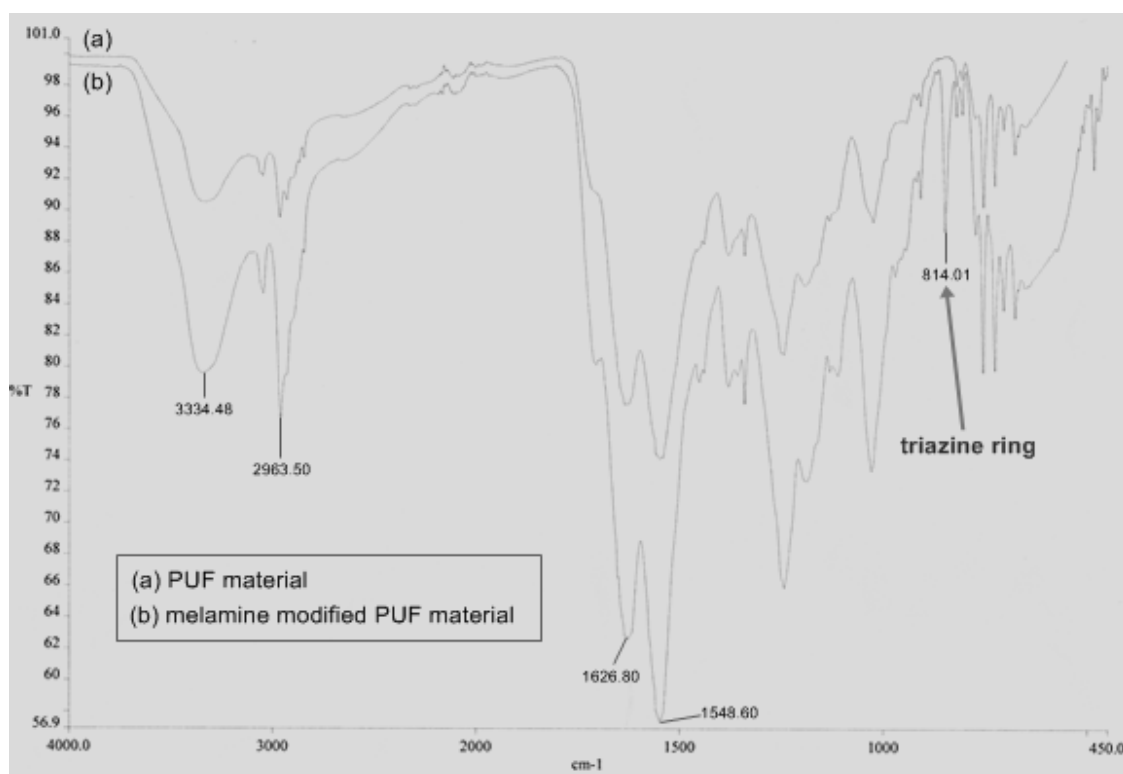


Figure 4-1 FTIR-ATR spectra of extracted neat PUF capsule shell matter in comparison with the extracted melamine modified PUF shell material.

The two curves match each other, except for one very obvious additional peak in the spectrum of the melamine modified microcapsule shell at 814 cm^{-1} . This distinct absorption peak corresponds to the vibration of the triazine ring which shows that the PUF microcapsule shell containing melamine had been formed. Hence, FTIR-ATR spectroscopy clearly proved that the melamine modification of the PUF microcapsule shell was successful.

4.4.1.4 Differentiation of Shell Composition by Thermoanalytical Methods

The DSC plots of both samples showed endothermic melting peaks. Figure 4-2 illustrates the heat flow curves of the extracted pure PUF microcapsule shell material in comparison with the curve of the sample in which 5% of the urea was replaced by melamine. The melting temperature (T_m) of the PUF material was $267\text{ }^\circ\text{C}$ and T_m of the melamine modified sample was reached at $264\text{ }^\circ\text{C}$.

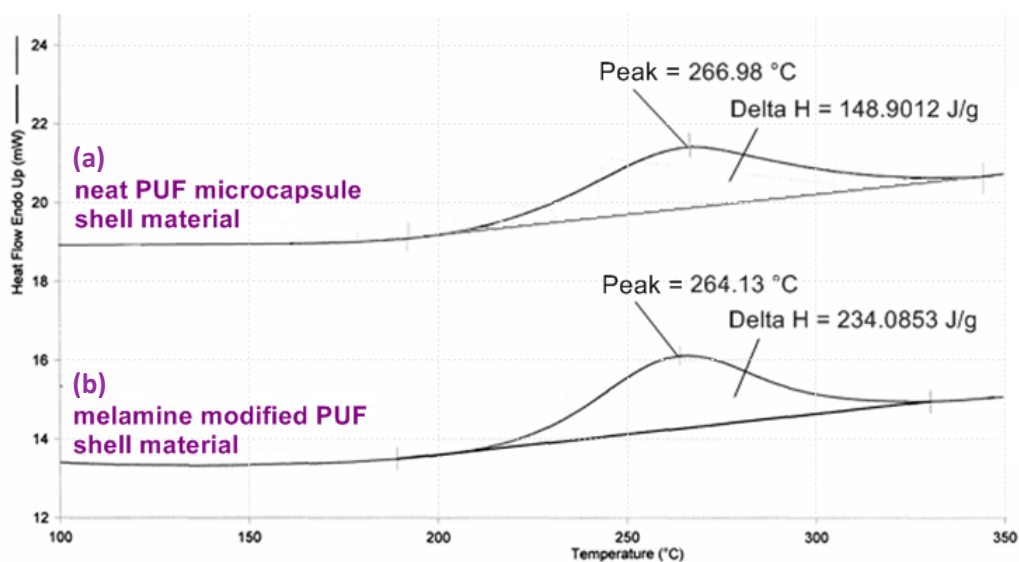


Figure 4-2 DSC plots of extracted PUF microcapsule shell matter: (a) neat PUF material and (b) the shell material in which 5% of the urea were replaced with melamine.

A distinct differentiation was provided by the enthalpy of melting (ΔH_m) which is calculated from the peak area. ΔH_m was considerably higher for the melamine modified sample (234 J/g) than for the neat PUF material (149 J/g). Since one melamine molecule possesses 3 amine groups with 2 hydrogen atoms each a highly cross-linked polymer network can be built. The urea molecule consists only of two of these amine functional groups with no more than 3 hydrogen atoms being able to react. Hence, the increased ΔH_m might be an indication for the higher amount of crystallinity with 5% of the urea being replaced with melamine.

The resulting TGA thermograms of the two different samples are compared in Figure 4-3 which displays both, the weight loss curve and the derivative weight. The weight percent of the pure PUF shell material showed a sudden drop of about 75 % starting around 200 °C and continuing until about 330 °C which demonstrates the decomposition of the PUF material. Further moderate weight loss until 650 °C might represent the decomposition of the higher thermally stable cross-linked PUF polymer.

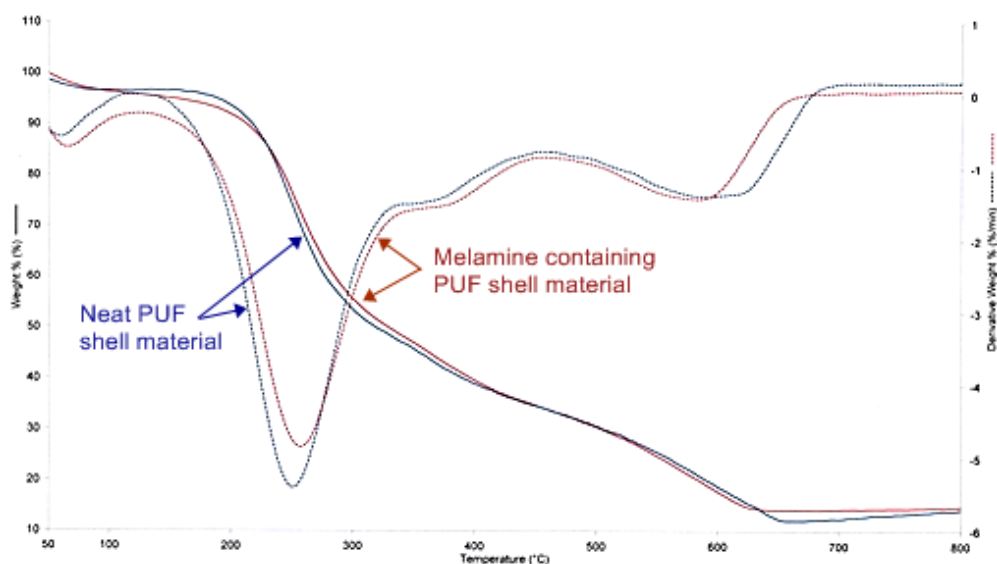


Figure 4-3 TGA curves of extracted PUF microcapsule shell material in comparison with the melamine modified shell material.

The melamine modified sample exhibited a little less abrupt mass loss in the same area (150-330 °C) of about 60 % and showed a maximum decomposition temperature of approximately 620 °C. The plot of the derivative weight displayed a peak at higher temperature for the melamine modified sample at approximately 260 °C than the one of the neat PUF material which was about 250 °C. In summary, the weight loss of the melamine modified microcapsule shell material occurred at a slower rate and slightly higher temperatures than that of the pure PUF material.

4.4.2 Characterization of Microcapsule Embedded Polymeric Material

The results of selected important mechanical properties to characterize dental restorative materials next to microscopic inspections are presented in the following sections. Toughness values and the modulus of elasticity could not be calculated from the mechanical measurements due to the brittleness of the dental material without filler.

4.4.2.1 Microcapsule Distribution in the Host Material

With the help of a stereo microscope the distribution of the 3 wt% and 6 wt% microcapsules in the dental host material were inspected. All samples showed a random distribution of the microcapsules throughout the host material as apparent from the example micrograph in Figure 4-4. This is a very important factor as well dispersed microcapsules increase the probability that an upcoming crack encounters the capsules in a self-healing system.

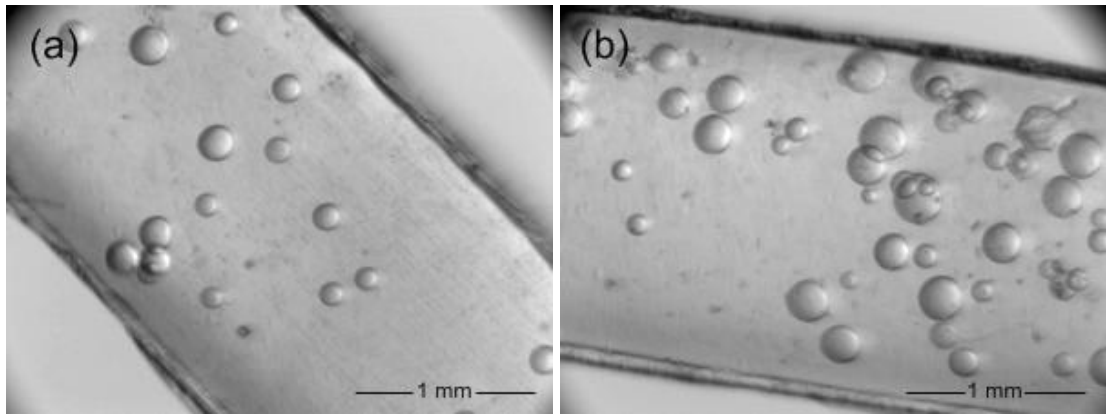


Figure 4-4 Optical micrographs of (a) 3 wt% and (b) 6 wt% PUF/DCPD microcapsules embedded in a dental host material.

4.4.2.2 Inspection of Microcapsule-Matrix Interface by FESEM

To achieve optimum crack-mending ability in a self-healing system an equal distribution of the microcapsules in the host material is required along with very good bonding ability of the capsule shell to the host resin. Images obtained from FESEM (Figure 4-5) show that the rough exterior shell wall of the embedded melamine modified PUF microcapsule is infiltrated by the matrix methacrylates. This is highly advantageous for promoting bonding of the capsules to the polymeric host material, and it increases the probability of the capsule rupture upon crack intrusion. The bonding ability of the pure PUF microcapsule shell to the dental methacrylic host material was not clear from the FESEM image.

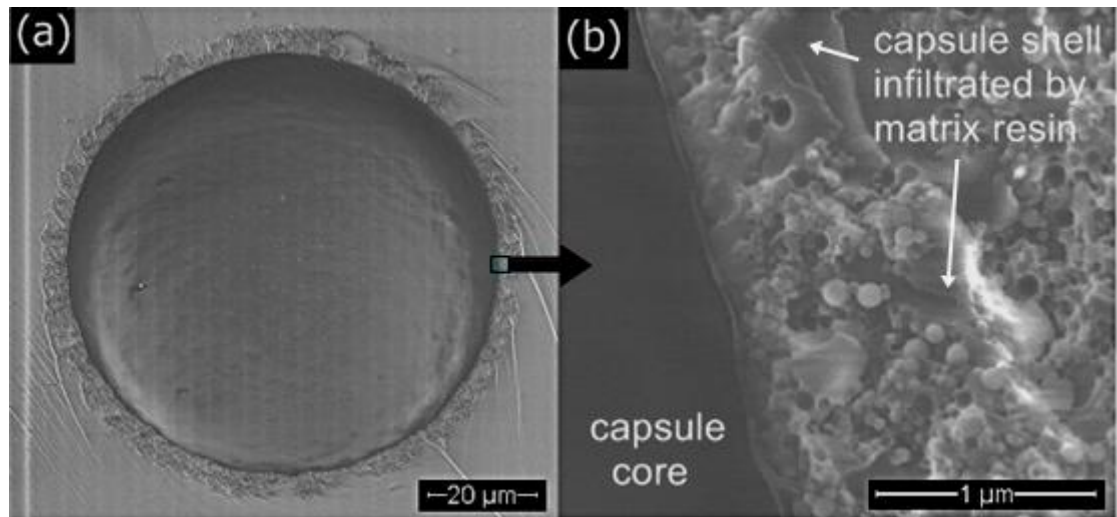


Figure 4-5 FESEM images of (a) melamine modified PUF/DCPD microcapsule embedded in a dental host material, and (b) the interface of the microcapsule shell and the dental matrix material.

4.4.2.3 Flexural Strength

Figure 4-6 illustrates the results obtained from the three-point-bending measurements of the test series that incorporated 3 wt% and 6 wt% microcapsules with different melamine amounts in the microcapsule shell (0–5% corresponding to the urea part). The average values were calculated from at least 7 measurements. The results were compared with the original dental material that did not contain any microcapsules which showed the highest flexural strength of 106.3 ± 19.8 MPa. Within the 3 wt% microcapsule test series (Fig. 4-6 a) the maximum value was reached for the sample with the pure PUF shell (105.1 ± 24.8 MPa). The flexural strength of the microcapsules comprising small amounts of melamine were in the range of 73.5 ± 4.7 MPa to 85.2 ± 7.1 MPa. The test results for the 6 wt% series (Fig. 4-6 b) were in the range of 64.6 ± 13.5 MPa to 87.1 ± 8.4 MPa with the lowest value obtained from the pure PUF/DCPD microcapsules (0% melamine) and the maximum value from the sample that contained 1% melamine in the capsule shell. Overall, the flexural strength

was not much affected by the incorporation of the microcapsules. There was no significant variation within each test series and the trend was not considerable.

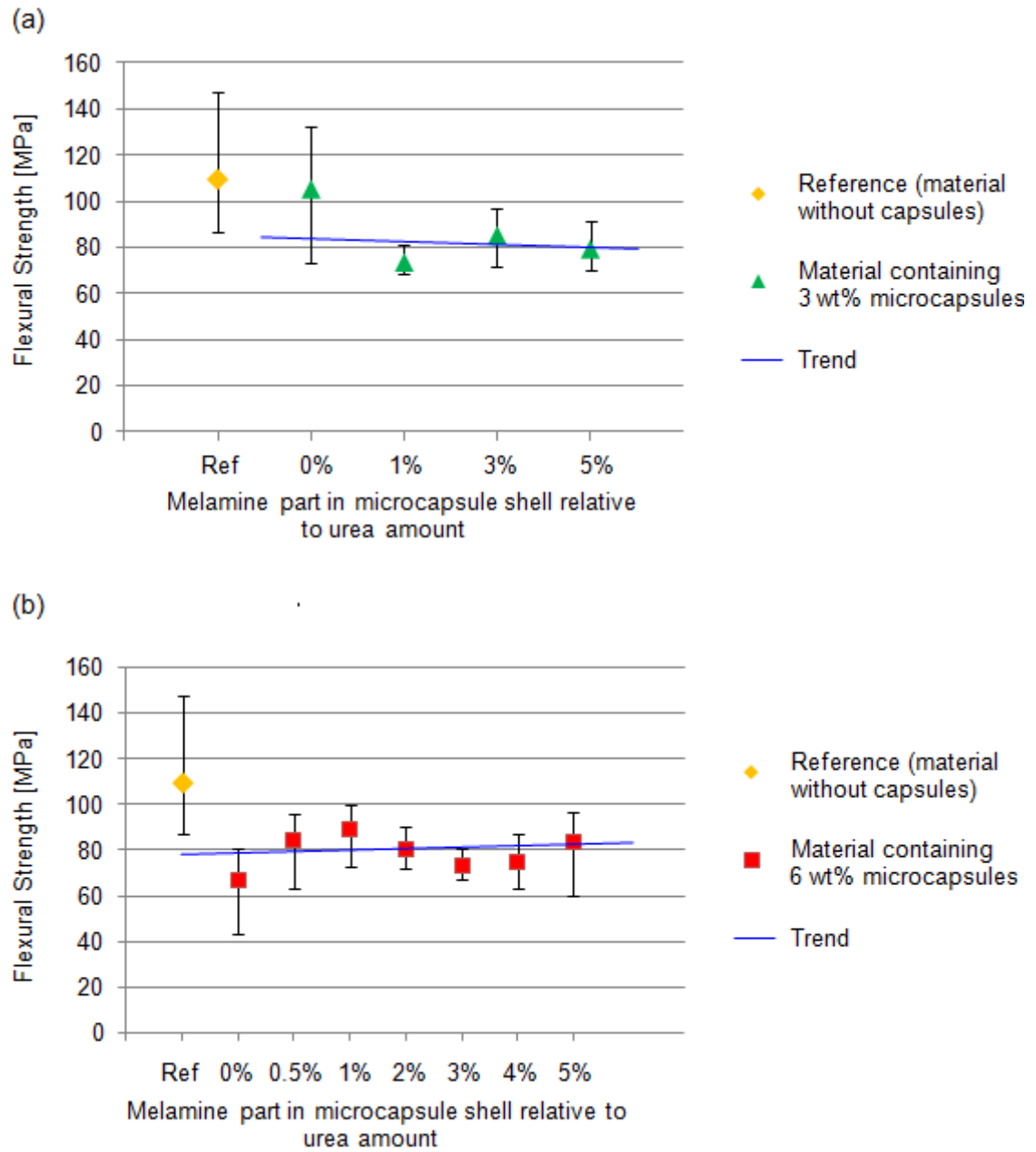


Figure 4-6 Flexural Strength of dental polymeric materials containing PUF/DCPD microcapsules which comprise different melamine amounts in their shell. The dental materials incorporated (a) 3 wt% and (b) 6 wt% microcapsules.

4.4.2.4 Vickers Hardness by Microindentation Measurement

Similar to the flexural strength, the Vickers hardness of the virgin material (30.7 ± 1.4 HV) did not differ much from the test results after the incorporation of microcapsules as displayed in Figure 4-7. There was no obvious trend within the two test series. The dental material containing 3 wt% microcapsules reached hardness values in the range of 24.1 ± 0.8 HV to 25.8 ± 0.9 HV with the minimum hardness obtained from the material containing the microcapsules of a neat PUF shell (Fig. 4-7 a). The maximum HV was reached by the sample with 5% urea being replaced by melamine in the PUF capsule shell. This observation leads to the assumption that an increasing melamine part in the PUF capsule shell can produce better bonding to the matrix material. However, this statement could not be backed by the 6 wt% microcapsule embedded material which resulted in a maximum hardness value of 28.8 ± 1.1 HV for the 0.5% melamine sample (Fig. 4-7 b); the minimum hardness was measured for the 2% melamine sample with 21.7 ± 1.1 HV. To conclude, the incorporation of the different melamine modified PUF/DCPD microcapsules into the dental material did not reveal any significant trend in the Vickers hardness measured by the microindentation method.

4.4.2.5 Nanoindentation Hardness

Nanoindentation test results were obtained from at least 8 measurements per sample. Figure 4-8 a displays the result of the material containing 3 wt% microcapsules which revealed slightly higher hardness values for the neat material (without capsules). In contrary, the nanoindentation test resulted in a lower hardness for the original material (177.4 ± 8.2 MPa) when compared with the 6 wt% microcapsule embedded samples (Fig. 4-8 b). Within this test series the peak value was achieved by

the material that incorporated microcapsules with 1% urea being replaced by melamine in the capsule shell (238.0 ± 24.8 MPa), followed by the 5% sample with 223.7 ± 33.9 MPa, and 194.4 ± 29.2 MPa for the 2% sample. The material containing capsules of a pure PUF shell had the lowest nanoindentation hardness values (149.7 ± 7.2 MPa).

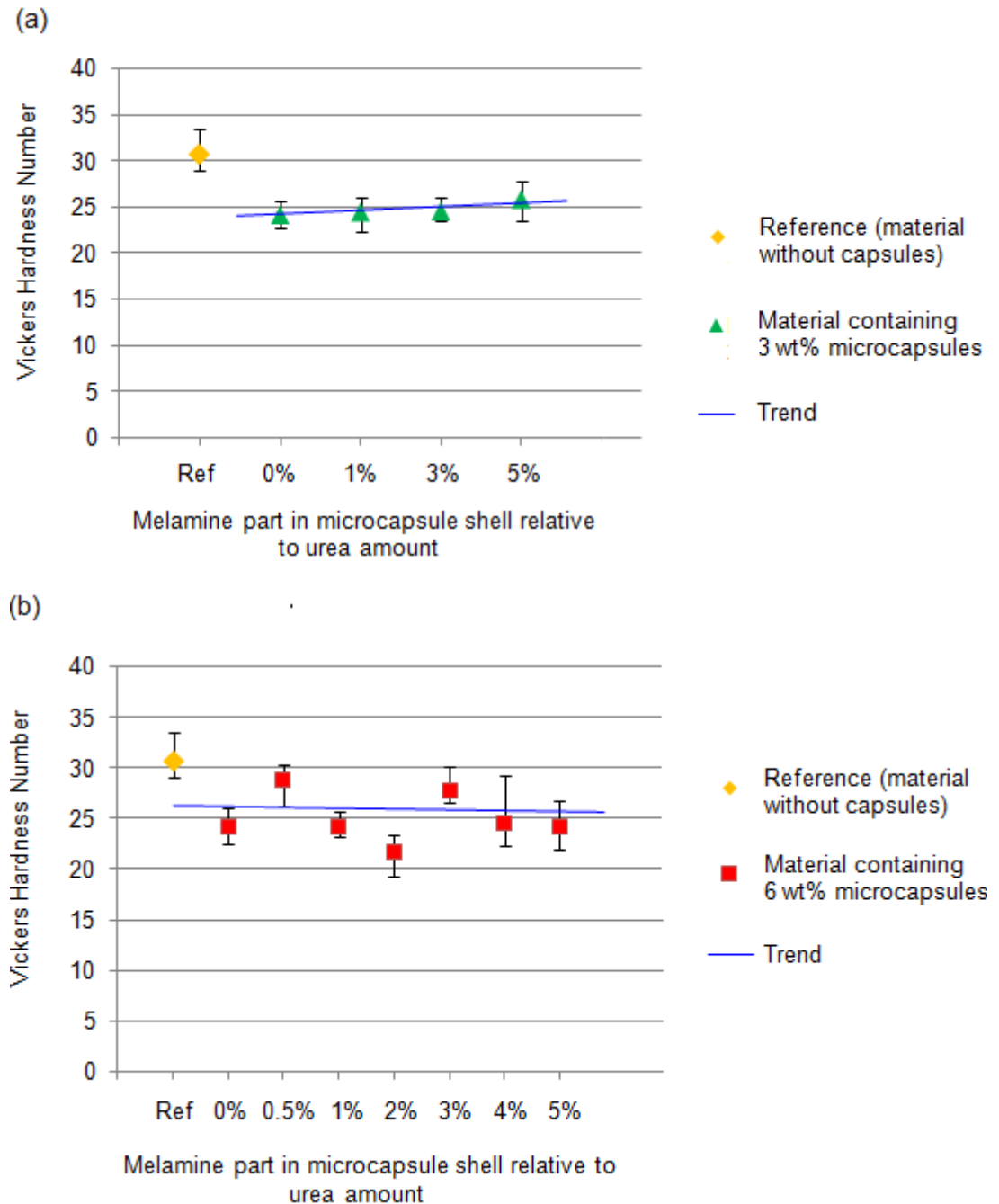


Figure 4-7 Vickers hardness of dental polymeric materials containing (a) 3 wt% PUF/DCPD microcapsules and (b) 6 wt% microcapsules with different melamine amounts in the PUF shell.

Based on these test results there is a probability that higher cross-linking of the melamine modified PUF material strengthened the capsule shell and enhanced the adhesion to the dental host material, although it may contradict the three-point-bending test results.

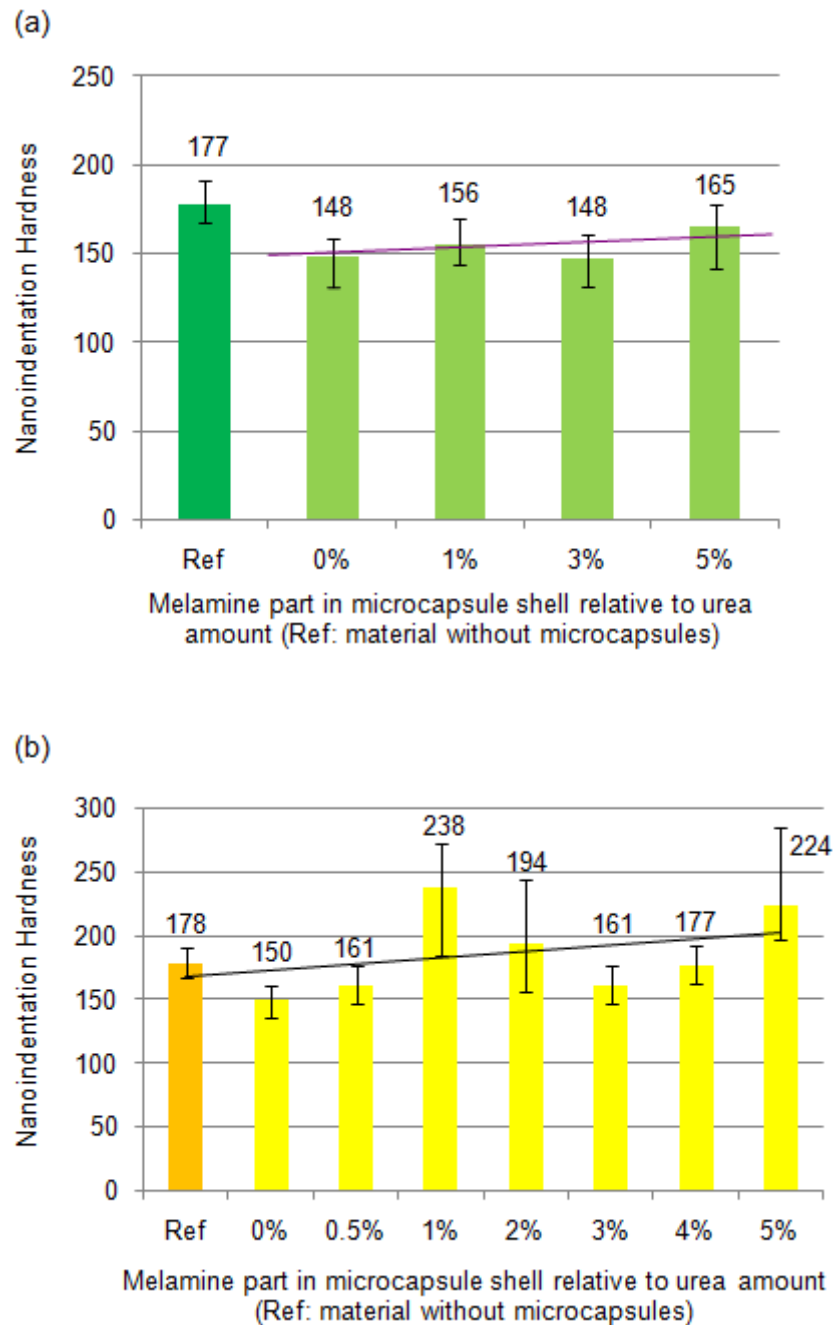


Figure 4-8 Nanoindentation hardness of dental polymeric materials containing (a) 3 wt% PUF/DCPD microcapsules and (b) 6 wt% PUF/DCPD microcapsules with different melamine amounts in the capsule shell.

4.4.2.6 Young's Modulus

The Young's Modulus was obtained from nanoindentation measurements. The average values as they are displayed in Figure 4-9 were calculated from at least eight measurements. The elastic properties of the reference material (without microcapsules) and the test series that incorporated 3 wt% microcapsules did not differ significantly as it is obvious from the bar chart in Figure 4-9 a. The elastic modulus of the 3 wt% test series was in the range of 2304 ± 121 MPa to 2628 ± 142 MPa. Whereas the resulting values of the 6 wt% test series (Fig. 4-9 b) showed much higher variations ranging from 1833 ± 156 MPa to 3072 ± 365 MPa with the lowest value obtained from the sample with the neat PUF microcapsule shell and the maximum reached by the 5% melamine modified capsule shell sample. The average elasticity of the neat material without incorporated microcapsules was 2618 ± 128 MPa. The bar chart reveals a slight tendency towards higher elastic modulus values with increasing melamine content in the capsules shell when 6 wt% microcapsules are embedded in the dental host material.

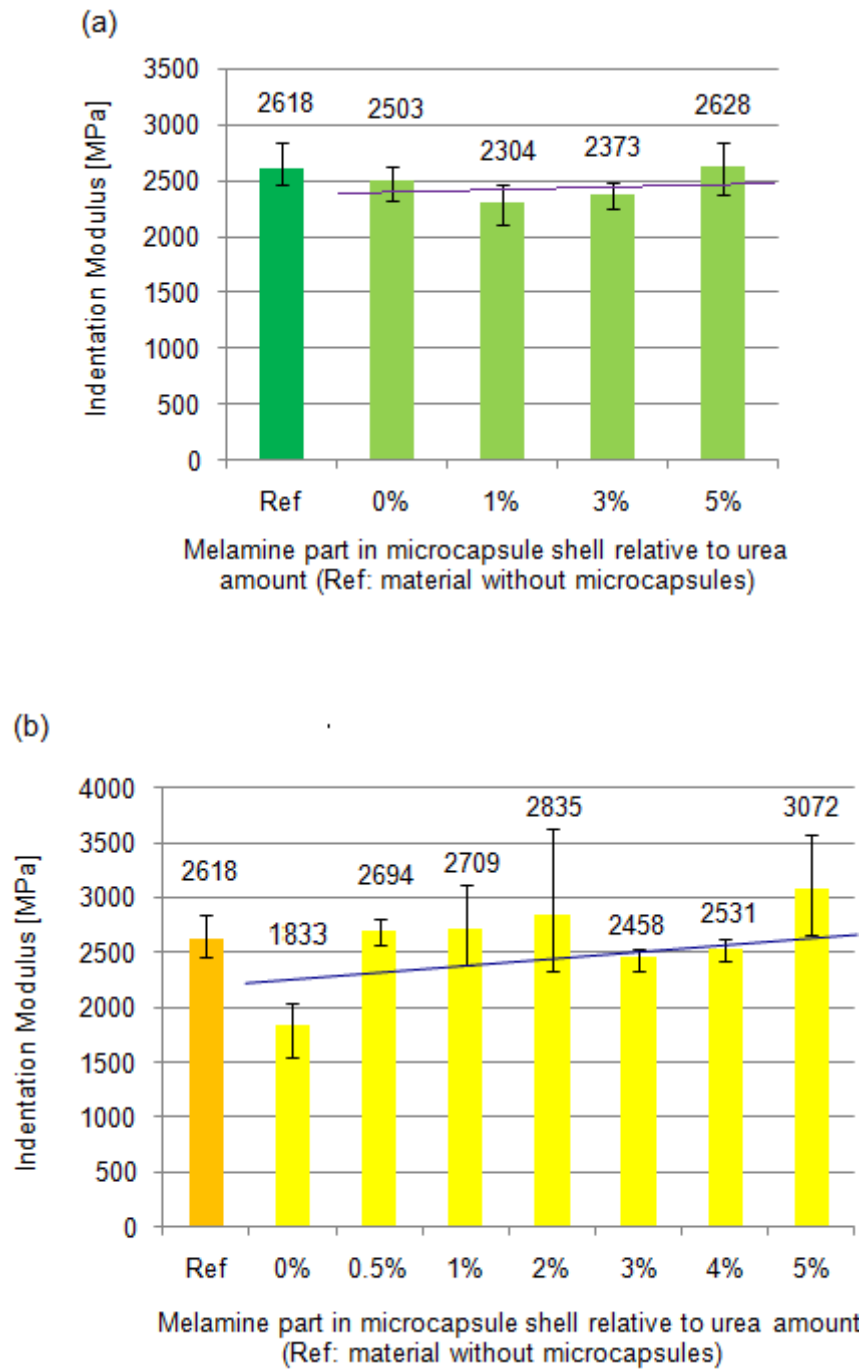


Figure 4-9 Young's Modulus obtained from nanoindentation hardness measurements of dental polymeric materials containing (a) 3 wt% PUF/DCPD microcapsules and (b) 6 wt% PUF/DCPD microcapsules with different melamine amounts in the microcapsule shell.

4.5 Summary and Conclusion

A series of microspheres that encapsulated DCPD were successfully prepared in which the melamine proportions in the UMF shell was varied. Annular shaped capsules of 50–500 microns in diameter were obtained with high yields (76-87%). The core content was proved by proton NMR and FTIR spectroscopies whereas the melamine modification of the PUF capsule shell was verified using FTIR and thermoanalytical methods.

A set of two different microcapsule amounts embedded in the dental host material was prepared and inspected by microscopy as well as mechanical tests. OM showed an optimum random distribution of the microcapsules throughout the dental host material which is important when applied in a self-healing system to guarantee that a crack encounters the capsules.

Furthermore, a good adhesion of the microcapsule shell and matrix is necessary to provide rupture of the capsule shell upon crack intrusion. When the microcapsules are incorporated into the dental host the rough exterior shell wall of the capsules is infiltrated by matrix methacrylates. The ability of the matrix resin to partially penetrate the rough exterior microcapsule shell wall is of utter importance to produce a good adhesion between the capsule shell and the host material. If the capsules are well-bonded the risk of creating predetermined breaking points within the structure of the material is significantly decreased. FESEM analysis confirmed the very good adhesion of the capsule shell to the dental host material. Enhanced bonding ability of the UMF microcapsule shell in comparison with the neat PUF capsule shell was not clear from the micrographs.

Finally, an excellent bonding is highly advantageous to maintain the good mechanical properties of the virgin material after the incorporation. Mechanical

measurements revealed rather high flexural strength, Vickers hardness, nanoindentation hardness, and modulus of elasticity which were not adversely affected by the incorporation of microcapsules. The partial substitution of urea by melamine up to 5% in the UMF microcapsule shell did not influence the mechanical properties when embedded in a dental matrix. Even though the robustness of the microcapsule shell might have been enhanced by the melamine modification, it is likely that the positive effect cannot be elucidated by mechanical measurements of the dental material that contains 3-6 wt% microcapsules since the amounts of melamine are too low considering the whole system.

CHAPTER V

PREPARATION OF PUF MICROCAPSULES CONTAINING EPOXY RESIN

5.1 Introduction

Epoxy resins are a highly interesting alternative to the common acrylate-based dental composite materials. In combination with a self-healing system the epoxy-based composite could offer a low-shrinkage restorative material of outstanding properties and extended life-time. Therefore, in this chapter a fundamental investigation on the encapsulation of epoxy compounds is reported to trigger further research work in this area. Microcapsules containing epoxy resins could be applied in the new silorane-based dental composite or other industrial epoxy-based products to create a self-healing functional material. They are typically cured with amines. An excess of the hardener in the matrix resin could function as curing agent for the healing monomer once the capsule is ruptured and the monomer distributed in the crack plane.

Another self-healing approach could include the incorporation of microcapsules that are filled with a healing monomer next to a set of microcapsules that are filled with the corresponding curing agent. The aim would be that if a crack ruptures both types of microcapsules the monomer and hardener compound would come in contact to react and seal the crack. Upon release of the curing agent it could also polymerize unreacted monomer that might be left in the cured epoxy host material.

In this study, a common epoxy resin was chosen as matrix material which was DGEBA. The healing agent was of the same chemistry. Since a wide range of curing agents is available with different functionalities that can polymerize epoxy monomers

three curing agents of different chemical nature were selected. These hardeners included a polyamide, an aliphatic amine and a cycloaliphatic amine which all possess the required ability to start the polymerization of the epoxy monomer at room temperature and provide rapid curing.

5.2 Materials

The microcapsule wall forming materials urea, ammonium chloride and resorcinol were purchased from Sigma-Aldrich whereas formalin was acquired from System. Epikote 828 (DGEBA) was provided by Asachem to function as core resin and host material. The curing agents Epikure F205, Epikure 3140 and DETA were also received from Asachem. The reactive diluent BGE, both surfactants sodium dodecylbenzene sulphonate (SDBS) and EMA copolymer (average $M_w = 100,000\text{--}500,000$ g/mol) were obtained from Sigma-Aldrich. NaOH pellets, 37% HCl solution, 5% sulphuric acid solution and the antifoaming agent 1-octanol were also received from Sigma-Aldrich whereas triethanolamine (TEA) was purchased from Merck and ethanol from HmbG Chemicals. The different powders of fumed silica (Aerosil) which were utilized as anti-caking agents were provided by Evonik-Degussa. For pH adjustments a 1 molar NaOH solution and a 1 molar HCl solution were prepared. The epoxy based materials, SDBS and the Aerosil samples were of technical grade. All other chemicals were of analytical grade and they were all used as received.

5.3 Method

5.3.1 Microencapsulation of Epoxy Compounds

First trials to manufacture PUF/epoxy microcapsules were carried out according to a two-step process as it was reported by Yuan *et al.* (2008). Therefore, a

UF prepolymer solution is prepared first which is only then followed by the actual encapsulation. In a second attempt the customary recipe for the preparation of PUF/DCPD microcapsules by *in situ* condensation polymerization of urea with formaldehyde was followed as it is described in chapter 3. A comparison of the steps of the two encapsulation methods is illustrated in Figure 5-1.

5.3.1.1 Two-Step Encapsulation Procedure

The first part includes the preparation of the UF prepolymer for which 5.0 g urea was added to 12.7 g formalin in a 50 mL glass beaker at room temperature. The mixture was agitated with the help of a magnetic stirrer. Once the urea was dissolved, the pH was adjusted to 8.5 using TEA. After this, the solution was heated to 65°C where it was kept under continuous stirring for one hour. Finally, the prepolymer solution was allowed to cool down to room temperature.

In the second step the prepolymer solution was transferred into a 500 mL glass beaker and agitated at 500 rpm with the help of a mechanical stirrer. Subsequently, 100 mL of the SDBS surfactant solution was added; the built foam was removed by the addition of 2 drops 1-octanol. This was followed by the slowly addition of the epoxy resin which were DGEBA or solutions of DGEBA and BGE; details are provided in Table 5-1. After 30 min the pH was adjusted to 3 using sulphuric acid. The reaction slurry was then heated to 65 °C at a rate of 2 °C/min and remained for 3 hours whilst continuous stirring. Finally, 100 mL distilled water were added and the reaction slurry was left to slowly cool down to room temperature. The product was filtered under suction and rinsed with water.

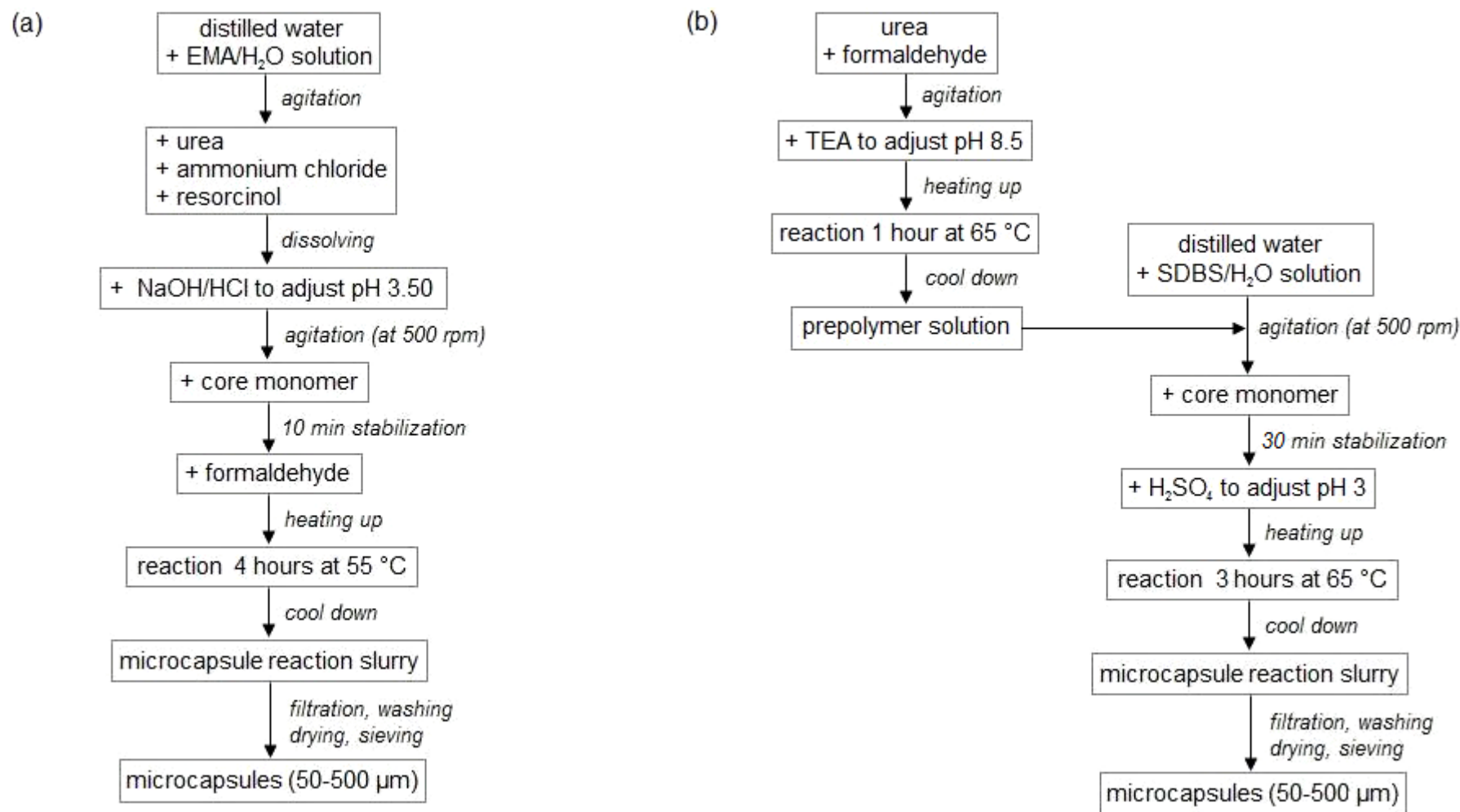


Figure 5-1 Comparison of two microencapsulation procedures utilizing (a) the acid-catalysed *in situ* condensation polymerization of urea with formaldehyde to form the microcapsule wall in a single-step procedure and (b) the two-step encapsulation procedure.

Further encapsulation attempts of the epoxy resin included variations in diverse process parameters such as the increase of the reaction temperature, the extension of the reaction time, and the initial pH which was raised from 3.0 to 3.5. Moreover, the concentrations of certain ingredients were varied. For instance, the concentration of the surfactant was decreased, and the epoxy core resin was diluted with BGE in different ratios. Finally, trials to encapsulate the curing agent were performed. All changes that were undertaken to obtain PUF microcapsules filled with the epoxy resin or microcapsules filled with the epoxy hardener by following the two-step method are summarized in Table 5-1.

5.3.1.2 Single-Step Encapsulation Procedure

For the preparation of PUF/epoxy microcapsules according to single-step encapsulation procedure the description in section 3.3.1 was followed. All the wall forming ingredients were added as reported beforehand. After the pH was adjusted to 3.5 the reaction slurry was agitated with a mechanical stirrer at a rate of 500 rpm. Then, 30 mL of the epoxy resin mixture (amounts as listed in Table 5-2) was added to form a suspension of fine droplets. After stabilization of the emulsion and the addition of the formalin, the temperature of the reaction mixture was raised to 55°C at a rate of 1.5°C/min. It was stirred for 4 hours continuously before the reaction slurry was allowed to cool down. Then, the suspension was filtered under suction and rinsed with water and ethanol. The capsules were separated by sieving through standardized test sieves of 50, 300, and 500 microns mesh size.

Table 5-1 Variations of parameters and ingredients during the course of the encapsulation trials of epoxy resin in a PUF shell following the two-step microencapsulation method

Experiment No.	Surfactant Concentration		PH		Encapsulation Reaction		Core Compound
	SDBS	EMA	Step 1*	Step 2**	Time	Temperature	
1	2.5 %	-	8.5	3	3 h	65 °C	Epikote 828
2	1.0 %	-	8.5	3	3 h	65 °C	Epikote 828
3	0.5 %	-	8.5	3	3 h	65 °C	Epikote 828
4	0.2 %	-	8.5	3	3 h	65 °C	Epikote 828
5	0.2 %	-	7	3	3 h	65 °C	Epikote 828
6	0.2 %	-	8.5	3.5	3 h	65 °C	Epikote 828
7	0.2 %	-	8.5	3	4 h	55 °C	Epikote 828
8	-	2.5 %	8.5	3	3 h	65 °C	Epikote 828
9	-	5.0 %	8.5	3	3 h	65 °C	Epikote 828
10	0.2 %	-	8.5	3	3 h	65 °C	Epikote 828 / BGE = 3:2
11	0.5 %	-	8.5	3	3 h	65 °C	Epikote 828 / BGE = 3:2
12	0.2 %	-	8.5	3	3 h	65 °C	Epikure F205
13	0.2 %	-	8.5	3	3 h	65 °C	Epikure 3140
14	-	2.5 %	8.5	3.5	4 h	55 °C	Epikote 828 / BGE = 3:2
15	-	2.5 %	8.5	3.5	4 h	55 °C	Epikure F205
16	-	2.5 %	8.5	3.5	4 h	55 °C	Epikure 3140

* Step 1: preparation of the prepolymer solution

** Step 2: actual microencapsulation

Table 5-2 Epoxy resin mixtures for the encapsulation in a PUF shell following the single-step microencapsulation method

Sample No.	Epikote 828 in (wt%)	BGE in (wt%)
1	100	0
2	80	20
3	60	40
4	50	50

5.3.1.3 Product Aftertreatment

The clusters of PUF/epoxy microcapsules that were obtained were separated in four portions and transferred into 250 mL glass beakers each. Then, the samples were filled with 150 mL of one of the following solvents: ethanol, acetone, distilled water and distilled water containing a drop of dishwashing liquid. This was followed by agitating the suspensions at room temperature using a mechanical stirrer to wash off any impurities and separate the agglomerations. After 6 hours, the individual suspensions were filtered under suction, except for the acetone sample which was stirred only 2 hours before filtration. Finally, the microcapsules were air dried under the fan and stored in a desiccator over night before they were examined by digital microscopy.

Another set of clustered microcapsules was separated into six parts which were weighed into a 250 mL glass beaker each. To every single sample 5% of a different type of fumed silica was added which are described in Table 5-3. The glass beakers containing the solid mixtures were then manually swirled to distribute the silica particles with the aim of breaking the microcapsule agglomerations without destroying the capsule shell.

Table 5-3 Description and properties of different types of fumed silica available under the trade name ‘Aerosil’ (Evonik-Degussa)

Aerosil Type	Surface Nature	Size* in (nm)	BET** in (m ² /g)	Typical Application	Conc.*** in (wt%)
200	Hydrophilic	12	200 ± 25	Epoxy, PUR, Acrylate/Methacrylate, PE, Silicone, PVC	1–10
300	Hydrophilic	7	300 ± 30	Acrylate/Methacrylate, PE	1–7
380	Hydrophilic	7	380 ± 30	Epoxy, PE	1–10
R202	Hydrophobic, poly-dimethylsiloxane treated	14	100 ± 20	Epoxy, PUR, Vinylester	1–8
R805	Hydrophobic, octylsilane treated	12	150 ± 25	Epoxy, PE	1–8
R7200	Hydrophobic, methacrylsilane treated	12	150 ± 25	Acrylate/Methacrylate, Vinylester, PE	5–15

* Average primary particle size

** Specific surface area analyzed by the technique which was developed by Brunauer et al. (1938)

*** Recommended concentration by the supplier (Evonik-Degussa)

5.3.1.4 Encapsulation of Amine Curing Agent

Following the two described oil-in-water emulsion encapsulation procedures it was attempted to enclose the curing agents Epikure 3140 and Epikure F205 in a PUF shell. DETA was not considered due to its higher water solubility (around 5g/L as it was illustrated in chapter 2, Table 2-4). Both selected catalysts possess relatively low viscosity which means when the PUF microcapsules containing the epoxy hardener were incorporated in a self-healing polymeric system they could easily distribute in the crack plane upon rupture.

For the two-step encapsulation procedure of the curing agents a 0.2 % solution of the SDBS surfactant was employed; all other compounds and parameters

were utilized as described above in section 5.3.1.1. The one-step microencapsulation procedure was carried out according to the description in 5.3.1.2 using the same materials and amounts of ingredients.

5.3.2 Analysis of PUF/Epoxy Microcapsules

5.3.2.1 Product Yield and Quality

The average yield was determined from the mass of capsules able to pass through a 500 μm sieve compared to the mass of the starting ingredients used for the preparation of the PUF/epoxy microcapsules. The starting compounds included the microcapsule shell forming materials urea, resorcinol, ammonium chloride and formaldehyde as well as the core materials Epikote 828 and BGE.

5.3.2.2 Examination of Microcapsules by Microscopic Methods

Digital microscopy was used to examine the shape and quality of the product. Further detailed inspection was then performed by OM whereas FESEM was employed for the study of the capsule shell morphology and membrane thickness measurements. For the latter part of the capsules were ruptured with a razor blade and mounted on a conductive stage next to a sample of intact capsules.

5.3.2.3 Determination of Microcapsule Core Content by ^1H -NMR Spectroscopy

To determine the core content part of the epoxy filled capsules were stirred in ethanol for 3 hours to wash off any residual material. The dry capsules were then ground with a mortar and extracted with deuterated acetone. ^1H -NMR spectroscopy was performed on the extract to verify the microcapsule core content which would be indicated by the presence of the characteristic signals corresponding to the epoxy group and the bisphenol-A spacer of the Epikote 828 resin.

5.3.2.4 Thermal Analysis of the Microcapsules

DSC of the intact PUF/epoxy microcapsules was measured from 35 °C to 350 °C at a heating rate of 10 °C/min to investigate the thermal stability of the capsules. The resulting spectrum was compared with a scan of the extracted PUF shell material which was obtained by grinding the microcapsules and clearing them from any epoxy resin. Therefore, the broken shell matter was suspended in ethanol and stirred for 2 hours using a magnetic stirrer. After this, the PUF material was filtered under suction and rinsed again with ethanol. The DSC measurement was performed on the dry material. The successful encapsulation of the epoxy monomer would be indicated by additional peaks being present in the curve of the intact microcapsules referring to chemical or physical changes of the epoxy core compound.

5.3.3 Incorporation of PUF/Epoxy Microcapsules in Epoxy Matrix

Sample moulds were prepared of a silicone rubber based material (Virtual Refill Putty, Fast Set, Vivadent) to obtain bar shaped test specimens of approximately 25 mm length, 2 mm height and 2 mm thickness. The matrix material for the incorporation of the PUF/epoxy microcapsules consisted of DGEBA and the hardener. Three samples were prepared using the different curing agents that are listed in Table 5-4 and the recommended proportions according to the supplier.

The ingredients were homogeneously mixed and degassed in an ultrasonic bath for 30 minutes to remove any entrapped air. The microcapsules were then added and the mixture was sonicated for another 30 minutes to distribute the capsules in the host material. 5% microcapsules of the size fraction 50 to 300 microns were incorporated. The resin and hardener without microcapsules served as a reference.

The specimens were left over night at room temperature before they were removed from the mould.

Table 5-4 Proportions of selected curing agents to be used with Epikote 828 as recommended by the supplier*

Curing Agent	Description	Proportion with Epikote 828
DETA	Aliphatic amine	12 phr**
Epikure F205	Modified cyclo-aliphatic amine	58 phr
Epikure 3140	Polyamide	50 phr

* *Hexion, Technical Data Bulletin for Epon Resin 828, RP: 3075*

** *Parts weight per 100 parts weight of resin*

5.3.4 Examination of Embedded Microcapsules by FESEM

After the incorporation of the microcapsules into the epoxy-based host material the adhesion of the PUF microcapsule shell to the matrix resin was inspected by FESEM. Therefore a test specimen was stored in the freezer for 24 hours to obtain a smooth surface when breaking afterwards. The interface between capsule shell and host resin on the broken surfaces was then examined by FESEM.

5.4 Results and Discussion

Microcapsules of a PUF shell that contain DCPD were successfully prepared by *in situ* polymerization as described in chapter 3. For the encapsulation of epoxy resins Yuan and co-workers (2008) reported that it is necessary to prepare a UF prepolymer solution first which is only then followed by the actual encapsulation. Therefore, first experiments were undertaken following their suggestion. However, it

was not possible to enclose neither the epoxy compounds nor the hardener with this two-step encapsulation method. Even after changing some distinct process parameters including the initial pH, reaction temperature and reaction time, microcapsules could not be obtained. Also, variations in the concentrations of certain ingredients such as the surfactant, the core monomer, the ratio of core monomer mixture and the ratio of urea to formaldehyde did not show any positive effect.

Further attempts to prepare the PUF/epoxy microcapsules were performed according to the single-step procedure. It was possible to encapsulate the different mixtures of the epoxy resin and the reactive diluent as described in Table 5-2. However, only with a ratio of 3 parts DGEBA to 2 parts BGE individual microcapsules were obtained. PUF microcapsules containing the curing agent were not produced. Hence, the following section concentrates solely on the product analysis of the PUF microcapsules incorporating the 3:2 DGEBA/BGE resin mixture which were successfully manufactured by the single-step procedure.

5.4.1 Microcapsule Yield, Size and Shape

The microcapsule yield was about 35% in the size range of 50–500 μm . Images obtained from digital microscopy illustrated that a variety of microcapsules of different diameters were produced and no other particulate matter was found in the product (Figure 5-2 a). The product left on the 500 micron test sieve consisted solely of agglomerations of smaller capsules as revealed by microscopy. These clusters were easily separated when added to any of the solvents tested which were ethanol, acetone, distilled water and water that contained a detergent. However, after filtration and drying the samples appeared again in the form of clusters. The optical

micrographs of the discrete microcapsules showed an uneven capsule shell as it is obvious in Figure 5-2 b.

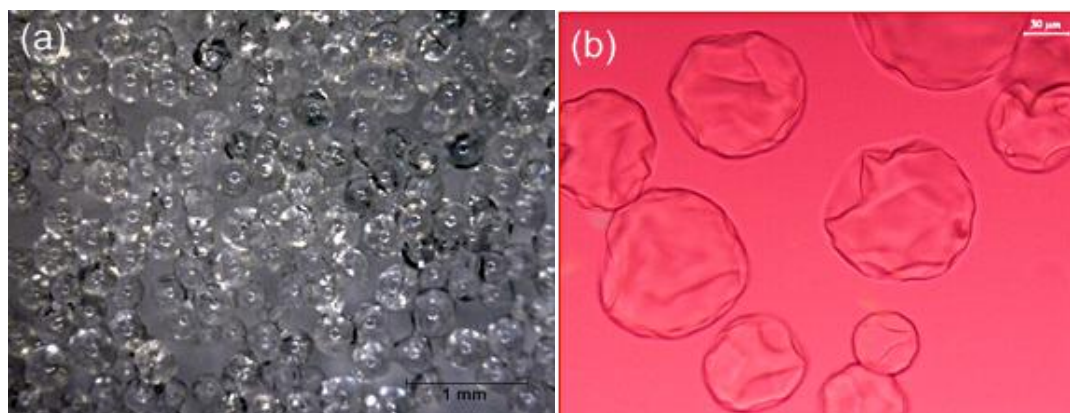


Figure 5-2 (a) Digital micrograph of PUF/epoxy microcapsules and (b) optical micrograph of the same capsules revealing their irregular shape.

The silica types used in this study differed from each other in the particle size, the surface nature, and the specific surface area (as described in Table 5-3). Generally, the surface of fumed silica is hydrophilic in nature; to improve the properties the particles are in most of the applications aftertreated with silanes or siloxanes resulting in their hydrophobic counterpart. Silica particles were considered to be a very interesting additive as they could function as an anti-caking agent for the microcapsules to improve their flowing behaviour and shelf-life, and at the same time the silica could act as strengthening filler within the dental composite matrix. Furthermore, the attachment of silica particles onto the surface of the outer capsule shell layer might improve the adhesion to the matrix resin when incorporated. However, none of the fumed silica types that were tested to aid in the separation of the agglomerations showed an immediate advantageous effect.

5.4.2 FESEM of Microcapsule Shell

FESEM confirmed the ‘wrinkled’ appearance of the microcapsules as shown in Figure 5-3 a. It was also revealed that the PUF/epoxy microcapsules produced lacked the rough porous outer shell that was observed for the PUF/DCPD capsules and discussed earlier in chapter 3 (e.g. Figs. 3-7 c and d, 3-11, and 3-12). Only at higher magnification single nano-sized particles became visible which were adhered to the outer surface of the smooth capsule shell layer (Fig. 5-3 b). The spherical nanoparticles measured about 50–350 nm in diameter. It was not possible to facilitate membrane thickness measurements on the ruptured capsule shell.

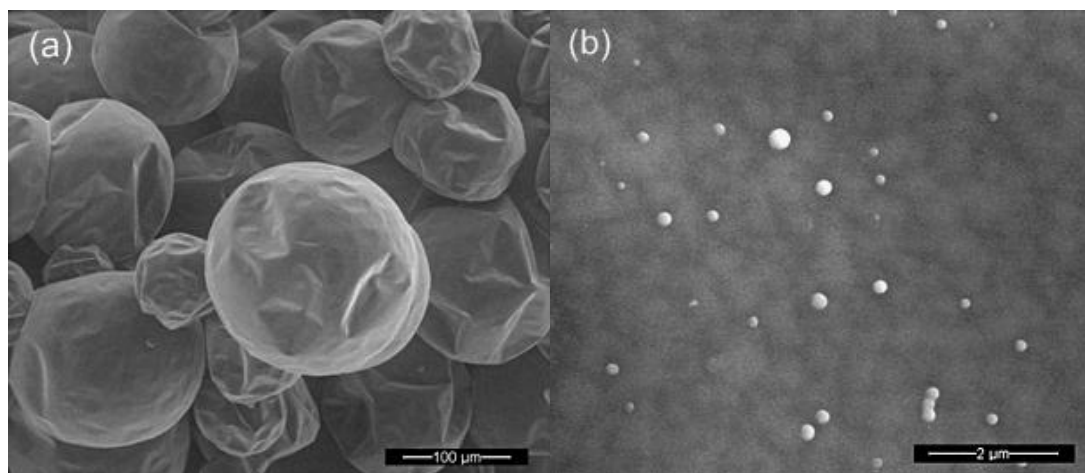


Figure 5-3 FESEM images illustrating (a) PUF/epoxy microcapsules and (b) the capsule surface on which individual spherical nanoparticles are attached.

5.4.3 Verification of Epoxy Core by $^1\text{H-NMR}$ Spectroscopy

Solution state $^1\text{H-NMR}$ analysis in acetone of the microcapsule extract verified the presence of the epoxy core monomers DGEBA and BGE. The spectrum in Figure 5-4 shows the characteristic peaks of the oxirane group of the DGEBA monomer at 2.63 ppm (dd, 2H), 2.76 ppm (dd, 2H) and 3.23 ppm (dd, 2H). The hydrogen resonance of the aromatic ring and methyl group of the bisphenol-A spacer

appears at 6.81 ppm (d, 4H), 7.11 ppm (d, 4H) and 1.57 ppm (s, 6H), respectively. Further peaks indicating methylene hydrogens that are contained in the structure of the DGEBA monomer are evident at 3.78 ppm (dd, 2H) and 4.21 ppm (dd, 2H).

The less intensive peaks at approximately 2.38 ppm, 2.63 ppm and 2.86 ppm refer to the hydrogen resonance of the oxirane ring of the reactive diluent which was present at lower concentration. The methyl group of the BGE monomer is indicated by the resonance at 0.86 ppm whereas methylene hydrogens are visible in the area of around 1.45 ppm, 1.51 ppm, 3.37 ppm, 3.38 ppm and 3.63 ppm. In summary, the typical resonances reflecting DGEBA and BGE are all obvious in the $^1\text{H-NMR}$ spectrum which proved the successful encapsulation of the epoxy monomers.

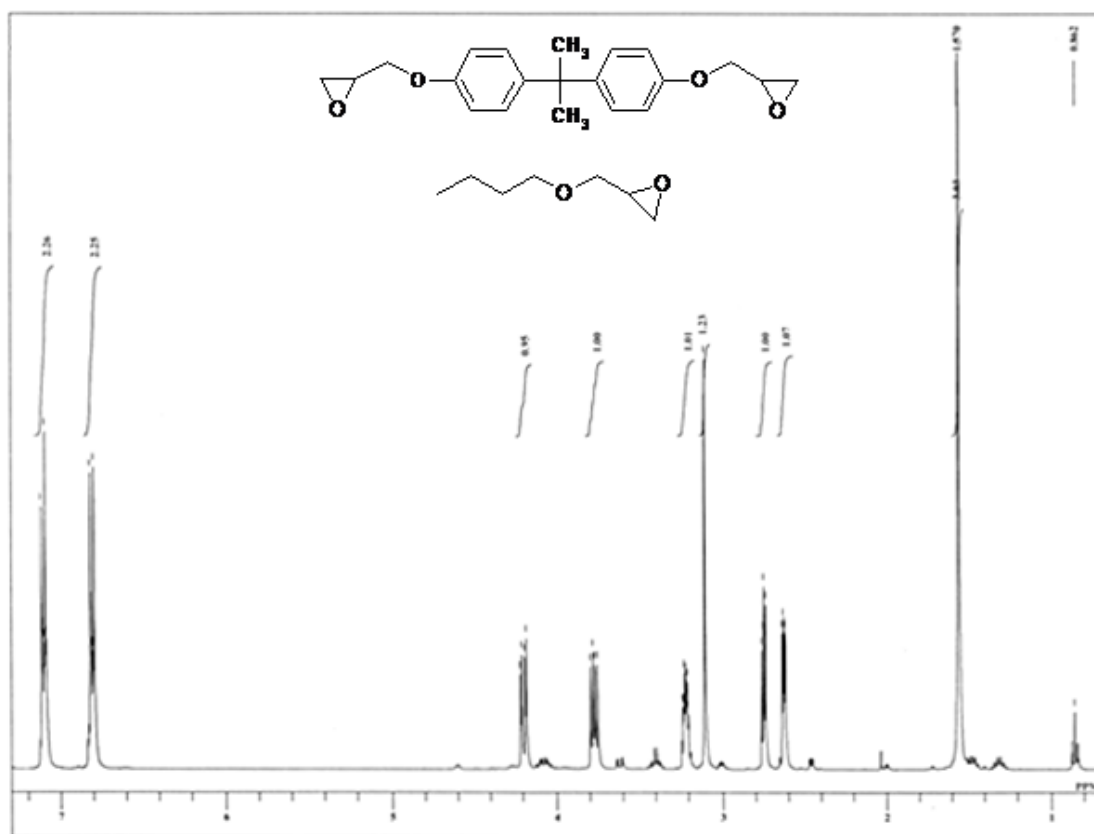


Figure 5-4 $^1\text{H-NMR}$ spectrum of the extracted ground PUF/epoxy microcapsules showing the characteristic peaks of the encapsulated epoxy resins DGEBA and BGE.

5.4.4 Characterization of the Microcapsules by DSC

The DSC scans of the PUF microcapsule shell material in comparison with the intact microcapsules are shown in Figure 5-5. The microcapsules are filled with an epoxy monomer mixture consisting of DGEBA diluted in BGE, with boiling temperatures of about 200 °C and 164 °C, respectively. Therefore, the endothermic peak at about 206 °C obvious in the heat flux curve of the microcapsules can be attributed to the evaporation of the epoxy core monomers upon capsule rupture. The following moderate increase in the heat flow might indicate the melting of the PUF shell material reaching a peak at about 330 °C. In the plot of the extracted PUF matter the heat flux slowly raises at about 150 °C to reach an endothermic melting peak of the shell material at 313 °C. To sum up, the two DSC plots clearly differ

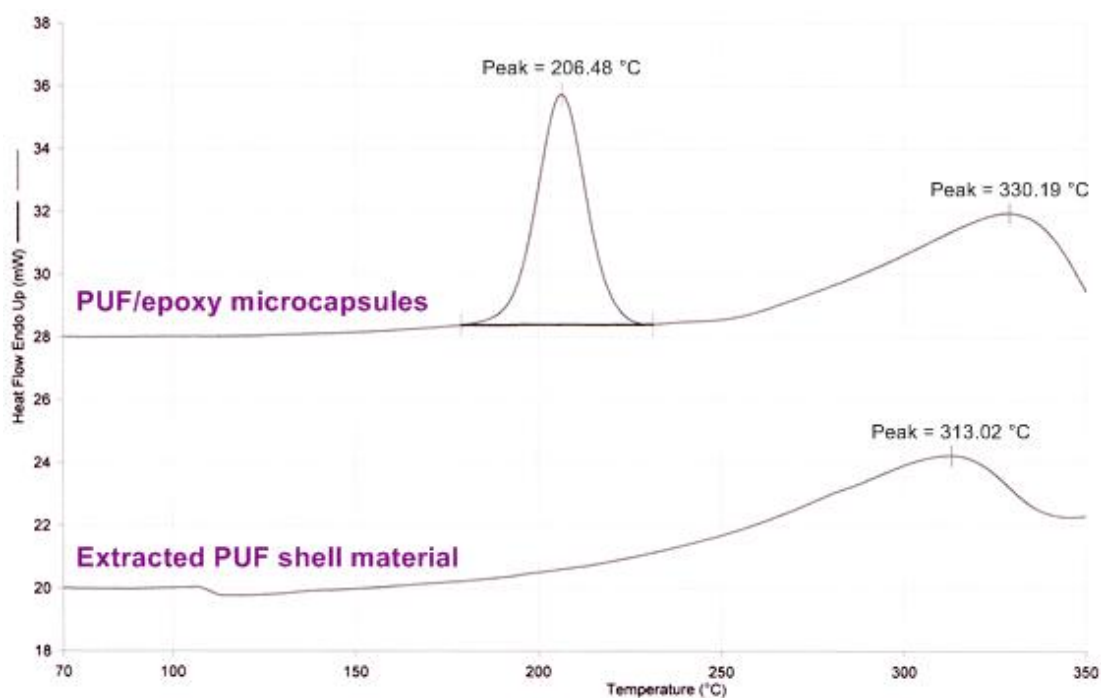


Figure 5-5 DSC curves representing the heat flow of PUF/epoxy microcapsules in comparison with the extracted PUF shell matter.

from each other by the distinct transition peak referring to the epoxy monomers which solely appears in the curve of the microcapsules and therefore verifies the core compound.

5.4.5 Incorporation of PUF/Epoxy Microcapsules in Epoxy Matrix

After the addition of the microcapsules to the host resin the sample was placed in the ultrasonic bath. The minimum exposure time to completely remove any entrapped air and to obtain a homogeneous mixture was 20 minutes. When adding the PUF/epoxy microcapsules to the resin consisting of Epikote 828 and Epikure 3140 hardening occurred almost instantly. The resin containing DETA started to gel 20 minutes after the microcapsule addition and the material was polymerized after another 10 minutes. With the epoxy/Epikure F205 mixture the microcapsule addition induced curing after 30 minutes. The polymerization of the epoxy matrix resin might have been initiated by urea derivatives that could be present in the PUF microcapsule shell.

5.4.6 Adhesion of PUF Microcapsule Shell to Epoxy Host Resin

Figure 5-6 displays the FESEM micrograph of a PUF/epoxy microcapsule embedded in the epoxy host material. Since the microcapsule shell did not possess the relatively thick porous outer layer which could be penetrated by the host resin mechanical retention is not provided. Hence, the bonding of capsule shell to the matrix material has to rely on chemical interactions. Figure 5-6 b shows that the interface does not contain any air inclusions and the smooth capsule shell layer directly adjoins to the matrix. The single nanoparticles that were stuck onto the

capsule shell (as displayed earlier in Figure 5-3 b) are visible in the adjacent resin area. Generally, it seems that the capsules are well fixed within the matrix resin.

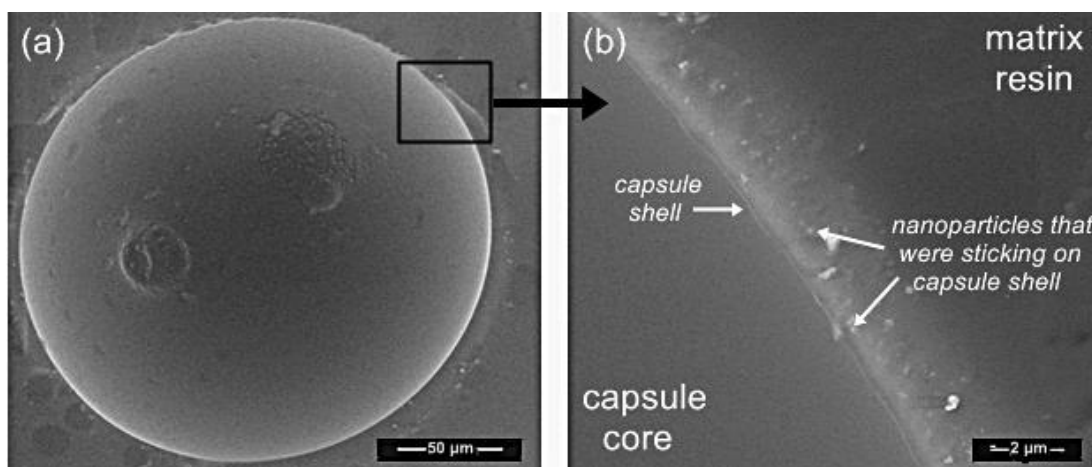


Figure 5-6 FESEM images of (a) PUF microcapsule containing Epikote 828/BGE embedded in an epoxy-based matrix material and (b) the interface of the microcapsule shell and the epoxy host material.

5.5 Summary and Conclusion

The epoxy resin mixture Epikote 828/BGE was successfully encapsulated in a PUF shell by the single-step *in situ* oil-in-water emulsion polymerization method. The product appeared in the form of a white free-flowing powder containing agglomerations of the microcapsules with diameters ranging from 50–500 microns. The agglomerated microcapsules could neither be separated by the treatment with different solvents nor by the addition of silica anti-caking agents. The yield of the individual capsules was 35 %. The other part of the product consisted of agglomerations of microcapsules which when exposed to a solvent or reactive diluent easily separated and distributed randomly.

DSC verified the epoxy core monomer and the PUF microcapsule shell. Proton NMR spectroscopy confirmed the presence of the epoxy core. Furthermore,

microscopy showed the wrinkled surface of the microcapsules, lacking the porous outer shell layer that was observed for the PUF/DCPD capsule. Still the capsule shell adhered well to the epoxy matrix resin as it was shown by FESEM. Besides, it was observed that when incorporating the microcapsules in an epoxy host material the hardening of the matrix resin is accelerated, probably due to urea derivatives in the PUF capsule shell.

CHAPTER VI

CONCLUSIONS AND FUTURE WORK

6.1 Conclusions

A self-healing concept has been explored for the development of a novel advanced dental restorative composite. If the microcapsule-based self-healing system is applied in a conventional dental polymeric material it has the ability to heal cracks that might occur within the structure of the material. Therefore, it would greatly improve the performance of the tooth filling material.

An applicable self-healing monomer-catalyst combination was identified which included DCPD and a Grubbs catalyst. The DCPD monomer was successfully encapsulated by acid-catalyzed *in situ* condensation polymerization of UF to form the microcapsule shell. After the adjustment of certain process parameters the microcapsules produced appeared in the form of a free-flowing white powder. Employing an initial pH of 3.5, an agitation rate of about 500 rpm, a minimum reaction time of 3 hours and a formaldehyde-urea ratio of 1.9 to 2.3, high yields of annular shaped microcapsules in the size range of 50–500 microns are obtained (up to 89%). Since the capsules generally tend to build agglomerations upon filtering and drying the aftertreatment with ethanol or acetone was found to be a crucial factor to receive individual spheres. The microcapsules were still intact after 2 years storage time at room temperature. The long shelf-life was confirmed by the unchanged results of ¹H-NMR spectroscopy of the core monomer and DSC measurements of the capsule shell after the certain time periods.

In addition to the microcapsule preparation, analytical methods were evaluated to characterize the product. DSC, ¹H-NMR spectroscopy and FTIR-ATR spectroscopy are all applicable methods for the verification of the capsule core monomer in the case of DCPD; whereas the PUF shell material is preferably inspected by thermoanalytical techniques such as TGA and DSC. Different microscopic methods are useful for the examination of the shape, size and the general quality of the product. FESEM revealed that the microcapsules possess an impervious shell membrane of about 130 nm thickness that surrounds the core monomer and prevents diffusion or leakage. On the surface of the continuous smooth shell membrane numerous PUF nano-beads are sticking to build an outer shell layer of approximately 10–15 μm thickness. The outer part is rough and porous in its structure which allows the penetration of the matrix resin when embedded in the polymeric host material. This ability is important as it promotes the adhesion of the capsule shell to the matrix resin by providing additional mechanical retention.

The modification of the PUF microcapsule shell with small melamine amounts did not show a significant strengthening effect as revealed by mechanical tests on the microcapsule embedded material. Nevertheless, the flexural strength, microhardness and nanoindentation hardness values of the virgin material were not adversely affected after the incorporation of the microcapsules. Furthermore, the random distribution of the embedded microcapsules throughout the host material which was evident in the optical micrographs is highly advantageous for a self-healing system as it increases the likeliness that an approaching crack encounters the microcapsules. The excellent adhesion of the capsules to the acrylic matrix resin which infiltrated the outer capsule shell layer was shown by FESEM. The capsules

need to be well bonded to maintain the good mechanical properties of the original material and also to enhance the rupture ability upon crack intrusion.

Finally, epoxy resins were successfully encapsulated in a PUF shell. The epoxy core monomer was verified by $^1\text{H-NMR}$ analysis and DSC. The latter also revealed a high thermal stability of the PUF/epoxy microcapsules. Even though FESEM revealed the lack of the outer porous shell layer the PUF shell adhered well to the epoxy-based host material as obvious from the micrographs.

6.2 Participations at Conferences and Exhibitions

- (i) Microencapsulation Process for Self-Healing Polymeric Material. Sonja Then¹, Gan Seng Neon¹ and Noor Hayaty Abu Kasim² (¹Department of Chemistry, ²Department of Conservative Dentistry, University of Malaya, 50603 Kuala Lumpur, Malaysia). Malaysia Polymer International Conference (MPIC), Palm Garden IOI Resort, Putrajaya, Malaysia, 21-22 October 2009.
- (ii) Microcapsules for Self-Healing Polymeric Material. Sonja Then¹, Gan Seng Neon¹ and Noor Hayaty Abu Kasim² (¹Department of Chemistry, ²Department of Conservative Dentistry, University of Malaya, 50603 Kuala Lumpur, Malaysia). 6th Singapore International Chemical Conference (SICC-6), Singapore International Convention & Exhibition Centre (Suntec), Singapore, 15-18 December 2009.
- (iii) Gold Medal: Microcapsules for Self-Healing Dental Material. Inventors: Gan Seng Neon¹, Noor Hayaty Abu Kasim² and Sonja Then¹ (¹Department of

Chemistry, ²Department of Conservative Dentistry, University of Malaya, 50603 Kuala Lumpur, Malaysia). 21st International Invention, Innovation & Technology Exhibition (ITEX 2010), Kuala Lumpur Convention Centre (KLCC), Kuala Lumpur, Malaysia, 14-16 May 2010.

- (iv) Preparation and Characterization of Microcapsules for Self-Healing Dental Restorative Materials. Sonja Then¹, Gan Seng Neon¹ and Noor Hayaty Abu Kasim² (¹Department of Chemistry, ²Department of Conservative Dentistry, University of Malaya, 50603 Kuala Lumpur, Malaysia). Integrating Nanomaterials in Formulations (NanoFormulation2010), Stockholm University, Stockholm, Sweden, 9-11 June 2010; in connection with Formulations for the Future – from Fundamentals to Processing (FormulaVI), Stockholm University, Stockholm, Sweden, 7-10 June 2010.

- (v) Preparation and Properties of Melamine Modified Poly(urea-formaldehyde) Microcapsules for the Application in Dental Polymeric Materials. Sonja Then¹, Gan Seng Neon¹ and Noor Hayaty Abu Kasim² (¹Department of Chemistry, ²Department of Conservative Dentistry, University of Malaya, 50603 Kuala Lumpur, Malaysia). 3rd International Conference on Functional Material and Devices (ICFMD-2010), Hotel Permai Inn, Kuala Terengganu, Malaysia, 14-17 June 2010.

- (vi) A Self-Healing Concept for the Development of an Advanced Dental Composite Material. Sonja Then¹, Gan Seng Neon¹ and Noor Hayaty Abu Kasim² (¹Department of Chemistry, ²Department of Conservative Dentistry,

University of Malaya, 50603 Kuala Lumpur, Malaysia). Emerging Trends in Chemistry – Bilateral Symposium between the University of Malaya and the University Hyderabad, Department of Chemistry, University of Malaya, Kuala Lumpur, 26-28 October 2010.

6.3 Suggestions for Future Work

Amongst others, a novel approach to modify the PUF microcapsule shell for the specific application in a methacrylate-based restorative composite material was followed in this work as reported in chapter 4. Further changes in the microcapsule composition to customize them for the use in a self-healing dental polymer shall be examined in future studies. For instance, higher amounts of melamine could be included to increase the strength and toughness of the microcapsule shell. A different option would be the exploration of polyurethane (PU, PUR) as possible microcapsule shell material.

Furthermore, during the course of this study it was shown that other acrylic monomers can be encapsulated by the *in situ* emulsion technique. To reduce costs and make use of local resources palm oil-based ingredients could be utilized as matrix material and may also be considered as healing agent. Other advantages of compounds derived from palm oil include the environmental friendliness and biocompatibility.

Next, future efforts should be aimed at the addition of the specific catalyst for the healing monomer in the composite system. First tests showed that by the addition of the ruthenium-based catalyst the dental acrylic resin starts to jell partly. Hence, it might be considered to surround the catalyst particles with a protective layer to avoid interactions with the matrix material. Furthermore, the strong colour of the Grubbs

catalyst requires the addition of colour pigments so that the composite filling material can match the tooth colour. Besides, biocompatibility aspects, costs and availability of the Grubbs type catalysts need to be evaluated in detail. Especially for the application in a dental restorative material it is of utter importance that the ingredients do not harm the patient. Therefore, in one of the next steps biocompatibility studies have to be performed not only of the single ingredients but also of the complete self-healing polymeric material system.

After the optimization of the monomer-catalyst system further work needs to focus on the assessment of the self-healing performance and efficiency of the system. Therefore, a suitable mechanical test set-up and method have to be chosen. To obtain an authentic evaluation of the self-healing function the result of three different types of tests are recommended to be compared. These include a reference in which the healing monomer and the corresponding catalyst are manually induced into the matrix material. Secondly, a specimen consisting of the host material and the catalyst; the healing monomer is then manually injected. And lastly, the material in which both, the self-healing monomer and the corresponding catalyst are embedded to measure the *in situ* self-healing performance.

Once a suitable method for the verification of the healing efficiency is established, the optimum amount of microcapsules to be embedded in the matrix resin has to be evaluated. Along with this the quantity of the corresponding catalyst needs to be adjusted. In a later step, the tests should preferably be repeated in simulated body fluid at 37 °C in order to assess the potential *in vivo* performance of the healing system in dental application.

Shelf-life tests of the microcapsules have been performed in this work as described in section 3.3.5 and 3.4.7, and a lot of data is available on the storage

ability of the conventional dental materials. However, the shelf-life of the dental material after the incorporation of the microcapsules and the corresponding catalyst as well as the functionality of the self-healing system after certain time periods is yet to be determined. This would include the measurement of the activity of the catalyst next to the analysis of the physical and chemical stability of the complete self-healing composite system.

An alternative, most interesting field of study is the development of self-healing epoxy-based materials as introduced in chapter 5 in this work. Specifically the enhancement of the durability of the novel silorane-based low-shrinkage restorative composites is of utter interest and should be considered for future research. Therefore, the first task would be the optimization of the production process of the PUF microcapsules containing epoxy resins. Amongst others, the ratio of the core to shell material influences the wall thickness which is one aspect to be considered to increase the strength and toughness of the PUF/epoxy capsules.

An additional suggestion is to further investigate the effect of silica particles when added to the PUF/epoxy microcapsules as silica can function in many ways. Fumed silica are able to prevent powders from caking together and keeping their free-flowing ability over an extended period of storage time by either absorbing moisture or by coating the particles, in this case the microcapsules. If the silica particles adhere well to the capsule shell surface they might promote the adhesion to the matrix resin. Moreover, silica filler particles are known for their strengthening effect in composite materials resulting in increased mechanical values and durability. There is a wide variety of differently surface treated silica types available that could be tested for this purpose. Once a suitable silica kind is identified, microscopic analyses and mechanical measurements are recommended to study the adhesion of

the PUF shell material to the epoxy-based host material and the strength and hardness of the novel system.

Generally, the application of the microcapsule-based self-healing system makes products safer, more reliable and robust, and longer lasting. This technology is not only able to improve the crack-resistance of a dental composite it can be utilized in any polymeric material. For instance, it is possible to be used in adhesives, coatings, and paints as this technique repairs cracks, scratches, and deterioration. Hence, future work might focus on the research in different other fields employing the knowledge gained during the course of this research work. It is suggested to include interdisciplinary collaborations and challenge researchers from different fields such as medicine, inorganic and organic chemistry, mechanical engineering, and other applied sciences to foster the progress in the development of self-healing materials.

REFERENCES

- ASTM Specification E 384 - 89 (1990). Standard test method for microhardness of materials. In *Annual Book of ASTM Standards* (Vol. E04.05). Philadelphia: American Society for Testing and Materials.
- ANSI/ADA Specification 27 (1993). Resin-based filling materials. Chicago: American National Standards Institute / American Dental Association.
- Abuin, S. P. (2010). Epoxy Adhesives: A View of the Present and the Future. In J.-P. Pascault & R. J. J. Williams (Eds.), *Epoxy Polymers* (1 ed., pp. 215-234). Weinheim: Wiley-VCH.
- Alexandridou, S., & Kiparissides, C. (1994). Production of oil-containing polyterephthalamide microcapsules by interfacial polymerization. An experimental investigation of the effect of process variables on the microcapsule size distribution. *Journal of Microencapsulation: Micro and Nano Carriers*, 11(6), 603-614.
- Allock, H. R., Lampe, F. W., & Mark, J. E. (2003). *Contemporary Polymer Chemistry* (3 ed.). New Jersey: Pearson.
- Anusavice, K. J. (2003). Mechanical Properties of Dental Materials. In *Phillips' Science of Dental Materials* (11 ed., pp. 73-102). St Louis: Saunders.
- Arenhold-Bindslev, D. (1998). Environmental aspects of dental filling materials. *European Journal of Oral Sciences*, 106(2), 713-720.
- Arenhold-Bindslev, D., & Larsen, A. H. (1994). Mercury levels and discharge in waste water from dental clinics. *Water, Air, & Soil Pollution*, 86(1-4), 93-99.
- Arshady, R. (1999). *Microspheres, Microcapsules and Liposomes* (1 ed.). London: Citus Books.
- Arshady, R., & Guyot, A. (2002). *Functional Polymer Colloids and Microparticles: Microspheres, Microcapsules and Liposomes* ((1 ed., Vol. 4). London: Citus Books.
- Bailey, W. J. (1990). Matrices that expand on curing for high strength composites and adhesives. *Materials Science and Engineering, A* 129, 271-279.
- Barszczewska-Rybarek, I. M. (2009). Structure-property relationships in dimethacrylate networks based on Bis-GMA, UDMA and TEGDMA. *Dental Materials*, 25(9), 1082-1089.
- Belfield, K. D., & Zhang, G. Y. (1997). Photoinitiated cationic ring-opening polymerization of a cyclosiloxane. *Polymer Bulletin*, 38(2), 165-168.

- Bell, T. J., Bendeli, A., Field, J. S., Swain, M. V., & Thwaite, E. G. (1991). The determination of surface plastic and elastic properties by ultra micro-indentation. *Metrologia*, 28(6), 463-470.
- Bell, T. J., & Thwaite, E. G. (1999). Recent developments in hardness testing and their implications for standardisation. *CIRP Annals - Manufacturing Technology*, 48(1), 449-452.
- Benita, S. (1996). *Microencapsulation: Methods and Industrial Applications*. New York: Marcel Dekker.
- Bleay, S. M., Loader, C. B., Hawyes, V. J., Humberstone, L., & Curtis, P. T. (2001). A smart repair system for polymer matrix composites. *Composites Part A: Applied Science and Manufacturing*, 32(12), 1767-1776.
- Bono, A., Beng, Y. K., & Siambun, N. J. (2003). Melamine-urea-formaldehyde (MUF) resin: the effect of the number of reaction stages and mole ratio on resin properties. *Jurnal Teknologi*, 38(F), 43-52.
- Bowen, R. L. (1956). Use of epoxy resins in restorative materials. *Journal of Dental Research*, 35(3), 360-369.
- Bowen, R. L. (1962). Dental filling material comprising vinyl silane treated fused silica and a binder consisting of the reaction product of bis phenol and glycidyl acrylate. US Patent No. 3,066,112.
- Bowen, R. L. (1965). Method of preparing a monomer having phenoxy and methacrylate groups linked by hydroxy glyceryl groups. US Patent No. 3,179,623.
- Bowen, R. L. (1965). Silica-resin direct filling material and method of preparation. US Patent No. 3,194,783 and 3,194,784.
- Braem, M., Finger, W., Van Doren, V. E., Lambrechts, P., & Vanherle, G. (1989). Mechanical properties and filler fraction of dental composites. *Dental Materials*, 5(5), 346-349.
- Brown, E. N. (2003). *Fracture and Fatigue of a Self-Healing Polymer Composite Material*. University of Illinois, Urbana-Champaign.
- Brown, E. N., Kessler, M. R., Sottos, N. R., & White, S. R. (2003). In situ poly(urea-formaldehyde) microencapsulation of dicyclopentadiene. *Journal of Microencapsulation*, 20(6), 719-730.
- Brown, E. N., Sottos, N. R., & White, S. R. (2002). Fracture testing of a self-healing polymer composite. *Experimental Mechanics*, 42(4), 372-379.
- Brown, E. N., White, S. R., & Sottos, N. R. (2004). Microcapsule induced toughening in a self-healing polymer composite. *Journal of Materials Science*, 39(5), 1703-1710.

- Brunauer, S., Emmett, P. H., & Teller, E. (1938). Adsorption of gases in multimolecular layers. *Journal of the American Chemical Society*, 60(2), 309-319.
- Chadwick, R. G. (1989). A review: the assessment of the durability of composite resin restorative materials in vivo. *Clinical Materials*, 4(3), 241-253.
- Chao, H. Y. (2002). Microencapsulated adhesive. US Patent No. 6,375,872.
- Chauvin, Y. (2006). Olefinmetathese: die frühen Tage (Nobel-Vortrag). *Angewandte Chemie*, 118(23), 3824-3831.
- Chen, M. H. (2010). Update on dental nanocomposites. *Journal of Dental Research*, 89(6), 549-560.
- Chen, X., Dam, M. A., Ono, K., Mal, A., Shen, H., Nutt, S. R., et al. (2002). A thermally re-mendable cross-linked polymeric material. *Science*, 295(5560), 1698-1702.
- Chiang, Y. C. (2009). *Polymerization shrinkage with light-initiated dental composites*. Ludwig-Maximilians-Universitaet, Muenchen.
- Cho, S., Andersson, H., White, S., Sottos, N., & Braun, P. (2006). Polydimethylsiloxane-based self-healing materials. *Advanced Materials*, 18(8), 997-1000.
- Christjanson, P., Pehk, T., & Siimer, K. (2006). Structure formation in urea-formaldehyde resin synthesis. *Proceedings of the Estonian Academy of Sciences. Chemistry*, 55(4), 212-225.
- Conner, A. H. (1996). Urea-Formaldehyde Adhesive Resins. In J. C. Salamone (Ed.), *Polymeric Materials Encyclopedia* (Vol. 11, pp. 8496-8501). Boca Raton: CRC Press.
- Cosco, S., Ambrogio, V., Musto, P., & Carfagna, C. (2006). Urea-formaldehyde microcapsules containing an epoxy resin: influence of reaction parameters on the encapsulation yield. *Macromolecular Symposia*, 234, 184-192.
- Cosco, S., Ambrogio, V., Musto, P., & Carfagna, C. (2007). Properties of poly(urea-formaldehyde) microcapsules containing an epoxy resin. *Journal of Applied Polymer Science*, 105(3), 1400-1411.
- Craig, R. G. (1981). Chemistry, composition, and properties of composite resins. *Dental Clinics of North America*, 25(2), 219-239.
- De Lange, C., Bausch, J. R., & Davidson, C. L. (1980). The curing pattern of photo-initiated dental composites. *Journal of Oral Rehabilitation*, 7(5), 369-377.
- Dewprashad, B., & Eisenbraun, E. J. (1994). Fundamentals of epoxy formulation. *Journal of Chemical Education*, 71(4), 290-300.

- Dry, C. (1996). Procedures developed for self-repair of polymer matrix composite materials. *Composite Structures*, 35(3), 263-269.
- Eichner, K., & Kappert, H. F. (2005). *Zahnaerztliche Werkstoffe und ihre Verarbeitung* (8 ed. Vol. 1). Stuttgart: Georg Thieme.
- Eick, J. D., Byerley, T. J., Chappell, R. P., Chen, G. R., Bowles, C. Q., & Chappelow, C. C. (1993). Properties of expanding SOC/epoxy copolymers for dental use in dental composites. *Dental Materials*, 9(2), 123-127.
- Eick, J. D., Kotha, S. P., Chappelow, C. C., Kilway, K. V., Giese, G. J., Glaros, A. G., *et al.* (2007). Properties of silorane-based dental resins and composites containing a stress-reducing monomer. *Dental Materials*, 23(8), 1011-1017.
- Eick, J. D., Smith, R. E., Pinzino, C. S., & Kostoryz, E. L. (2006). Stability of silorane dental monomers in aqueous systems. *Journal of Dentistry*, 34(6), 405-410.
- Eick, J. D., Smith, R. E., Pinzino, C. S., Kotha, S. P., Kostoryz, E. L., & Chappelow, C. C. (2005). Photopolymerization of developmental monomers for dental cationically initiated matrix resins. *Dental Materials*, 21(4), 384-390.
- Feldman, J., & Schrock, R. R. (1991). Recent advances in the chemistry of d(0) alkylidene and metallacyclobutane complexes. *Progress in Inorganic Chemistry*, 39, 1-74.
- Ferracane, J. L. (2001). *Materials in Dentistry: Principles and Applications* (2 ed. Vol. 5). Baltimore: Lippincott Williams & Wilkins.
- Floyd, C. J. E., & Dickens, S. H. (2006). Network structure of Bis-GMA- and UDMA-based resin systems. *Dental Materials*, 22(12), 1143-1149.
- Fogg, D. E., Foucault, H. M., Robert, H. C., & Mingos, D. M. P. (2007). Ring-opening Metathesis Polymerization (ROMP). In *Comprehensive Organometallic Chemistry III* (pp. 623-652). Oxford: Elsevier.
- Franck, A. (1996). *Kunststoff-Kompendium* (4 ed.). Wuerzburg: Vogel.
- Ghosh, S. K. (2006). Functional Coatings and Microencapsulation: A General Perspective. In *Functional Coatings by Polymer Microencapsulation* (pp. 1-28). Weinheim: Wiley-VCH.
- Goovaerts, K., Lambrechts, P., De Munck, J., Bergmans, L., Van Meerbeek, B., Buschow, K. H. J., *et al.* (2002). Composite Dental Materials: Wear. In *Encyclopedia of Materials: Science and Technology* (pp. 1-8). Oxford: Elsevier.
- Green, B. K. (1957). Oil-containing microscopic capsules and method of making them. US Patent No. 2,800,458.

- Green, B. K., & Schleicher. (1953). US Patent No. 2,800,457.
- Grubbs, R. H. (2003). *Handbook of Metathesis* (1 ed.). Weinheim: Wiley-VCH.
- Grubbs, R. H. (2006). Olefinmetathesekatalysatoren zur Synthese von Molekülen und Materialien (Nobel-Vortrag). *Angewandte Chemie*, 118(23), 3845-3850.
- Grubbs, R. H., & Chang, S. (1998). Recent advances in olefin metathesis and its application in organic synthesis. *Tetrahedron*, 54(18), 4413-4450.
- Grubbs, R. H., & Trnka, T. M. (2005). *Ruthenium-Catalyzed Olefin Metathesis*. Weinheim: Wiley-VCH.
- Grubbs, R. H., & Tumas, W. (1989). Polymer synthesis and organotransition metal chemistry. *Science*, 243(4893), 907-915.
- Guggenberger, R., & Weinmann, W. (2000). Exploring beyond methacrylates. *American Journal of Dentistry*, 13, 82D-84D.
- Gupta, S., Zhang, Q., Emrick, T., Balazs, A. C., & Russell, T. P. (2006). Entropy-driven segregation of nanoparticles to cracks in multilayered composite polymer structures. *Nature Materials*, 5(3), 229-233.
- Hansen, C. J., Wu, W., Toohey, K. S., Sottos, N. R., White, S. R., & Lewis, J. A. (2009). Self-healing materials with interpenetrating microvascular networks. *Advanced Materials*, 21(41), 4143-4147.
- Hayes, S. A., Jones, F. R., Marshiya, K., & Zhang, W. (2007). A self-healing thermosetting composite material. *Composites Part A: Applied Science and Manufacturing*, 38(4), 1116-1120.
- Hayworth, L. T. (1985). Microencapsulation Process. US Patent No. 4,521,352.
- Hellerich, W., Harsch, G., & Haenle, S. (1996). *Werkstoff-Fuehrer Kunststoffe: Eigenschaften, Pruefungen* (7 ed.). Muenchen: Carl Hanser.
- Hickel, R. (2009). Trends in materials science from the point of view of a practicing dentist. *Journal of the European Ceramic Society*, 29(7), 1283-1289.
- Hong, K., & Park, S. (2000). Polyurea microcapsules with different structures: preparation and properties. *Journal of Applied Polymer Science*, 78(4), 894-898.
- Hoveyda, A. H. (2008). *Catalytic Asymmetric Olefin Metathesis*. Weinheim: Wiley-VCH.
- Huang, J., Stevens, E. D., Nolan, S. P., & Petersen, J. L. (1999). Olefin metathesis-active ruthenium complexes bearing a nucleophilic carbene ligand. *Journal of the American Chemical Society*, 121(12), 2674-2678.

- Ilie, N., & Hickel, R. (2006). Silorane-based dental composite: behavior and abilities. *Dental Materials Journal*, 25(3), 445-454.
- Ilie, N., Jelen, E., Clementino-Luedemann, T., & Hickel, R. (2007). Low-shrinkage composite for dental application. *Dental Materials Journal*, 26(2), 149-155.
- Inui, K., & Shigemura, T. (2004). Microencapsulated insecticidal composition. US Patent No. 20040120976.
- ISO Specification 4049 (2000). Dentistry - Polymer-based filling, restorative and luting materials. Geneva: International Organization for Standardization.
- Janda, J., Bernacchi, D., & Frieders, S. (1995). Microencapsulation Process. US Patent No. 5,418,010.
- Jandt, K. D., & Sigusch, B. W. (2009). Future perspectives of resin-based dental materials. *Dental Materials*, 25(8), 1001-1006.
- Jimenez-Planas, A., Martin, J., Abalos, C., & Llamas, R. (2008). Developments in polymerization lamps. *Quintessence International*, 39(2), E74-E84.
- Jordan, O., Aebischer, P., & Clemence, J.-F. (2000). Pharmaceutical microencapsulation. US Patent No. 6,080,412.
- Jyothi, N. V., Prasanna, M., Prabha, S., Seetha, R. P., Srawan, G., & Sakarkar, S. N. (2009). Microencapsulation techniques, factors influencing encapsulation efficiency: a review [Electronic Version]. *The Internet Journal of Nanotechnology*, 3, from <http://www.ispub.com>.
- Kawaguchi, M., Fukushima, T., & Horibe, T. (1989). Effect of monomer structure on the mechanical properties of light-cured composite resins. *Dental Materials Journal*, 8(1), 40-45.
- Keller, M. W. (2007). *A Self-Healing Poly(Dimethyl Siloxane) Elastomer*. University of Illinois, Urbana-Champaign.
- Kessler, M. R. (2002). *Characterization and Performance of a Self-Healing Composite Material*. University of Illinois, Urbana-Champaign.
- Kessler, M. R. (2007). Self-healing: a new paradigm in materials design. *Proceedings of the Institution of Mechanical Engineers - Part G: Journal of Aerospace Engineering*, 221(4), 479-495.
- Klosiewicz, D. W. (1983). Method for making a dicyclopentadiene thermoset polymer. US Patent No. 4,400,340.
- Koerber, K., & Ludwig, K. (1993). *Zahnaerztliche Werkstoffkunde und Technologie* (2 ed.). Stuttgart: Georg Thieme.

- Kostoryz, E., Zhu, Q., Zhao, H., Miller, M., & Eick, J. (2006). Assessment of the relative skin sensitization potency of siloranes and bis-GMA using the local lymph node assay and QSAR predicted potency. *Journal of Biomedical Materials Research Part A*, 79A(3), 684-688.
- Kuestermann, B. J. (2009). *Einfluss von Kavitaetentiefe, Komposit und Schichttechnik auf die Hoeckerdeformation waehrend der Polymerisation bei Klasse II-Fuellungen*. Julius-Maximilians-Universitaet, Wuerzburg.
- Lee, H. Y., Lee, S. J., Cheong, I. W., & Kim, J. H. (2002). Microencapsulation of fragrant oil via in situ polymerization: effects of pH and melamine-formaldehyde molar ratio. *Journal of Microencapsulation*, 19(5), 559-569.
- Lee, W., Scholz, R., Nielsch, K., & Gösele, U. (2005). A template-based electrochemical method for the synthesis of multisegmented metallic nanotubes. *Angewandte Chemie*, 117(37), 6204-6208.
- Leitgeb, A., Wappel, J., & Slugovc, C. (2010). The ROMP toolbox upgraded. *Polymer*, 51(14), 2927-2946.
- Li, V. C., Lim, Y. M., & Chan, Y.-W. (1998). Feasibility study of a passive smart self-healing cementitious composite. *Composites Part B: Engineering*, 29(6), 819-827.
- Li, Y., Swartz, M. L., Phillips, R. W., Moore, B. K., & Roberts, T. A. (1985). Materials science effect of filler content and size on properties of composites. *Journal of Dental Research*, 64(12), 1396-1403.
- Lien, W., & Vandewalle, K. S. (2010). Physical properties of a new silorane-based restorative system. *Dental Materials*, 26(4), 337-344.
- Lloyd, H., & Jeffrey, R. (1947). A micro-hardness tester. *Journal of Scientific Instruments*, 24(7), 186-188.
- Lu, H., Stansbury, J. W., & Bowman, C. N. (2004). Towards the elucidation of shrinkage stress development and relaxation in dental composites. *Dental Materials*, 20(10), 979-986.
- Mackert, J. R. (1991). Dental amalgam and mercury. *The Journal of the American Dental Association*, 122(8), 54-61.
- Manners, I. (1995). Ring-Opening Polymerization of Metallocenophanes: A new Route to Transition Metal-Based Polymers. In *Advances in Organometallic Chemistry* (Vol. 37, pp. 131-168). San Diego: Academic Press.
- Marxkors, R., & Meiners, H. (1993). *Taschenbuch der zahnaerztlichen Werkstoffkunde*. Muenchen: Carl Hanser.
- Marxkors, R., Meiners, H., & Geis-Gerstorfer, J. (2008). *Taschenbuch der zahnaerztlichen Werkstoffkunde* (6 ed.). Koeln: Deutscher Zahnärzte Verlag.

- Maxson, P. (2007). Mercury in dental use: environmental implications for the European Union [Electronic Version], from <http://www.zeromercury.org>.
- May, C. A. (1988). *Epoxy Resins: Chemistry and Technology* (1 ed.). New York: Marcel Dekker.
- May, C. A., & Nixon, A. C. (1961). Reactive diluents for epoxy adhesives. *Industrial & Engineering Chemistry*, 53(4), 303-304.
- McCabe, J. F., & Walls, A. W. G. (1998). *Applied Dental Materials* (8 ed. Vol. 12). London: Blackwell Science.
- Mjoer, I. A. (1997). Selection of restorative materials in general dental practice in Sweden. *Acta Odontologica Scandinavica*, 55(1), 53-57.
- Morishita, M., Inaba, Y., Fukushima, M., Kobari, S., Nagata, A., & Abe, J. (1976). Preparation of microcapsules. US Patent No. 3,943,063.
- Moszner, N., Fischer, U. K., Angermann, J., & Rheinberger, V. (2006). Bis-(acrylamide)s as new cross-linkers for resin-based composite restoratives. *Dental Materials*, 22(12), 1157-1162.
- Moszner, N., & Salz, U. (2001). New developments of polymeric dental composites. *Progress in Polymer Science*, 26(4), 535-576.
- Moszner, N., Voelkel, T., Fischer, U. K., & Rheinberger, V. (1999). Polymerisation of cyclic monomers, 8. Synthesis and radical polymerisation of hybrid 2-vinylcyclopropanes. *Macromolecular Rapid Communications*, 20(1), 33-35.
- Motuku, M., Vaidya, U. K., & Janowski, G. M. (1999). Parametric studies on self-repairing approaches for resin infused composites subjected to low velocity impact. *Smart Materials and Structures*, 8(5), 623-638.
- Moy, J. (1998). Microcapsules with reduced shell wall permeability. US Patent No. 5,804,298.
- Mueller-Schneemayer, I. (2004). *Die Amalgamkontroverse in den Zwanziger Jahren des 20. Jahrhunderts*. Ludwig-Maximilians-University Munich, Munich.
- Nagem-Filho, H., Nagem, H. D., Francisconi, P. A. S., Franco, E. B., Mondelli, R. F. L., & Coutinho, K. Q. (2007). Volumetric polymerization shrinkage of contemporary composite resins. *Journal of Applied Oral Science*, 15(5), 448-452.
- Needleman, H. L. (2006). Mercury in dental amalgam - a neurotoxic risk? *The Journal of the American Medical Association*, 295(15), 1835-1836.
- Ni, P. H., Zhang, M. Z., & Yan, N. X. (1995). Effect of operating variables and monomers on the formation of polyurea microcapsules. *Journal of Membrane Science*, 103(1-2), 51-55.

- Oeev, B., Citak, B., Oeztemel, D., Balbas, A., Peker, S., & Cakir, S. (1997). Variation of droplet sizes during the formation of microcapsules from emulsions. *Journal of Microencapsulation*, 14(4), 489-499.
- Oliver, W. C., & Pharr, G. M. (1992). An improved technique for determining hardness and elastic-modulus using load and displacement sensing indentation experiments. *Journal of Materials Research*, 7(6), 1564-1583.
- Oliver, W. C., & Pharr, G. M. (2004). Measurement of hardness and elastic modulus by instrumented indentation: advances in understanding and refinements to methodology. *Journal of Materials Research*, 19(1), 3-20.
- Osborn, J. A., & Schrock, R. R. (1971). Coordinatively unsaturated cationic complexes of rhodium(I), iridium(I), palladium(II), and platinum(II). Generation, synthetic utility, and some catalytic studies. *Journal of the American Chemical Society*, 93(12), 3089-3091.
- Osborn, J. A., & Schrock, R. R. (1971). Preparation and properties of some cationic complexes of rhodium(I) and rhodium(III). *Journal of the American Chemical Society*, 93(10), 2397-2407.
- Pang, J. W. C., & Bond, I. P. (2005). 'Bleeding composites'--damage detection and self-repair using a biomimetic approach. *Composites Part A: Applied Science and Manufacturing*, 36(2), 183-188.
- Pang, J. W. C., & Bond, I. P. (2005). A hollow fibre reinforced polymer composite encompassing self-healing and enhanced damage visibility. *Composites Science and Technology*, 65(11-12), 1791-1799.
- Panich, N., & Yong, S. (2005). Improved method to determine the hardness and elastic moduli using nano-indentation. *King Mongkut's Institute of Technology Ladkrabang Science Journal*, 5(2), 483-492.
- Petrie, E. M. (2005). *Epoxy Adhesive Formulations* (1 ed.). New York: McGraw-Hill.
- Peutzfeldt, A. (1997). Resin composites in dentistry: the monomer systems. *European Journal of Oral Sciences*, 105(2), 97-116.
- Phillips, R. W., Avery, D. R., Mehra, R., Swartz, M. L., & McCune, R. J. (1971). One-year observations on a composite resin for class II restorations. *The Journal of Prosthetic Dentistry*, 26(1), 68-77.
- Phillips, R. W., Avery, D. R., Mehra, R., Swartz, M. L., & McCune, R. J. (1972). Observations on a composite resin for class II restorations: two-year report. *The Journal of Prosthetic Dentistry*, 28(2), 164-169.
- Phillips, R. W., Avery, D. R., Mehra, R., Swartz, M. L., & McCune, R. J. (1973). Observations on a composite resin for class II restorations: three-year report. *The Journal of Prosthetic Dentistry*, 30(6), 891-897.

- Pizzi, A. (1989). *Wood Adhesives: Chemistry and Technology* (Vol. 2). New York: Marcel Dekker.
- Pizzi, A. (1994). *Advanced Wood Adhesives Technology* (1 ed.). New York: Marcel Dekker.
- Pizzi, A., & Mittal, K. L. (2003). *Handbook of Adhesive Technology* (2 ed.). New York: Marcel Dekker.
- Prasetya, R. A., & Hasakowati, W. (2010). Mechanism of microencapsulation with urea-formaldehyde polymer. *American Journal of Applied Sciences*, 7(6), 739-745.
- Puckett, A. D., Fitchie, J. G., Kirk, P. C., & Gamblin, J. (2007). Direct composite restorative materials. *Dental Clinics of North America*, 51(3), 659-675.
- Puckett, A. D., & Smith, R. (1992). Method to measure the polymerization shrinkage of light-cured composites. *Journal of Prosthetic Dentistry*, 68(1), 56-58.
- Ranney, M. W. (1969). *Microencapsulation Technology* (1 ed.). Park Ridge: Noyes Development Corporation.
- Ratna, D. (2005). *Epoxy Composites: Impact Resistance and Flame Retardancy* (Vol. 16). Shrewsbury: iSmithers.
- Rawls, H. R. (2003). Dental Polymers. In K. J. Anusavice (Ed.), *Phillips' Science of Dental Materials* (11 ed., pp. 143-169). St Louis: Saunders.
- Rawls, H. R., & Esquivel-Upshaw, J. F. (2003). Restorative Resins. In K. J. Anusavice (Ed.), *Phillips' Science of Dental Materials* (11 ed., pp. 399-442). St. Louis: Elsevier.
- Rey, L., Duchet, J., Galy, J., Sautereau, H., Vouagner, D., & Carrion, L. (2002). Structural heterogeneities and mechanical properties of vinyl/dimethacrylate networks synthesized by thermal free radical polymerisation. *Polymer*, 43(16), 4375-4384.
- Roulet, J.-F., & Meyer, G. (2006). Komposit - Meilensteine der Entwicklung der letzten 50 Jahre [Electronic Version]. *Die Zahnarzt Woche*, 15, from <http://www.dzw.de>.
- Rule, J. D. (2005). *Polymer Chemistry for Improved Self-Healing Composite Materials*. University of Illinois, Urbana-Champaign.
- Rule, J. D., Sottos, N. R., & White, S. R. (2007). Effect of microcapsule size on the performance of self-healing polymers. *Polymer*, 48(12), 3520-3529.
- Sadhir, R. K., & Luck, R. M. (1992). *Expanding Monomers: Synthesis, Characterization, and Applications* (1 ed.). Boca Raton: CRC Press.

- Samadzadeh, M., Boura, S. H., Peikari, M., Kasiriha, S. M., & Ashrafi, A. (2010). A review on self-healing coatings based on micro/nanocapsules. *Progress in Organic Coatings*, 68(3), 159-164.
- Scher, H. B., & Rodson, M. (1990). Microencapsulation process. US Patent No. 4,956,129.
- Schmalz, G., & Arentholt-Bindslev, D. (2005). *Biokompatibilitaet zahnaerztlicher Werkstoffe* (1 ed.). Munich: Elsevier, Urban & Fischer.
- Scholl, M., Ding, S., Lee, C. W., & Grubbs, R. H. (1999). Synthesis and activity of a new generation of ruthenium-based olefin metathesis catalysts coordinated with 1,3-dimesityl-4,5-dihydroimidazol-2-ylidene ligands. *Organic Letters*, 1(6), 953-956.
- Schrock, R. R. (1990). Living ring-opening metathesis polymerization catalyzed by well-characterized transition-metal alkylidene complexes. *Accounts of Chemical Research*, 23(5), 158-165.
- Schrock, R. R. (2006). Metall-Kohlenstoff-Mehrfachbindungen in katalytischen Metathesereaktionen (Nobel-Vortrag). *Angewandte Chemie*, 118(23), 3832-3844.
- Schrock, R. R., & Hoveyda, A. H. (2003). Complexes as efficient olefin-metathesis catalysts. *Angewandte Chemie*, 42(38), 4592-4633.
- Schrock, R. R., & Hoveyda, A. H. (2003). Molybdän- und Wolframimidoalkylidenkomplexe als effiziente Olefinmetathesekatalysatoren. *Angewandte Chemie*, 115(38), 4740-4782.
- Schrock, R. R., & Osborn, J. A. (1976). Catalytic hydrogenation using cationic rhodium complexes. I. Evolution of the catalytic system and the hydrogenation of olefins. *Journal of the American Chemical Society*, 98(8), 2134-2143.
- Schwab, P., Grubbs, R. H., & Ziller, J. W. (1996). Synthesis and applications of RuCl₂(CHR')(PR₃)₂: the influence of the alkylidene moiety on metathesis activity. *Journal of the American Chemical Society*, 118(1), 100-110.
- Schwarz, O. (1992). *Kunststoffkunde* (4 ed.). Wuerzburg: Vogel.
- Schweikl, H., G., S., & W., W. (2002). Mutagenic activity of structurally related oxiranes and siloranes in salmonella typhimurium. *Mutation Research/Genetic Toxicology and Environmental Mutagenesis*, 521(1-2), 19-27.
- Schweikl, H., Schmalz, G., & Weinmann, W. (2004). The induction of gene mutations and micronuclei by oxiranes and siloranes in mammalian cells in vitro. *Journal of Dental Research*, 83(1), 17-21.

- Sideridou, I., Tserki, V., & Papanastasiou, G. (2002). Effect of chemical structure on degree of conversion in light-cured dimethacrylate-based dental resins. *Biomaterials*, 23(8), 1819-1829.
- Sliwka, W. (1975). Mikroverkapselung. *Angewandte Chemie*, 87(16), 556-567.
- Smith, R. E., Pinzino, C. S., Chappelow, C. C., Holder, A. J., Kostoryz, E. L., Guthrie, J. R., *et al.* (2004). Photopolymerization of an expanding monomer with an aromatic dioxirane. *Journal of Applied Polymer Science*, 92(1), 62-71.
- Sriram, S. R. (2002). *Development of self-healing polymer composites and photoinduced ring opening metathesis polymerization*. University of Illinois, Urbana-Champaign.
- Stansbury, J. W. (1992). Synthesis and evaluation of new oxaspiro monomers for double ring-opening polymerization. *Journal of Dental Research*, 71(7), 1408-1412.
- Stansbury, J. W. (2000). Curing dental resins and composites by photopolymerization. *Journal of Esthetic and Restorative Dentistry*, 12(6), 300-308.
- Stansbury, J. W., & Bailey, W. J. (1990). Evaluation of Spiro Orthocarbonate Monomers Capable of Polymerization with Expansion as Ingredients in Dental Composite Materials. In C. G. Gebelein & R. L. Dunn (Eds.), *Progress in Biomedical Polymers* (pp. 133-139). New York: Plenum Press.
- Stansbury, J. W., & Dermann, M. H. (1997). Radical/cationic photopolymerization of spiro orthocarbonate-modified methacrylate resins. *Journal of Dental Research*, 76, 215-215.
- Steeger, U., Weber, R., & Baehren, A. (2009). Scratching, biting, scoring, scraping - new micro and ultra-micro harness testers. *Shimadzu News*, pp. 11-12.
- Strickling, W. (1988). *Vergleichende Untersuchungen zur Härte von Aufbrennlegierungen und die klinische Relevanz von Härteangaben*. Philipps Universitaet, Marburg.
- Sumii, M., & Yoshimura, Y. (1996). Microencapsulation process. US Patent No. 5,503,781.
- Syrett, J. A., Becer, C. R., & Haddleton, D. M. (2010). Self-healing and self-mendable polymers. *Polymer Chemistry*, 1, 978-987.
- Tabor, D. (1951). *The Hardness of Metals*. New York: Oxford University Press.

- Tan, H. S., Ng, T. H., & Mahabadi, H. K. (1991). Interfacial polymerization encapsulation of a viscous pigment mix: emulsification conditions and particle size distribution. *Journal of Microencapsulation: Micro and Nano Carriers*, 8(4), 525 - 536.
- Thao, T. D. P., Johnson, T. J. S., Tong, Q. S., & Dai, P. S. (2009). Implementation of self-healing in concrete - proof of concept. *The IES Journal Part A: Civil & Structural Engineering*, 2(2), 116 - 125.
- Tilbrook, D. A., Clarke, R. L., Howle, N. E., & Braden, M. (2000). Photocurable epoxy-polyol matrices for use in dental composites I. *Biomaterials*, 21(17), 1743-1753.
- Tohmura, S.-I., Inoue, A., & Sahari, S. H. (2001). Influence of the melamine content in melamine-urea-formaldehyde resins on formaldehyde emission and cured resin structure. *Journal of Wood Science*, 47(6), 451-457.
- Toohey, K. S., Hansen, C. J., Lewis, J. A., White, S. R., & Sottos, N. R. (2009). Delivery of two-part self-healing chemistry via microvascular networks. *Advanced Functional Materials*, 19(9), 1399-1405.
- Toohey, K. S., Sottos, N. R., Lewis, J. A., Moore, J. S., & White, S. R. (2007). Self-healing materials with microvascular networks. *Nature Materials*, 6(8), 581-585.
- Trask, R. S., Williams, H. R., & Bond, I. P. (2007). Self-healing polymer composites: mimicking nature to enhance performance. *Bioinspiration & Biomimetics*, 2(1), 1-9.
- Trnka, T. M., & Grubbs, R. H. (2000). The development of L2X2RuCHR olefin metathesis catalysts: an organometallic success story. *Accounts of Chemical Research*, 34(1), 18-29.
- Truong, V. T., & Tyas, M. J. (1988). Prediction of in vivo wear in posterior composite resins: a fracture mechanics approach. *Dental Materials*, 4(6), 318-327.
- Van Landuyt, K. L., Snauwaert, J., De Munck, J., Peumans, M., Yoshida, Y., Poitevin, A., *et al.* (2007). Systematic review of the chemical composition of contemporary dental adhesives. *Biomaterials*, 28(26), 3757-3785.
- Van Meerbeek, B., Perdigão, J., Lambrechts, P., & Vanherle, G. (1998). The clinical performance of adhesives. *Journal of Dentistry*, 26(1), 1-20.
- Watkins, N., Quigley, P., & Orton, M. (1994). Ring opening metathesis polymerization of cyclic alkenes containing heteroatoms. *Macromolecular Chemistry and Physics*, 195(4), 1147-1164.

- Weinmann, W., Luchterhandt, T., Guggenberger, R., Stippschild, A., Then, S., & Dede, K. (2002). Comparative testing of volumetric shrinkage and sealing of silorane and methacrylate filling materials. *Journal of Dental Research*, *81*, 417.
- Weinmann, W., Thalacker, C., & Guggenberger, R. (2005). Siloranes in dental composites. *Dental Materials*, *21*(1), 68-74.
- Wengrovius, J. H., Schrock, R. R., Churchill, M. R., Missert, J. R., & Youngs, W. J. (1980). Tungsten-oxo alkylidene complexes as olefin metathesis catalysts and the crystal structure of $W(O)(CHCMe_3)(PEt_3)Cl_2$. *Journal of the American Chemical Society*, *102*, 4515.
- White, S. R., Sottos, N. R., Geubelle, P. H., Moore, J. S., Kessler, M. R., Sriram, S. R., *et al.* (2001). Autonomic healing of polymer composites. *Nature*, *409*(6822), 794-797.
- Wijnendaele, K., De Jaeger, F., & Haegglund, S. (2010). Reduktion der Formaldehyd-Exposition in der Holzverarbeitenden Industrie. from <http://www.vhi.de>.
- Willems, G., Lambrechts, P., Braem, M., & Vanherle, G. (1993). Three-year follow-up of five posterior composites: in vivo wear. *Journal of Dentistry*, *21*(2), 74-78.
- Woirgard, J., Dargenton, J. C., Tromas, C., & Audurier, V. (1998). A new technology for nanohardness measurements: principle and applications. *Surface and Coatings Technology*, *100-101*, 103-109.
- Wool, R. P. (2001). A material fix [Electronic Version]. *Nature*, *409*, 773, from <http://autonomic.beckman.illinois.edu/files/RWool.pdf>.
- Wu, D. Y., Meure, S., & Solomon, D. (2008). Self-healing polymeric materials: a review of recent developments. *Progress in Polymer Science*, *33*(5), 479-522.
- Yuan, L., Aijuan, G., Liang, G., Wu, J., Wang, W., & Sun, Z. (2009). Novel glass fiber-reinforced cyanate ester/microcapsule composites. *Journal of Composite Materials*, *43*(16), 1679-1694.
- Yuan, L., Gu, A., & Liang, G. (2008). Preparation and properties of poly(urea-formaldehyde) microcapsules filled with epoxy resins. *Materials Chemistry and Physics*, *110*(2-3), 417-425.
- Zako, M., & Takano, N. (1999). Intelligent material systems using epoxy particles to repair microcracks and delamination damage in GFRP. *Journal of Intelligent Material Systems and Structures*, *10*(10), 836-841.
- Zalucha, D. J., & Abbey, K. J. (2007). *Kent and Riegel's Handbook of Industrial Chemistry and Biotechnology* (11 ed. Vol. 1). New York: Springer.

Zimmermann, A. (1991). *Untersuchungen zur Haerte an der Oberflaeche von Gipsproben*. Philipps-Universitaet, Marburg.

APPENDIX A: Raw Data of FESEM – EDX Analysis

EDX analysis of microcapsule surface, smooth shell layer

Test Parameters

Label :	A
Collected :	6-May-2009 09:40 PM
Livetime (s) :	40.00
Real time (s) :	41.49
Detector :	Silicon
Window :	SATW
Tilt (deg) :	-0.2
Elevation (deg) :	35.0
Azimuth (deg) :	0.0
Magnification :	10000 X
Accelerating voltage (kV) :	10.00
Process time :	5
Spectrum processing :	No peaks omitted
Processing option :	All elements analyzed (Normalised)
	Number of iterations = 3

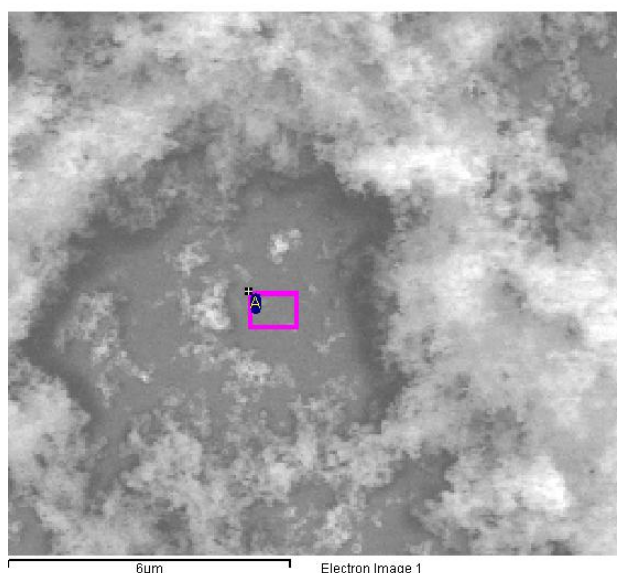


Figure A1 Area of FESEM-EDX measurement on smooth microcapsule shell surface.

Table A1 Standard Measurement FESEM-EDX

C	CaCO ₃	1-Jun-1999 12:00 AM
N	Not defined	1-Jun-1999 12:00 AM
O	SiO ₂	1-Jun-1999 12:00 AM
Al	Al ₂ O ₃	1-Jun-1999 12:00 AM

Table A2 Composition of smooth microcapsule shell;
elemental analysis by FESEM-EDX

Element	Weight%	Atomic%
Carbon	53.81	58.85
Nitrogen	30.25	28.37
Oxygen	15.00	12.32
Aluminium	0.93	0.45
Totals	100.00	100.00

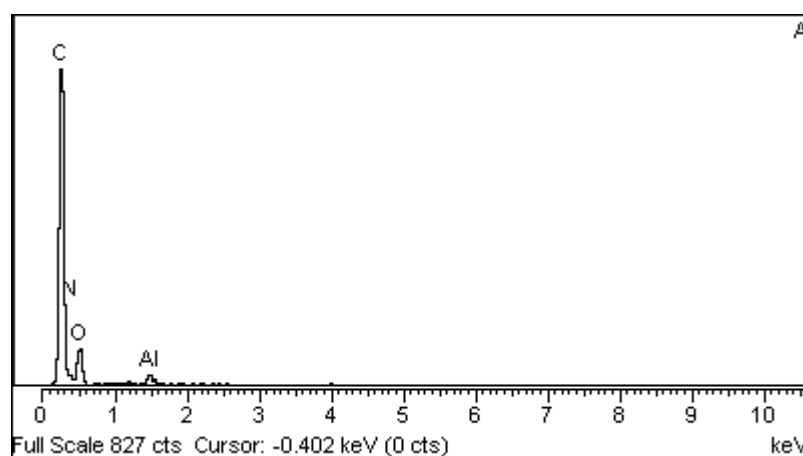


Figure A2 FESEM-EDX spectra obtained from elemental analysis of the smooth microcapsule shell surface.

EDX analysis of microcapsule surface, rough outer shell layer

Test Parameters

Label :	B
Collected :	6-May-2009 09:41 PM
Livetime (s) :	40.00
Real time (s) :	41.51
Detector :	Silicon
Window :	SATW
Tilt (deg) :	-0.2
Elevation (deg) :	35.0
Azimuth (deg) :	0.0
Magnification :	10000 X
Accelerating voltage (kV) :	10.00
Process time :	5
Spectrum processing :	No peaks omitted
Processing option :	All elements analyzed (Normalised)
	Number of iterations = 3

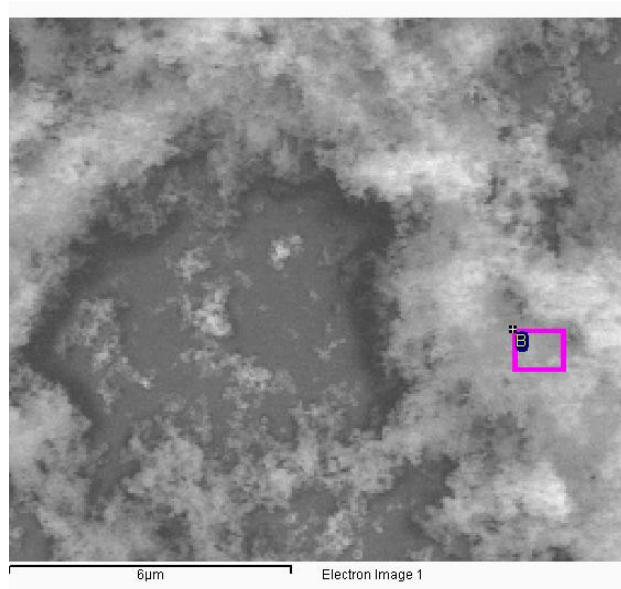


Figure A3 Area of FESEM-EDX measurement on outer microcapsule shell layer.

Table A3 Composition of outer microcapsule shell layer; elemental analysis by FESEM-EDX

Element	Weight%	Atomic%
Carbon	43.99	49.22
Nitrogen	33.91	32.54
Oxygen	21.16	17.78
Aluminium	0.94	0.47
Totals	100.00	100.00

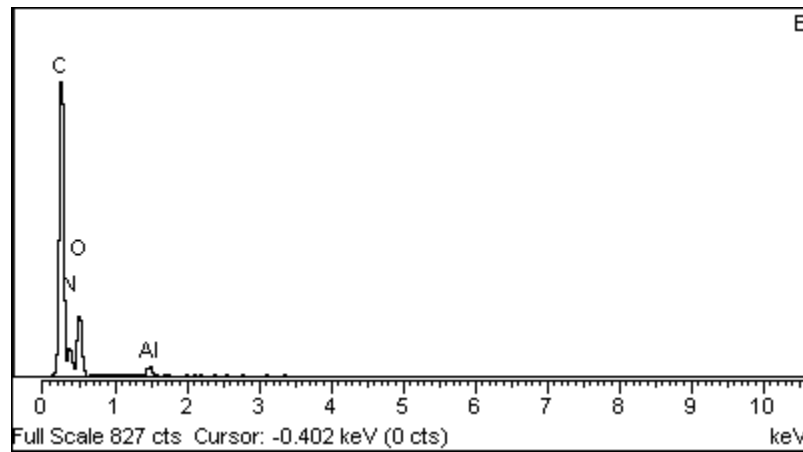


Figure A4 FESEM-EDX spectra obtained from elemental analysis of the outer microcapsule shell layer.

APPENDIX B: Thermograms of Shelf-Life Test

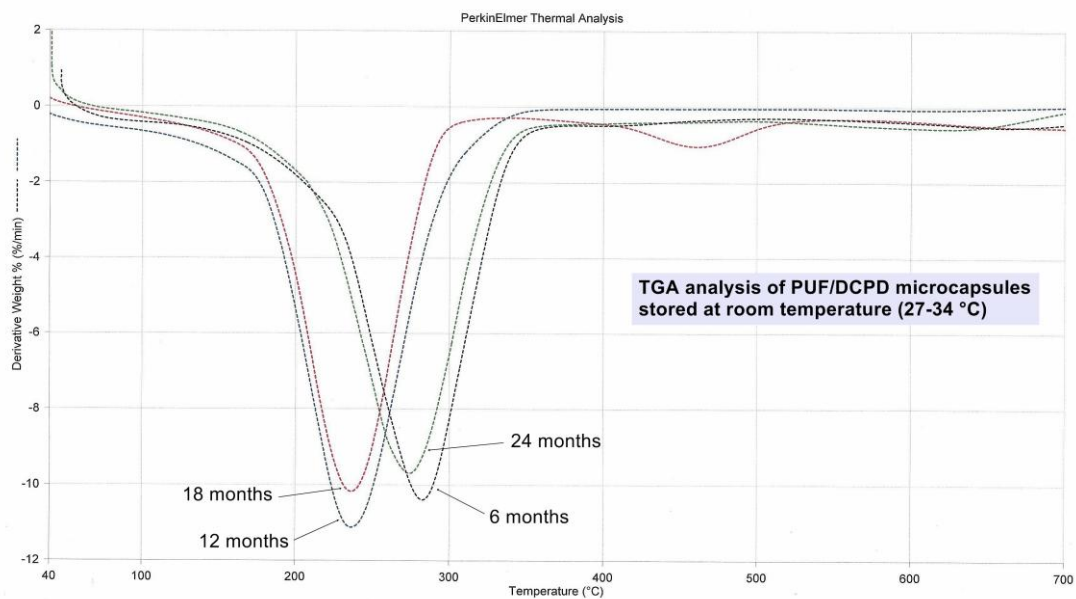


Figure B1: TGA traces of PUF/DCPD microcapsules after ageing.

APPENDIX C: Raw Data of Mechanical Measurements

1. Three-Point-Bending Test

Test Parameters

Instrument: Shimadzu AG-X high precision universal testing machine
Test Mode: Single
Test Type: 3 Point Bend
Speed: 0.75 mm/min
Shape: Plate
Qty/Batch: 8
Test result: Max Stress in [MPa]
Test date: 11-Nov-2009 / 1-Dec-2009 / 22-Jan-1009

Table C1 Flexural strength of dental resin material incorporating 3% microcapsules with different melamine amounts in the capsule shell; reference: without capsules

Sample No.	Reference	Melamine Part Relative to Urea Amount			
		0%	1%	3%	5%
1	101.8600	129.5500	80.3110	87.1580	70.2455
2	92.2730	105.2880	81.1519	96.5000	79.0099
3	122.4410	132.5900	72.0332	89.4696	76.9582
4	147.2830	73.4096	69.5274	71.4755	88.2380
5	105.1400	78.3573	74.1178	81.6996	80.6885
6	86.5176	113.7570	70.3228	85.1212	91.0691
7	93.8544	127.8450	68.7846	85.0000	70.0000
8	100.6340	79.9499	72.0485	85.2000	77.4854
Average	106.2504	105.0934	73.5372	85.2030	79.2118
Std. Dev.	19.7711	24.7784	4.7461	7.0752	7.5366
Minimum	86.5176	73.4096	68.7846	71.4755	70.0000
Maximum	147.2830	132.5900	81.1519	96.5000	91.0691

Table C2 Flexural strength of dental resin material incorporating 6% microcapsules with different melamine amounts in the capsule shell; reference: without capsules

Sample No.	Reference	Melamine Part Relative to Urea Amount						
		0%	0.5%	1%	2%	3%	4%	5%
1	101.8600	78.3120	96.0378	84.2399	77.3902	67.0378	77.3597	76.2884
2	92.2730	59.0596	94.5288	89.6568	77.7284	80.8808	69.5977	96.7427
3	122.4410	72.8335	75.5798	90.0235	89.5837	77.2271	81.0925	72.3460
4	147.2830	64.9834	81.6694	93.8814	71.9537	70.0525	70.3882	88.7806
5	105.1400	43.8643	63.3842	72.8880	85.3145	72.2812	70.5336	60.3435
6	86.5176	53.1309	87.8673	78.9621	90.1160	73.3971	87.3448	96.2448
7	93.8544	80.3010	84.5794	87.5137	68.6445	72.0332	62.9476	96.2959
8	100.6340	—	91.5169	99.4850	—	—	78.2551	81.5155
Average	106.2504	64.6407	84.3955	87.0813	80.1044	73.2728	74.6899	83.5697
Std. Dev.	19.7711	13.5072	10.8736	8.3753	7.4134	4.5698	7.7512	13.3415
Minimum	86.5176	43.8643	63.3842	72.8880	71.9537	67.0378	62.9476	60.3435
Maximum	147.2830	80.3010	96.0378	99.4850	90.1160	80.8808	87.3448	96.7427

2. Microhardness Measurement

Test Parameters

Instrument: Shimadzu Micro Hardness Tester HMV-2 Series
 Test loads: HV 0.1 = 100 g
 Measurement mode: Simple test
 Duration time: 5 sec
 Indenter type: Vickers
 Objective lens: 40
 Eyepiece: 10
 Test result: Vickers Hardness

Test date: 13-Aug-2009
 Sample: Reference: virgin dental material, and dental material incorporating 6% PUF/DCPD microcapsules

Table C3 Vickers hardness test results of neat dental resin material

Sample No.	Vickers Hardness Measurement					Test Result	HV
	M1	M2	M3	M4	M5		
S1	29.6	31.1	30.4	30.5	30.8	Total Average	30.7
S2	30.4	33.5	33.3	32.4	33.0	Std. Dev.	1.4
S3	29.4	29.7	29.2	29.4	29.8	Minimum	29.0
S4	31.6	32.0	31.9	31.7	32.1	Maximum	33.5
S5	29.4	29.1	29.8	29.0	29.2		

Table C4 Vickers hardness test results of dental resin material incorporating 6% PUF/DCPD microcapsules

Sample No.	Vickers Hardness Measurement					Test Result	HV
	M1	M2	M3	M4	M5		
S1	24.9	26.1	24.7	25.2	25.8	Total Average	24.1
S2	23.9	23.8	22.5	23.4	24.0	Std. Dev.	0.8
S3	23.6	24.0	23.6	23.7	23.5	Minimum	22.5
S4	23.0	23.9	24.1	23.3	23.2	Maximum	26.1
S5	24.7	24.6	23.9	24.4	23.8		

Test date: 12-13 Nov 2009 / 02 Dec 2009
 Sample: Dental material incorporating 6% melamine modified PUF/DCPD microcapsules

Table C5 Vickers hardness test results of dental resin material incorporating 6% microcapsules with 0.5% of the urea part in the capsule shell replaced by melamine

Sample No.	Vickers Hardness Measurement					Test Result	HV
	M1	M2	M3	M4	M5		
S1	29.9	30.3	28.3	29.5	29.6	Total Average	28.8
S2	30.3	28.4	29.9	29.5	28.9	Std. Dev.	1.1
S3	29.2	26.4	26.2	27.3	27.4	Minimum	26.2
S4	29.8	29.3	29.3	29.5	29.6	Maximum	30.3
S5	28.9	28.5	28.3	28.6	27.9		

Table C6 Vickers hardness test results of dental resin material incorporating 6% microcapsules with 1% of the urea part in the capsule shell replaced by melamine

Sample No.	Vickers Hardness Measurement					Test Result	HV
	M1	M2	M3	M4	M5		
S1	25.6	25.5	24.0	24.0	24.3	Total Average	24.2
S2	25.1	24.5	24.1	23.5	23.3	Std. Dev.	0.7
S3	24.8	24.3	23.5	24.0	24.0	Minimum	23.1
S4	25.2	24.2	23.4	23.1	24.1	Maximum	25.6
S5	25.1	24.3	23.9	23.5	23.3		

Table C7 Vickers hardness test results of dental resin material incorporating 6% microcapsules with 2% of the urea part in the capsule shell replaced by melamine

Sample No.	Vickers Hardness Measurement					Test Result	HV
	M1	M2	M3	M4	M5		
S1	20.9	23.4	22.2	22.3	21.5	Total Average	21.7
S2	21.0	23.3	22.1	23.0	21.3	Std. Dev.	1.1
S3	19.3	21.4	23.3	21.3	22.1	Minimum	19.3
S4	19.9	20.9	22.4	21.1	20.2	Maximum	23.4
S5	20.7	22.9	22.4	22.0	22.3		

Table C8 Vickers hardness test results of dental resin material incorporating 6% microcapsules with 3% of the urea part in the capsule shell replaced by melamine

Sample No.	Vickers Hardness Measurement					Test Result	HV
	M1	M2	M3	M4	M5		
S1	26.7	28.7	30.1	28.5	30.0	Total Average	27.8
S2	26.8	26.7	26.9	26.8	26.9	Std. Dev.	1.1
S3	27.2	27.9	29.6	28.2	29.1	Minimum	26.5
S4	26.5	27.1	27.2	26.9	27.1	Maximum	30.1
S5	27.9	27.6	27.8	27.8	28.3		

Table C9 Vickers hardness test results of dental resin material incorporating 6% microcapsules with 4% of the urea part in the capsule shell replaced by melamine

Sample No.	Vickers Hardness Measurement					Test Result	HV
	M1	M2	M3	M4	M5		
S1	23.0	23.4	22.3	25.5	27.2	Total Average	24.6
S2	22.3	23.6	22.8	26.2	26.8	Std. Dev.	2.4
S3	23.1	22.7	22.9	29.0	26.8	Minimum	22.3
S4	22.3	22.5	22.5	28.9	27.0	Maximum	29.0
S5	22.5	22.6	22.6	28.7	26.7		

Table C10 Vickers hardness test results of dental resin material incorporating 6% microcapsules with 5% of the urea part in the capsule shell replaced by melamine

Sample No.	Vickers Hardness Measurement					Test Result	HV
	M1	M2	M3	M4	M5		
S1	25.5	26.1	25.7	23.4	23.0	Total Average	24.1
S2	23.4	26.7	24.5	22.8	22.4	Std. Dev.	1.5
S3	26.5	25.0	25.3	22.9	21.9	Minimum	21.9
S4	24.7	24.9	24.1	23.1	22.0	Maximum	26.7
S5	25.0	26.2	23.7	22.8	21.9		

Test date: 02-03 Dec 2009
 Sample: Dental material incorporating 3% melamine modified PUF/DCPD microcapsules

Table C11 Vickers hardness test results of dental resin material incorporating 3% PUF/DCPD microcapsules (reference, without melamine modification)

Sample No.	Vickers Hardness Measurement					Test Result	HV
	M1	M2	M3	M4	M5		
S1	24.9	25.1	24.6	25.0	25.7	Total Average	24.1
S2	22.8	23.8	22.9	23.7	23.0	Std. Dev.	0.8
S3	23.2	24.1	23.6	23.4	24.2	Minimum	22.8
S4	24.1	24.5	24.8	24.2	24.3	Maximum	25.7
S5	23.6	23.9	22.9	23.9	24.0		

Table C12 Vickers hardness test results of dental resin material incorporating 3% microcapsules with 1% of the urea part in the capsule shell replaced by melamine

Sample No.	Vickers Hardness Measurement					Test Result	HV
	M1	M2	M3	M4	M5		
S1	25.8	26.0	23.7	25.2	25.0	Total Average	24.4
S2	23.1	22.4	23.0	22.8	23.2	Std. Dev.	1.0
S3	24.9	24.8	25.5	25.1	25.1	Minimum	22.4
S4	25.0	25.2	24.8	25.0	25.2	Maximum	26.0
S5	23.7	24.1	23.9	24.6	24.0		

Table C13 Vickers hardness test results of dental resin material incorporating 3% microcapsules with 3% of the urea part in the capsule shell replaced by melamine

Sample No.	Vickers Hardness Measurement					Test Result	HV
	M1	M2	M3	M4	M5		
S1	23.9	23.8	24.1	23.7	25.5	Total Average	24.5
S2	24.4	23.7	26.0	24.4	24.4	Std. Dev.	0.8
S3	23.5	24.2	25.7	24.7	24.3	Minimum	23.5
S4	23.7	23.6	24.5	26.1	25.1	Maximum	26.0
S5	23.8	23.9	26.0	25.5	24.9		

Table C14 Vickers hardness test results of dental resin material incorporating 3% microcapsules with 5% of the urea part in the capsule shell replaced by melamine

Sample No.	Vickers Hardness Measurement					Test Result	HV
	M1	M2	M3	M4	M5		
S1	27.0	25.6	25.9	26.1	26.2	Total Average	25.8
S2	25.5	25.8	24.8	25.3	25.1	Std. Dev.	0.9
S3	27.1	26.3	23.5	26.6	25.9	Minimum	23.5
S4	27.0	25.1	24.4	27.4	26.2	Maximum	27.4
S5	26.1	25.7	24.5	26.9	25.6		

3. Ultra-Microhardness Testing

Test Parameters

Instrument:	Shimadzu Dynamic Ultra Micro Hardness Tester DUH-211
Test mode:	Load-unload
Test force:	490.33 mN (50 gf)
Loading speed:	10.0 mN/sec
Hold time at unoad:	5 s
Poisson's ratio:	0.300
Cf-Ap,As Correction:	OFF
Read times:	3
Indenter elastic	1.140e+006 N/mm ²
Indenter type:	Triangular115
Objective lens:	50
Indenter poisson's ratio:	0.070
Test result:	Nanoindentation Hardness (Hit) in [N/mm ²] Indentation Modulus (Nit) in [MPa]
Sample:	3% Microcapsules embedded in dental matrix material
Test date:	09 Feb 2010 / 29 Mac 2010
Sample:	6% Microcapsules embedded in dental matrix material
Test date:	04 Feb 2010 / 09 Feb 2010

Table C15 Nanoindentation hardness of dental resin material incorporating 3% microcapsules with part of the urea in the capsule shell being replaced by melamine

Indentation No.	Reference	Melamine Part Relative to Urea Amount			
		0%	1%	3%	5%
1	168.3	/	145.3	137.3	/
2	175.1	131.3	155.5	131.5	141.5
3	172.3	132.9	148.6	147.2	168.5
4	167.9	153.9	168.8	147.3	156.8
5	186	148.3	161.8	144	177.5
6	183.8	141.9	149.6	161.1	165.2
7	179.0	157.1	169.4	157.6	165.4
8	173.2	158.4	157.5	154.8	176.2
9	191.7	158.1	143.7	/	171.3
Average	177.4	147.7	155.6	147.6	165.3
Std. Dev.	8.2	11.2	9.6	10.1	11.7
Minimum	167.9	131.3	143.7	131.5	141.5
Maximum	191.7	158.4	169.4	161.1	177.5

Table C16 Indentation modulus of dental resin material incorporating 3% microcapsules with part of the urea in the capsule shell being replaced by melamine

Indentation No.	Reference	Melamine Part Relative to Urea Amount			
		0%	1%	3%	5%
1	2483	/	2303	2191	/
2	2543	2319	2342	2098	2366
3	2520	2337	2238	2368	2740
4	2469	2564	2492	2316	2562
5	2731	2493	2385	2246	2852
6	2704	2451	2347	2466	2659
7	2653	2611	2487	2420	2590
8	2609	2623	2440	2328	2671
9	2852	2627	2329	/	2585
Average	2618	2503	2374	2304	2628
Std. Dev.	128	125	86	121	142
Minimum	2469	2319	2238	2098	2366
Maximum	2852	2627	2492	2466	2852

Table C17 Nanoindentation hardness of dental resin material incorporating 6% microcapsules in which part of the urea in the capsule shell was replaced by melamine

Indentation No.	X-coordinate [mm]	Y-coordinate [mm]	Reference	Melamine Content in Microcapsule Shell Relative to Urea Part						
				0%	0.5%	1%	2%	3%	4%	5%
1	0.000	0.000	168.323	148.983	152.379	—	165.843	145.895	—	199.103
2	0.500	0.000	175.109	157.862	148.657	272.592	189.707	152.379	163.034	201.585
3	1.000	0.000	172.345	151.491	164.845	233.772	193.774	148.657	172.562	201.644
4	0.000	0.500	167.872	149.845	165.752	243.891	244.570	164.845	164.263	196.652
5	0.500	0.500	186.020	146.180	163.110	257.895	230.407	165.752	184.654	285.264
6	1.000	0.500	183.809	135.460	175.832	183.777	208.291	163.110	181.675	206.690
7	0.000	1.000	179.011	159.973	171.837	222.758	156.282	175.832	172.443	227.017
8	0.500	1.000	173.175	152.511	145.895	245.563	188.141	171.837	192.015	285.026
9	1.000	1.000	191.730	145.304	—	243.966	172.946	—	185.762	210.299
Average			177.488	149.734	161.038	238.027	194.440	161.038	177.051	223.698
Standard Deviation			8.254	7.231	10.916	24.775	29.148	10.916	10.559	33.900
Minimum			167.872	135.460	145.895	183.777	156.282	145.895	163.034	196.652
Maximum			191.730	159.973	175.832	272.592	244.570	175.832	192.015	285.264

Table C18 Indentation modulus of dental resin material incorporating 6% microcapsules in which part of the urea in the capsule shell was replaced by melamine

Indentation No.	Reference	Melamine Content in Microcapsule Shell Relative to Urea Part						
		0%	0.5%	1%	2%	3%	4%	5%
1	2483	1999	2571	2442	2786	/	2418	3402
2	2543	1957	2630	2391	2753	2400	2457	3660
3	2520	1781	2604	2666	3099	2333	2468	3338
4	2469	1853	2709	3107	2993	2537	2546	3572
5	2731	1719	2722	2470	3513	2491	2605	3035
6	2704	1549	2726	2883	2786	2418	2522	2751
7	2653	2035	2802	3076	2753	2536	2605	3430
8	2609	1875	2788	2641	3099	2499	2630	4638
9	2852	1725	/	2709	2993	2447	/	3156
Average	2618	1833	2694	2709	2975	2458	2531	3442
Std. Dev.	128	156	84	264	248	72	79	528
Min	2469	1549	2571	2391	2753	2333	2418	2751
Max	2852	2035	2802	3107	3513	2537	2630	4638

APPENDIX D: Publications

Optimization of Microencapsulation Process for Self-Healing Polymeric Material

Sonja Then¹, Seng Neon Gan¹, Noor Hayaty Abu Kasim²

¹ Department of Chemistry, University of Malaya, 50603 Kuala Lumpur, Malaysia

² Department of Conservative Dentistry, University of Malaya, 50603 Kuala Lumpur, Malaysia

Abstract: A series of poly(urea-formaldehyde) (PUF) microcapsules filled with dicyclopentadiene (DCPD) was successfully prepared by in situ polymerization. The effect of diverse process parameters and ingredients on the morphology of the microcapsules was observed by SEM, optical microscopy (OM) and digital microscopy. Different techniques for the characterization of the chemical structure and the core content were considered such as FT-IR and ¹H-NMR as well as the characterization of thermal properties by DSC. High yields of free flowing powder of spherical microcapsules were produced. The synthesized microcapsules can be incorporated into another polymeric host material. In the event the host material cracks due to excessive stress or strong impact, the microcapsules would rupture to release the DCPD, which could polymerize to repair the crack.

Then, S., Gan, S. N., Abu Kasim, N. H. (2011). Optimization of Microencapsulation Process for Self-Healing Polymeric Material. *Sains Malaysiana*, 40(7), 795-802.

Performance of Melamine Modified Urea-Formaldehyde Microcapsules in a Dental Host Material

Sonja Then¹, Seng Neon Gan¹, Noor Hayaty Abu Kasim²

¹ Department of Chemistry, University of Malaya, 50603 Kuala Lumpur, Malaysia

² Department of Conservative Dentistry, University of Malaya, 50603 Kuala Lumpur, Malaysia

Abstract: Urea-formaldehyde (UF) microcapsules filled with dicyclopentadiene (DCPD) show potential for making self-healing dental restorative materials. To enhance the physical properties of the capsules, the urea was partially replaced with 0-5% melamine. The microcapsules were analyzed by different microscopic techniques. DSC was used to examine the capsule shell, and the core content was confirmed by ¹H-NMR spectroscopy. Capsules in the range of 50-300 μm were then embedded in a dental composite matrix consisting of bisphenol-A-glycidyl dimethacrylate (Bis-GMA) and triethylene-glycol dimethacrylate (TEGDMA). Flexural strength, microhardness and nanoindentation hardness measurements were performed on the light-cured specimens. Optical microscopy (OM) examination showed a random distribution of the microspheres throughout the host material. The incorporation of small amounts of the microcapsules did not affect the performance of the matrix material. SEM analysis revealed excellent bonding of the microcapsules to the host material which is a characteristic of utter importance for maintaining the very good mechanical properties of a dental composite with self-healing ability.

Then, S., Gan, S. N., Abu Kasim, N. H. (2011). Performance of Melamine Modified Urea-Formaldehyde Microcapsules in a Dental Host Material. *Journal of Applied Polymer Science*, 122(4), 2557–2562.